Lawrence Berkeley National Laboratory
Recent Work

Title
CONTROLLED THERMONUCLEAR RESEARCH QUARTERLY REPORT Sept., Oct., Nov. 1960

Permalink
https://escholarship.org/uc/item/4hm5q93r

Author
Lawrence Berkeley National Laboratory

Publication Date
1960-12-15

eScholarship.org Powered by the California Digital Library
University of California

UCRL-9500

Cy. 2

UNIVERSITY OF CALIFORNIA

Ernest O. Lawrence Radiation Laboratory

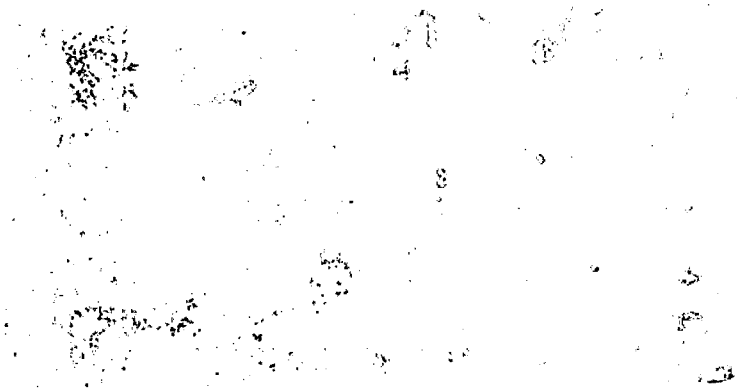

BERKELEY, CALIFORNIA

DISCLAIMER

This document was prepared as an account of work sponsored by the United States Government. While this document is believed to contain correct information, neither the United States Government nor any agency thereof, nor the Regents of the University of California, nor any of their employees, makes any warranty, express or implied, or assumes any legal responsibility for the accuracy, completeness, or usefulness of any information, apparatus, product, or process disclosed, or represents that its use would not infringe privately owned rights. Reference herein to any specific commercial product, process, or service by its trade name, trademark, manufacturer, or otherwise, does not necessarily constitute or imply its endorsement, recommendation, or favoring by the United States Government or any agency thereof, or the Regents of the University of California. The views and opinions of authors expressed herein do not necessarily state or reflect those of the United States Government or any agency thereof or the Regents of the University of California.

UCRL-9500
UC-20 Controlled
Thermonuclear Processes

UNIVERSITY OF CALIFORNIA
Lawrence Radiation Laboratory
Berkeley and Livermore, California

Contract No. W-7405-eng-48

CONTROLLED THERMONUCLEAR RESEARCH QUARTERLY REPORT

September, October, November 1960

December 15, 1960

CONTROLLED THERMONUCLEAR RESEARCH QUARTERLY REPORT

September, October, November 1960

Contents

I. PYROTRON (MAGNETIC MIRROR) PROGRAM

1. Introduction and Summary 5
2. Magnetic High-Compression Experiments (Table Top) . . . 6
3. Electron Energy Distribution and Scintillator Probe Calibration 9
4. Measurements of Velocity-Space Hydromagnetic Instability on Table Top 13
5. Accel-Decel Electrostatic Particle Energy Analyzer . . . 19
6. Plasma Diagnostics in Table Top 21
7. Rejuvenation of Electron Multipliers 23
8. Grid Source Development (ALICE) 23
9. Beam Neutralization 25
10. Vacuum and Surface Studies 25
11. P-4 (Steady-State Plasma) System 29

II. ASTRON PROGRAM

1. Introduction 34
2. Astron Accelerator Components 35

III. LIVERMORE PINCH PROGRAM

1. Summary 38
2. Electron-Beam Pinch 38
3. Conical Pinch Plasma Accelerator 43
4. Collisionless Plasma Shock 43
5. Liquid Sodium Experiment 44
6. 12-Inch Levitron 44
7. High-Field Research 47
8. The Unipolar Generator 47
9. Theory 49

IV. BERKELEY PLASMA RESEARCH

1. Sheet Pinch Studies 52
2. Homopolar Program 55
3. Hydromagnetic Wave and Cyclotron Heating 56
4. Ion Cyclotron Resonance 66
5. Plasma Physics and Microwave Diagnostics 66
6. Further Analysis of the "Switch-On" Ionizing Wave 71

*Preceding Quarterly Reports UCRL-9393, UCRL-9243

V. THEORETICAL AND BASIC EXPERIMENTAL PLASMA PHYSICS

1. The Interchange Instability 74
2. Cyclotron Radiation from a Plasma 75
3. The Magnetic Compression of a Partially Ionized Gas . . . 76
4. Resistive Relaxation of a Perturbed Sheet Pinch 76
5. A Computation for Studying the Formation of the Astron E-Layer 78
6. Stability of Infinitely Thin Electron Layers 79
7. Plasma Potential in a Magnetic Mirror System 80
8. Secondary Processes in a Hydrogen Gas Neutralizer . . . 83
9. Vibrational States of the HD^+ and HT^+ Ions 86
10. Penetration of Charged Particles through the Picket Fence 88
11. Atomic and Molecular Beam Research 88
12. Containment of Positrons in Mirror and Cusp Geometries . 91

VI. ENGINEERING AND TECHNOLOGICAL DEVELOPMENT

1. Ultrahigh-Vacuum Development 96
2. Mechanical Engineering Development 97
3. Electrical Engineering Development 103

VII. TALKS AND PUBLICATIONS 116

CONTROLLED THERMONUCLEAR RESEARCH QUARTERLY REPORT *

September, October, November 1960

Lawrence Radiation Laboratory
University of California
Berkeley and Livermore, California

December 15, 1960

I. PYROTRON (MAGNETIC MIRROR) PROGRAM

1. INTRODUCTION AND SUMMARY

Richard F. Post

The most significant event of the past quarter was the successful operation of two stages of Toy Top III (the three-stage multiple-compression mirror machine). As described in the accompanying reports, a deuterium plasma with a measured mean ion energy of 3 kev, an ion density of 2×10^{13} ions/cm^3, and a volume of 2000 cm^3 was confined for nearly a millisecond, during which time neutrons were emitted from the body of the plasma. From the observations three very important facts can already be deduced:

(a) Heating of the plasma occurs at a rate in agreement with adiabatic theory.

(b) Apparently stable confinement of a plasma in which the ions are hotter than the electrons is possible. Thus, we now have evidence in both cases ($T_e > T_i$, Table Top, and $T_i > T_e$, Toy Top III) that plasma instabilities can be avoided, at least in special cases, in the mirror machine.

(c) Neither excessive transfer of energy to the electrons nor excessively rapid scattering of ions has been observed.

Since the plasma volume was small, and the value of β was low, we do not at all consider that these results settle the question of plasma stability in the mirror machine; they are obviously very encouraging to us, nevertheless.

Other significant developments include the first operation of the high-current ion source for use in the ALICE experiment. Well-focused ion beams with a total current approaching our design values have already been achieved.

Experimental work on the velocity-space instabilities that can be induced in the Table Top plasma has come to a successful conclusion.

* This work done under the auspices of the U. S. Atomic Energy Commission.

We have found it possible to corroborate the important predictions of the theory of such instabilities, and to learn much of the anatomy of the transport effects caused by the presence of the instability. A paper is in preparation.

Demonstration of the workability of plasma injection and the creation and confinement of a hot-ion plasma in Toy Top III has prompted a re-examination of the entire Mirror program. A projected program which should answer the many crucial confinement questions yet outstanding has been set down. Plans are being considered for possible future extensions of the multistage and ALICE experiments. The Table Top machine is now being modified to permit studies of the confinement of small volumes of hot-ion plasmas for periods up to 1 second. Looking toward the future, it now appears that a reasonable extrapolation of the techniques now developed in the Mirror program should permit obtaining "yes" or "no" answers to the crucial questions within a few years.

2. MAGNETIC HIGH-COMPRESSION EXPERIMENTS

Frederic H. Coensgen

Two-Stage Operation of Toy Top III

At the time of the preceding Quarterly Report, the assembly of the first two stages of the three-stage experiment had been completed and the system was under vacuum. Preliminary operation of the system as a two-stage experiment began in early September, 1960. The first evidence of ion heating was obtained about the second week in September. These measurements, as well as all subsequent measurements of ion heating, were obtained through the determination of the ion energy distributions in the compressed and transferred plasma. These measurements were made with the ion-energy analyzer described in previous reports. For maximum compression ($a \approx 33$) the final mean ion energy was found to be ≈ 3000 ev, which agrees within experimental accuracy with the 2700 ev predicted by adiabatic theory. The mean energy of the D^+ ions in the injected plasma was 850 ev.

By properly adjusting the dc and pulsed fields, it was possible to form a mirror containment region between the 9-in. and 4-in. sections. Although the mirror ratio was only 1.08, about 1/3 of the plasma could be retained in this region.

From various measurements we believe that we have produced and contained a plasma with the following characteristics:

mean ion energy	≈ 3000 ev
mean electron temperature	20 to 100 ev
volume	≈ 2000 cc
diameter	≈ 10 cm
mean density	$\approx 2 \times 10^{13}$ ions/cc
containment time	$\geqslant 900$ μsec, and apparently limited only by the decay time of the pulsed magnetic field
neutron production	$\approx 10^4$ neutrons per operation

The mean ion energy was determined, by means of the ion-energy analyzer, for the transferred plasma, when the entire plasma was transferred and when part of it was trapped. The energy distribution of the trapped ions was obtained by the difference of the distributions. In all these cases, all the distributions extended from 750 ev to nearly 10,000 ev, and the mean energy values were approx 3000 ev.

The electron temperature was determined by means of a microwave radiometer.

The volume was estimated from the distance between the mirrors of the containment region and the radius as given by adiabatic theory. Previous measurements by Franklin C. Ford have shown for other cases that plasma boundary moves as predicted from simple adiabatic theory.

An electrostatic extraction probe was used to measure the total positive charge and its radial distribution for the transferred plasma. The quantity of positive charge retained in the containment region was obtained by subtracting the measured transferred charge in a partial transfer from that in a totally transferred plasma. The fraction of retained plasma also agrees with that computed by integrating the ion energy distributions in the two cases.

The containment time was taken equal to the period of neutron production. The neutron production rate as a function of time was obtained by detecting the fast neutrons in a large plastic scintillator. Identification of these counts as due to neutrons was made by measurement of their absorption length in lead.

The total neutron production was obtained through the use of LiI crystal scintillator which was calibrated in place by using a PuBe neutron source. Neutron identification was made by the characteristic light pulses produced in the crystal from the reaction $Li^6(n, H^3)He^4$. No evidence of large x-ray bursts which could have confused the identification was detected by a 2×2-in. NaI crystal scintillator. The absence of x rays is consistent with the low compression ratio of 30 (compression ratios of the order of 1000 are used in experiments in which energetic x rays are detected).

Protons from the other branch of the d-d reaction were detected by means of nuclear emulsions placed inside the vacuum chamber. The reaction rate found from the proton measurements agreed with that from the neutron measurements.

The question arises for this plasma (as for all other plasmas of a few kilovolts ion energy) whether or not the neutron production is from the plasma or due to a few high-energy ions bombarding a target of cold gas. The latter assumption is inconsistent with the 900-μsec containment time, as the neutral density necessary to account for the observed rate would, through charge exchange, lead to a much shorter lifetime of the high-energy group. It is therefore necessary to postulate containment of the observed plasma either as a target or as a reacting plasma. The evidence favors the latter interpretation. We conclude that the plasma is contained for times that exceed the e-folding time for hydromagnetic instabilities by three orders of

magnitude. Furthermore, the close agreement of the observed ion energy gain with that predicted from adiabatic theory indicates that the energy transport from ions to electrons does not greatly exceed the rate calculated on the basis of Coulomb collisions.

These results have been published: F. H. Coensgen, W. F. Cummins, W. E. Nexsen, Jr., and A. E. Sherman, Phys. Rev. Letters 5, 459 (1960).

Three-Stage Toy Top III

The operation of the two-stage experiment was carried out at night to allow the construction of the banks and transmission lines for the third-stage magnets to proceed during the day. All the complex lines have been completed and the installation work is proceeding. It should be completed within 4 to 6 weeks.

On November 23, 1960, the two-stage vacuum system and coil system was dismantled, and installation of the three-stage system is under way. This construction should be completed within a month, provided the third-stage magnets do not fail when tested. Such a failure would delay the schedule by at least 3 weeks.

Plasma Generators

All members of the Toy Top crew have been engaged in the two-stage experiment or in construction of the third stage, so that no plasma source work is in progress. It is not planned to start any major plasma source effort until the three-stage experiment has been successfully operated.

Future Multistage Facilities

Encouraged by the results of the two-stage experiment, we have spent some time considering future facilities to extend the work, provided the three-stage experiment is successful. It is our opinion that a reasonable goal would be the production of a 100-kev plasma of 10% β, in a period of 3 to 4 years. The study of such a plasma would provide answers to many of the fundamental physical and technical questions that arise in any thermonuclear reactor. It would, of course, be most useful in solving the problems related to the mirror machine. Preliminary designs of a 10× and 5× scale-up of Toy Top III were made. These designs appear to be technically feasible, requiring only an extension of present engineering practice. More accurate cost estimates are being prepared, but the preliminary estimates are quite reasonable in comparison with other major Sherwood installations.

3. ELECTRON ENERGY DISTRIBUTION AND SCINTILLATOR PROBE CALIBRATION

Robert E. Ellis and Norris W. Carlson

Calibration measurements of scintillator probes have been continued. A probe with a plastic fluor approximately 1/2 in. in diameter and 1/8 in. thick, coated with approx 2000 angstroms of aluminum and mounted in a 1-in. -diameter probe stem,[1] was used to determine the relative efficiency of the coated plastic fluor as a function of electron energy and electron beam current. Figure 1 is a plot of the signal per unit beam current as a function of the residual energy $[E - E_A]$ which an electron of energy E has after passing through the aluminum coating whose thickness corresponds to an energy loss E_A. Q is the signal height in volts and I is the beam current in microamperes. The points were run for four values of current--I = 0.04, 0.02, 0.004, and 0.0004 μa. The uncertainty of the value of each point is about 7%. Within the accuracy of the data, it appears that a nearly constant slope of approximately the same value may be assigned to all four sets of points. Since the extrapolation of this curve does not go through zero, the relative fluor efficiency is less than approx 1.0 at energies below 40 or 50 kev, and goes to zero at $E-E_A \approx 4$ kev. The equation for the pulse height (in volts) is[1]

$$Q = 6.25 \times 10^{12} K \epsilon I [E-E_A] \quad . \tag{1}$$

Here K is a constant characteristic of the given probe being used, and ϵ is the relative efficiency of the fluor. Figure 2 is a plot of the relative fluor efficiency ϵ. Here the extrapolation of the curve to zero efficiency would, as indicated by Fig. 1, result in a low-energy cutoff of approx E_A + 4 kev for this fluor and these beam currents. With a beam current of 0.95 μa, we have obtained a curve that indicates a saturation effect at energies above about 30 kev. We have not confirmed this result yet because of a burned-out electron-gun filament. So far as results on previous Table Top measurements are concerned, a drop in fluor efficiency at this high beam voltage and current is not believed applicable. The actual maximum pulse height in the tests was limited to less than 30 volts, this being achieved where necessary by screening the phototube so that only 1/20 of the light reaching the phototube was used. This means that the fluor was actually generating from 10 to 20 times the light produced in the Table Top experiments. At beam energies below 30 kev, the fluor efficiency appears to be essentially the same at 0.95 μa of beam as it is at lower beam currents.

A test of a similar type of probe with a small 1/8-in. -diameter cesium iodide fluor in place of the plastic fluor yielded a signal approximately 1/150 of the signal with plastic fluor for comparable beam current and energy. Perhaps further checks should be made on this result, although the back-scattering of the low-energy electrons (20 kev in this case) from the high-Z cesium iodide might account for a considerable diminution of the signal.

---

[1] Robert E. Ellis and Norris W. Carlson, in Controlled Thermonuclear Research Quarterly Report UCRL-9243, Aug. 1960.

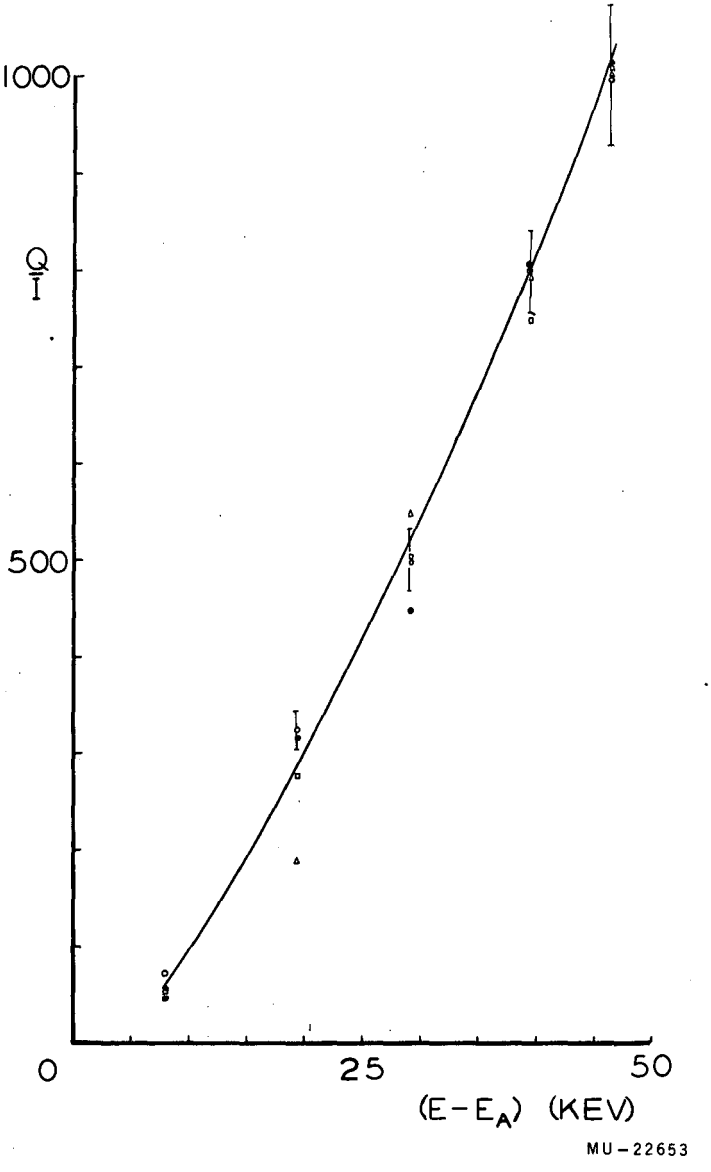

Fig. 1. The signal height Q (in v) per unit beam current I (in μa) as a function of the residual electron energy $E-E_A$ (in kev). The symbols represent data for four different values of beam current: □ - 0.04 μa; ● - 0.02 μa; O - 0.004 μa; and Δ - 0.0004 μa. The approximate uncertainty for each set of points at a given energy is shown for the 0.02-μa data only. The relative value of Q/I vs $E-E_A$ is of relevance here, since the quantity $K\epsilon$ (the probe constant K and relative fluor efficiency ϵ) would differ according to the probe geometry, photomultiplier voltage, etc., used in a particular case.

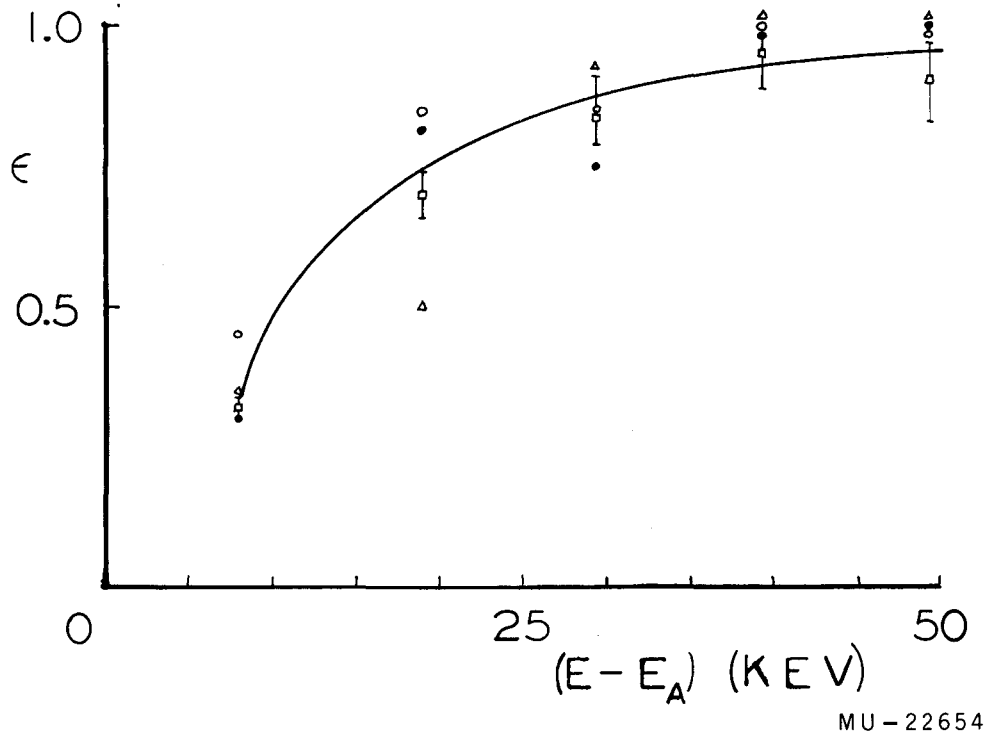

Fig. 2. The relative fluor efficiency ϵ as a function of the residual electron energy $E-E_A$ (in kev). The probe constant K is evaluated so that $\epsilon = 1$ when $E-E_A = 50$ kev.

The 21-channel scintillator probe head has been redesigned to better utilize flexible glass fiber light pipes. The over-all diameter of the probe is now approx 3 in. Electron beam tests of the transistorized photomultiplier bases and the 3/4-in. -diameter nine-stage phototubes to be used with this probe have shown a necessity for some more electronic design work which was not evident in the initial tests with a Co^{60} source. Some additional gain is required, as well as elimination of excessive hash on the signal. Although other larger phototubes can be used, their reduced size and the fact they use a battery source of B+ voltage make the smaller tubes quite convenient when so many are used at once.

The light-conducting properties of a flexible 5-ft-long 1/8-in. -diameter glass fiber light pipe[2] have been found satisfactory for use with scintillator probes. We have tested such a light pipe with the scintillator probe mentioned in the preceding progress report.[3] In this case, the electron beam was directed upon a small (1/8-in. -long 1/8-in. -diameter) cylindrical plastic fluor which was glued with epoxy resin to a 4-in. -long 1/8-in. -diameter lucite rod. An optical connection, using Canada balsam, was made between the lucite rod and one end of the flexible glass fiber light pipe, the other end of which was placed about an inch from a DuMont-6292 photomultiplier tube with no optical connection between light pipe and photomultiplier. The resulting pulse signal was comparable to the signal obtained by using only the 4-in. section of lucite rod (mentioned above) with a straight light path in air of about 5 ft from lucite rod to photomultiplier. No change in signal height was observed with two 1-in. -radius circular bends in the flexible glass fiber light pipe. It thus appears that such light pipes will be better by a factor of at least 400 than lucite rods of the same diameter (1/8 in.) for lengths of 4 to 5 ft.[3]

---

[2]Manufactured by American Optical Company, Southbridge, Massachusetts.

[3]Robert E. Ellis and Norris W. Carlson, in Controlled Thermonuclear Research Quarterly Report, UCRL-9393, Sept. 1960, p. 8.

4. MEASUREMENTS OF VELOCITY-SPACE HYDROMAGNETIC INSTABILITY ON TABLE TOP

Walton A. Perkins

We have continued the experimental investigation[4-6] of an instability that occurs for an anisotropic velocity distribution in which the ratio of perpendicular to parallel rms velocity is large.

The variation with radius of the end-escaping electron flux was measured with a scintillation detector. The 1/8-in. -diameter plastic scintillator could be moved along the radius on a belt by a rotary motion through a Wilson seal. The light was transmitted along a flexible glass-fiber light pipe to an RCA-6810A phototube.

The radial density of the escaping end flux was measured with an initial field of H_i = 0 gauss and H_i = 40 gauss. If the initial radii are roughly the same, a smaller final radius should be obtained with the lower initial magnetic field (i. e., larger compression ratio). The experimental results are shown in Fig. 3, giving a smaller final radius for an initial field of 40 gauss. This indicates that the larger plasma radius is caused by an instability which is prevented from occurring or at least diminished by the larger initial field. This result is in good agreement with the decrease[4] in the ratio of radial energy flux to end energy flux with increasing initial magnetic field.

The radii for medium and low density and H_i = 0 gauss are shown in Fig. 4. Here the instability has been avoided by trapping only a low-density plasma, whose β (plasma pressure) $\div$ $(B^2/8\pi)$ is less than the critical β.[1, 3] This result was expected again from the earlier reported decrease[8] in the ratio of the radial-probe signal to end-probe signal with decreasing density.

The radial-probe signal is composed of two parts--a large pulse occurring for the first millisecond and a late signal lasting about 5 msec (see Fig. 5). A comparison of the radial diffusion velocity of the two components was made by using an obstacle probe. Both the radial scintillation probe and the obstacle probe protruded into the vacuum chamber in the midplane as shown in Fig. 6.

---

[4] Richard F. Post and Walton A. Perkins, in Controlled Thermonuclear Research Quarterly Report, UCRL-9243, June 1960, p. 11-19.

[5] Walton A. Perkins, in Controlled Thermonuclear Research Quarterly Report, UCRL-9393, Sept. 1960, p. 11.

[6] R. F. Post, Velocity-Space Instabilities in a Mirror Machine, UCRL-6079, Aug. 1960.

[7] See Fig. 5 of Reference 1 or Fig. 6 of Reference 3.

[8] See Fig. 2 of Reference 5 or Fig. 8 of Reference 6.

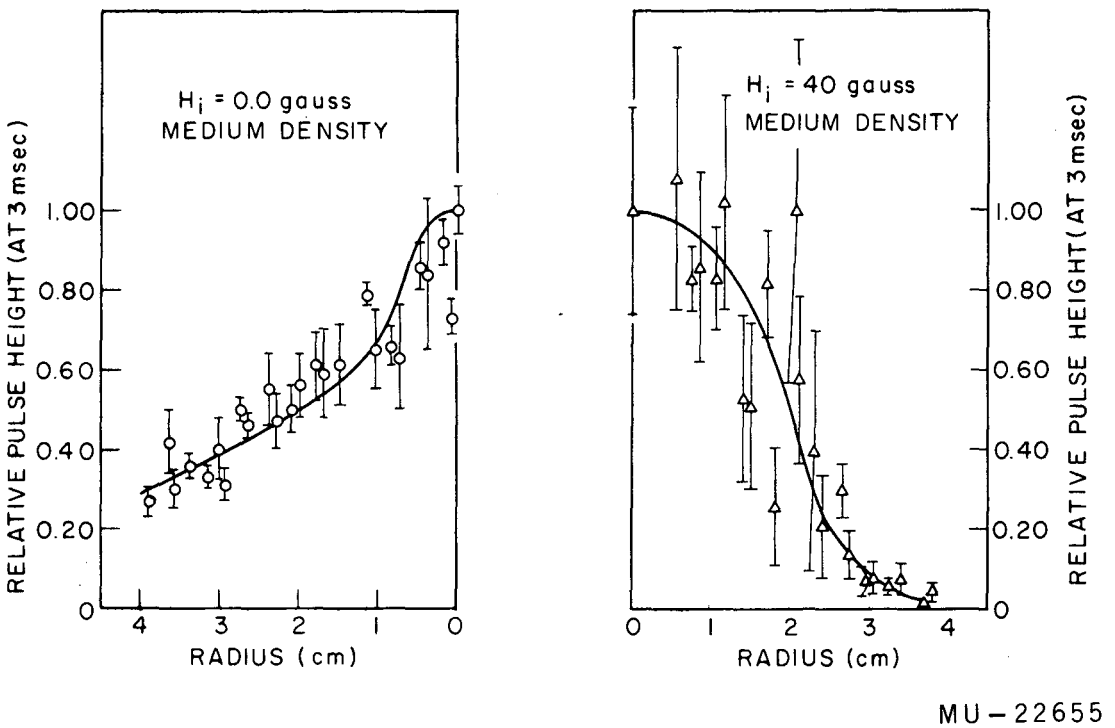

Fig. 3. End-escaping flux as a function of radius for initial magnetic fields of 0.0 gauss and 40 gauss.

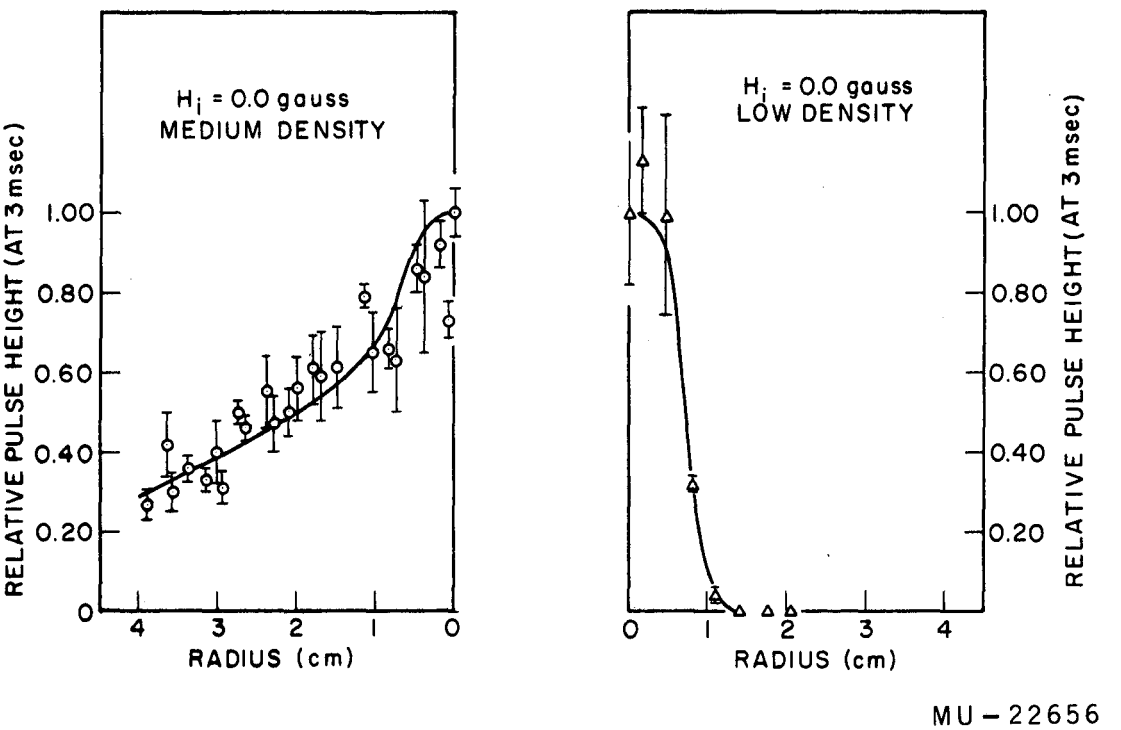

Fig. 4. End-escaping flux as a function of radius for an initial magnetic field of 0.0 gauss for medium and low densities.

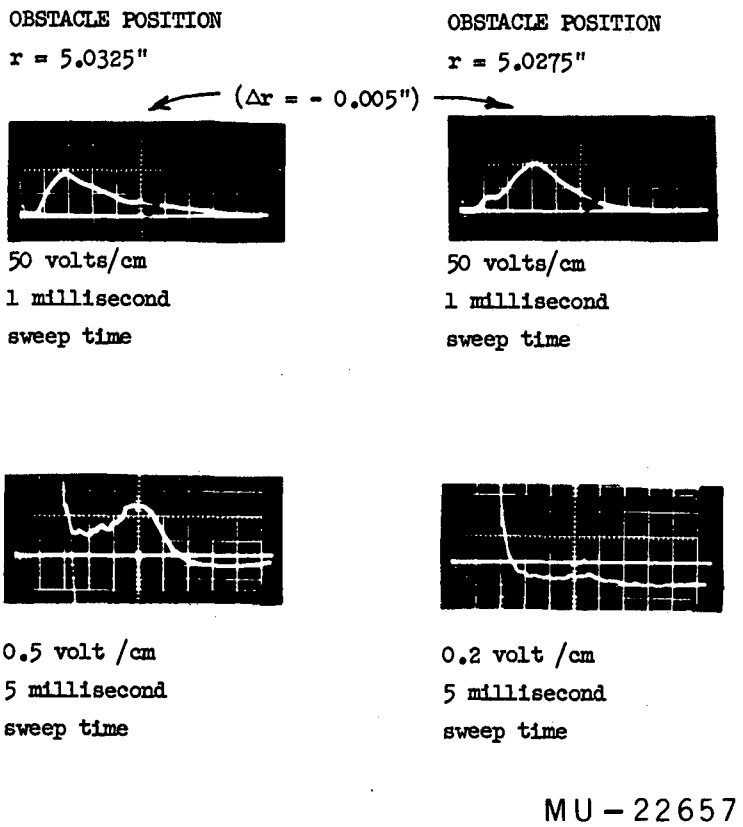

Fig. 5. Radial probe signals for two positions of the obstacle. The upper traces show the large early signal which is off scale in the lower traces.

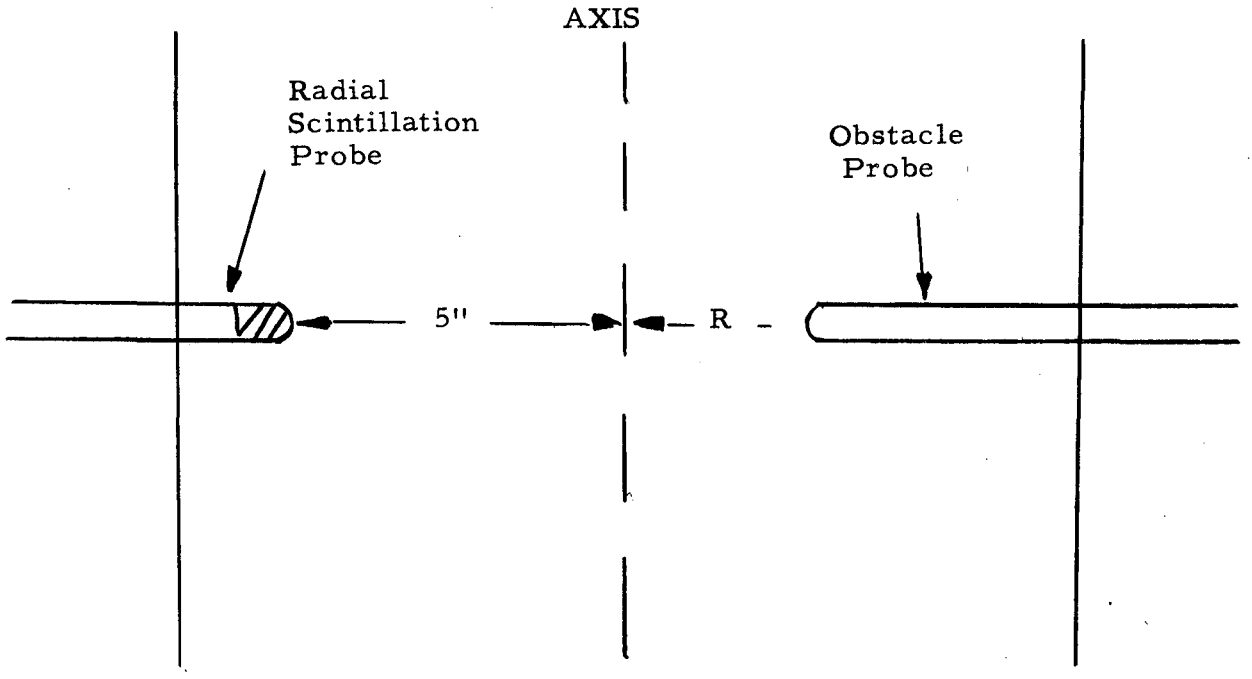

Fig. 6. Probe positions in vacuum chamber.

If the electrons missed the obstacle probe at a radius R and diffused outward to a radius greater than 5 in. during their 1/2 revolution of precession, they struck the radial scintillation probe. Therefore, the smaller the R of the obstacle needed to scatter the particles, the larger the radial diffusion velocity. The velocities of the early and late signals were quite different, as can be seen from Fig. 7. The early signal is the fast component and the late signal is the slow component. The slow component is wiped out by a movement of only 0.005 in. of the obstacle probe, whereas it takes a movement of 0.100 in. to decrease the fast component to 10% of its original value.

The fall-off of the slow-component signal shown in Fig. 7 is in agreement (within experimental accuracy) with the radial velocity that could be caused by the particles' being carried outward on the field lines of the decaying magnetic field. The slow component is interpreted as being caused by particles that were unstable at smaller radii, but became stable as the plasma diffused outward to larger radii, so that its β dropped below the critical β. The fast component is indicate of an unstable plasma diffusing across the field lines.

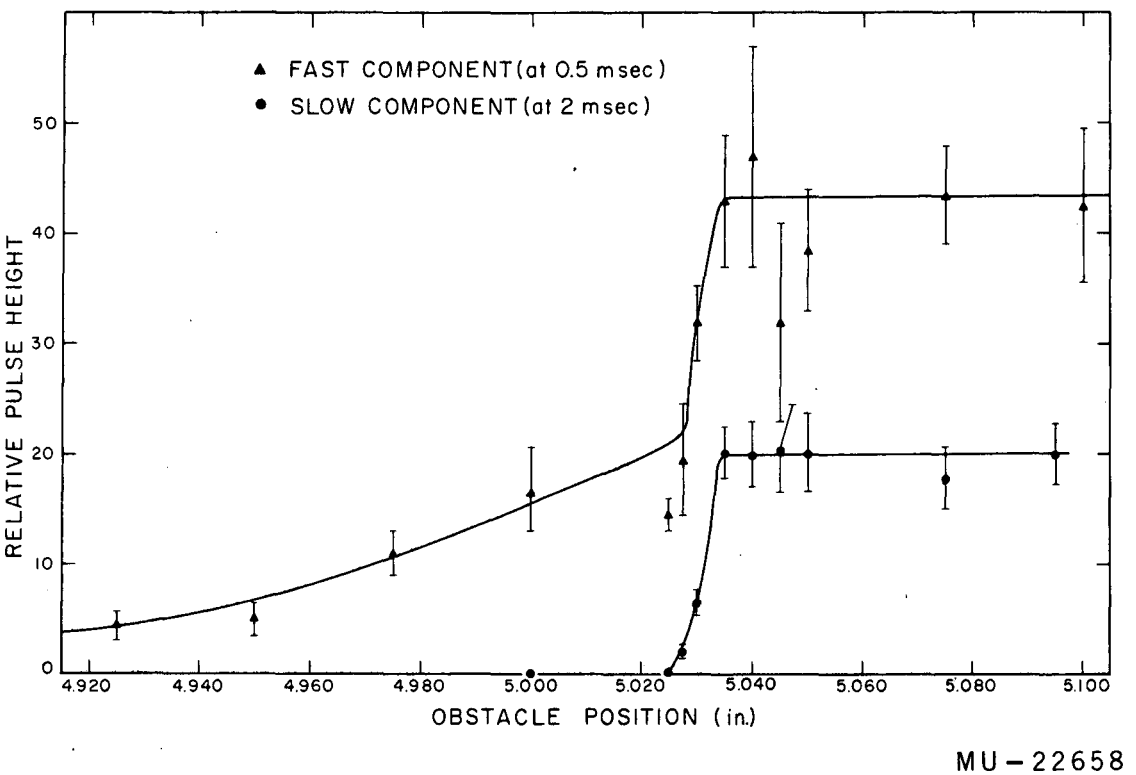

Fig. 7. Fast and slow components of the radial probe signal vs the position of the obstacle probe.

5. ACCEL-DECEL ELECTROSTATIC PARTICLE-ENERGY ANALYZER

Robert E. Ellis

The construction and preliminary testing of an electrostatic particle-energy analyzer has been completed. The analyzer consists of a cylindrical tank, 30 in. long and 12 in. in diameter, with three coaxial cylindrical electrodes on the longitudinal axis of the tank. The electrodes are approx 3 in. in diameter and 6 in. long. The tank is made of a high-nickel-content iron to provide magnetic shielding, and large alumina insulators provide the insulation between tank and electrodes. A variable slit in the front vacuum plate of the analyzer determines the flux of particles entering the electrode system. A 3-in. -diam thin plastic fluor is attached to the back of the electrode farthest from the entrance slit, so that light generated by particles striking the fluor can pass through a lucite light pipe extending through a vacuum seal in the rear vacuum cover, and then into an RCA-6810 photomultiplier tube.

It was originally planned that this detector should be capable of measuring the energy spectra of electrons or deuterons within the energy range 0 to 150 kev. For the detection of deuterons, a thin deuterated polyethylene film (not more than 0.001 in.) was to be placed in front of the plastic fluor so that the fusion protons from the reaction D(d, p)T would scintillate. Other ion species would thus be discriminated against by the presence of the foil, which would absorb them. Electrons would be discriminated against by the foil as well as by the negative-ion accelerating voltage on the first and last electrodes. For ion detection, a high negative voltage of perhaps 100 kev is applied to Electrodes 1 and 3 (numbered 1, 2, 3 from front to rear), and a positive voltage, variable from zero to as high as needed, is applied to Electrode 2. All electrode potentials are referenced to the same ground potential as that to which the initial particle energy is referenced. Thus electrons in a flux of ionized plasma are repelled from the entrance slit and do not enter the system at all if the negative voltage on electrode 1 is sufficiently high. Ions are accelerated through the first electrode, and only those with initial energy E greater than the voltage on Electrode 2 will pass through the second electrode and be accelerated into the deuterated foil by the negative voltage on Electrode 3. The resulting signal should depend only on the number of ions reaching the foil, provided the voltage on Electrode 3 is sufficiently high that the variation of the D(d, p)T cross section due to the initial spectrum of ion energies is negligible.

The equation for the output signal in volts is given by

$$Q = K \int_{E_0}^{\infty} (E + E_a) S(E, E_a) \phi(E) dE, \qquad (1)$$

where

K = constant, characteristic of the entrance slit size, final accel electrode voltage, light collection geometry, phototube voltage, fluor efficiency, etc.;

E = initial particle energy (kev);

E_0 = minimum particle energy required to pass through repel Electrode 2;

$S(E, E_a)$ = relative fusion cross section as a function of energy;

$\phi(E)$ = particle flux;

E_a = particle energy (kev) gained from acceleration through the voltage on Electrode 3.

Because the integrand does not involve E_0, we may solve for ϕ by differentiating once with respect to E_0. Thus,

$$\frac{dQ}{dE_0} = -K\,[E_0 + E_a]\,S(E_0, E_a)\,\phi(E_0)$$

and

$$\phi(E_0) = -\frac{1}{K[E_0 + E_a]S(E_0, E_a)}\,\frac{dQ}{dE_0}\,.$$

The function $S(E_0, E_a)$ becomes the relative scintillation efficiency of the fluor if no deuterated foil is used. This would be the case for electron detection or if no attempt were made to discriminate between ion species. The same equation applies to electron detection, for which all electrode voltages would, of course, be reversed.

It was hoped that because of the probably very small entrance slit (say, about 0.020-in. diameter) required for detection of the particle flux from such devices as the Table Top machine, the relatively large aperture of the electrode system would eliminate secondary emission from Electrode 2, as well as minimize focusing and space-charge problems. The integral nature of the signal might yield considerably larger signals than a differential type of analyzer.

At this point the analyzer has been tested with a titanium deuteride stacked-washer source, located approximately 1 ft. from the entrance slit with no magnetic guide field. With a slit diameter of 0.030 in., and essentially no light pipe between the fluor and the photomultiplier located about 2 ft away, 100-v signals are observed for electrons with the RCA-6810 photomultiplier at 850 v (very low) and a final accelerating voltage of (+) 25 kv. With no deuterated foil in front of the fluor, pulses of the same size were observed for ions with a photomultiplier voltage of 1050 v and a final accelerating voltage of (-) 102 kv. It remains to be seen what effect a 1000-angstrom aluminum coating on the fluor (to prevent light from reaching the phototube directly from the source) will have on the signal from ions. The light pulse from the source at present limits the photomultiplier voltage to low values. Much of this light might be eliminated with a double slit system and operation of the source at considerably greater distances from the slit, as would normally be the case. The source was operated at a voltage of 10 kev and at a repetition rate of 15 sec.

A rough analysis of the ion energy distribution obtained from this source indicates that the distribution is peaked at about 100 ev, in agreement with the results shown by H. W. Bandel[9] for deuterons from this type of source, using the differential analyzer he developed. This result, and a similar result for the electron energy distribution, cannot be taken too seriously, however, until present plans for an electrolytic-tank study of equipotential distributions and particle trajectories is completed, along with electron-beam calibration of the analyzer. It is quite likely that with the present electrode configuration a potential saddle point on the axis in the region of the center of the repel electrode results in an effective repel voltage significantly smaller than the actual electrode voltage.

Conclusive tests of the ion-detection efficiency with deuterated foil in front of the fluor have not yet been made, because of some delay in obtaining a satisfactory thin foil.

A circuit is being designed which will provide a linear sawtooth voltage pulse of variable pulse width and repetition rate, to be applied to the repel electrode. This should permit the measurement of the particle energy distribution several times during the life of a plasma such as that in the Table Top machine.

6. PLASMA DIAGNOSTICS IN TABLE TOP

Thomas O. Passell*

Calorimetric measurements of the plasma escaping Table Top have been completed. The most useful data were obtained from calorimeters consisting of bare disc thermistors from 1 to 2 cm in diameter and from 0.75 to 1.5 mm thick. The uniformity of each particular type of thermistor was such that once the calibration constant was determined the calibrating heater was not required for future constructions. Constancy of the calibration constant was checked periodically by observing the calorimeter self-heating from the pulsed magnetic field of Table Top.

The calorimetric data analyzed thus far can be summarized as follows:

1. A typical average electron density in the 300-cm^3 compressed plasma spindle is 2×10^{12} e/cm^3 (assuming a mean electron energy of 10 kev). This average density is for a peak compression field at the median plane of 10.6 kG, mirror ratio of 2, axial injection 10 μsec before compression field pulse, electrically conducting vacuum system walls, 10 kv on injection source, and an initial dc magnetic field of 100 gauss. Peak density for these

[9] H. W. Bandel, Study of an Ion Energy Analyzer and its Application to Table Top Mirror Machine, Sylvania Electric Products, Inc., Microwave Physics Laboratory, Mountain View, California, December 31, 1959.

*Stanford Research Institute, Menlo Park, California.

conditions is 8×10^{12} e/cm^3 if scattering into the loss cone is controlled by background gas ($\propto n_e$). The peak density becomes 1.6×10^{13} if scattering is controlled by the compressed plasma itself ($\propto n_e^2$). Actual conditions lie somewhere between these two extremes.

2. Radial energy losses at the median plane divided by end energy losses are 0.1 to 0.2 for nonconducting vacuum system walls at zero dc field, compared with about 0.05 for conducting walls. For dc magnetic fields greater than 20 or 30 gauss each of these values decreased by about a factor of 10.

3. The radial distribution of the plasma exiting through the east mirror is less peaked at the magnetic axis for zero dc magnetic field than it is for 100 gauss dc magnetic field. For the conditions given above in the discussion of density, full width at half maximum is 4.6 cm for zero dc field and 2.8 cm for 100 gauss dc field. These conditions are observed at a position outside the mirror where the peak field is about 10% greater than at the median plane.

Detailed results of these studies are being prepared as a UCRL report.

Development continued on various facets of the problem of measuring ambipolar electric fields in Table Top by E×B deflection of a particle beam. Specifically, the thermal detection of a pulsed particle beam (electrons in this test) has proved feasible for beam pulses giving only 0.2 millijoule to a 0.5-cm diam by 1.9-mm-thick disk thermistor. A sensitivity of 0.01 millijoules can easily be obtained from smaller thermistors and higher voltages on the bridge measuring circuit. However, the 0.5-cm-diam thermistors have a thermal cooling time constant of about 7 seconds and the smaller ones will be 2 to 5 sec. Hence a multichannel recorder must be used to record the thermal transients on a row of such sensors arrayed along the expected beam deflection path. Since our present 12-channel recorder has a cycle time of 12 sec, some faster device must be used.

The lithium ion gun design is now essentially firm--simply a cathode and a Pierce ion-extracting electrode. A few problems remain to be solved to improve a lifetime and output of the hot anode. Work at Stanford University using the lithium mineral furnished by us has shown that this type of source simply combines a lithium gas supply with a high-work-function surface. For example, the beta-eucryptite mineral was placed at one end of a closed tube and heated separately from a porous tantalum plug at the other end. It was discovered that 10 ma/cm^2 of lithium ions could be obtained by proper separate adjustment of the temperatures of the eucryptite and porous plug respectively. Consideration is being given to means of avoiding the gradual poisoning of the tantalum plug due to the formation of oxides. The use of noble metals such as platinum is complicated by their tendency to flow at the 1200-to-1300°C operating temperatures, thus filling the pores of an initially porous plug. A possible solution to the problem may be in the use of alloys of platinum with 5 to 20% of iridium or rhenium. These alloys are more resistant to flow than pure platinum, while retaining platinum's nobility.

7. REJUVENATION OF ELECTRON MULTIPLIERS

James T. Mattingly

The gaseous-discharge rejuvenation of electron multipliers was found to be applicable to both silver-magnesium and copper-beryllium dynode multiple structures.[10] From an analysis of the data, it appeared that the actual rejuvenation was caused by a fast heating and cleaning of the multiplier structure. Although no temperatures were measured during the gaseous discharging of the structure, it is probable that the clean-up temperature in in the temperature range used in outgassing and activation of the structure.

A small cylindrical heater of tungsten wire in ceramic was made that fitted closely around the dynode structure inside the vacuum tank. Next to the structure itself was placed an iron-constantan thermocouple. The electron-multiplier structure was heated to about 400°C. There was no rejuvenation. The structure was heated at 400°C for a longer period. Still no rejuvenation occurred. Apparently the temperature used was too high in this case.

Another copper-beryllium structure that was being tested showed a large decrease in gain within a very short time in the test vacuum environment. An infrared lamp, placed outside the chamber, heated the glass vacuum vessel. The pyrex glass, by reradiation, heated the copper-beryllium structure immediately. An increase in gain was observed. This was repeated a number of times with success. Study of simple rejuvenation means will continue.

8. GRID SOURCE DEVELOPMENT

Frank J. Gordon

The ion source has now been in operation for approximately one month. In this time, the electronics and vacuum systems have been finished and changed where necessary.

We are having shakedown difficulties with the source, so that our detailed examination of various parameters has barely started. However, we have had 165 ma of protons on a 1-by-3-1/4-in. target 3 ft from the source.

This is enough to partially verify the plotted beam trajectories and make it appear that with proper neutralization there will be sufficient beam for meaningful experiments in ALICE. Naturally, we expect some increase in this beam with further optimization of parameters.

A special target for analyzing beam profile is in manufacture. Also in process are regulators to control ripple and drift in the magnet and high-voltage supplies.

---

[10] James T. Mattingly, Rejuvenation of Electron Multiplier Structures by Gaseous Discharge, UCRL-6204, in preparation.

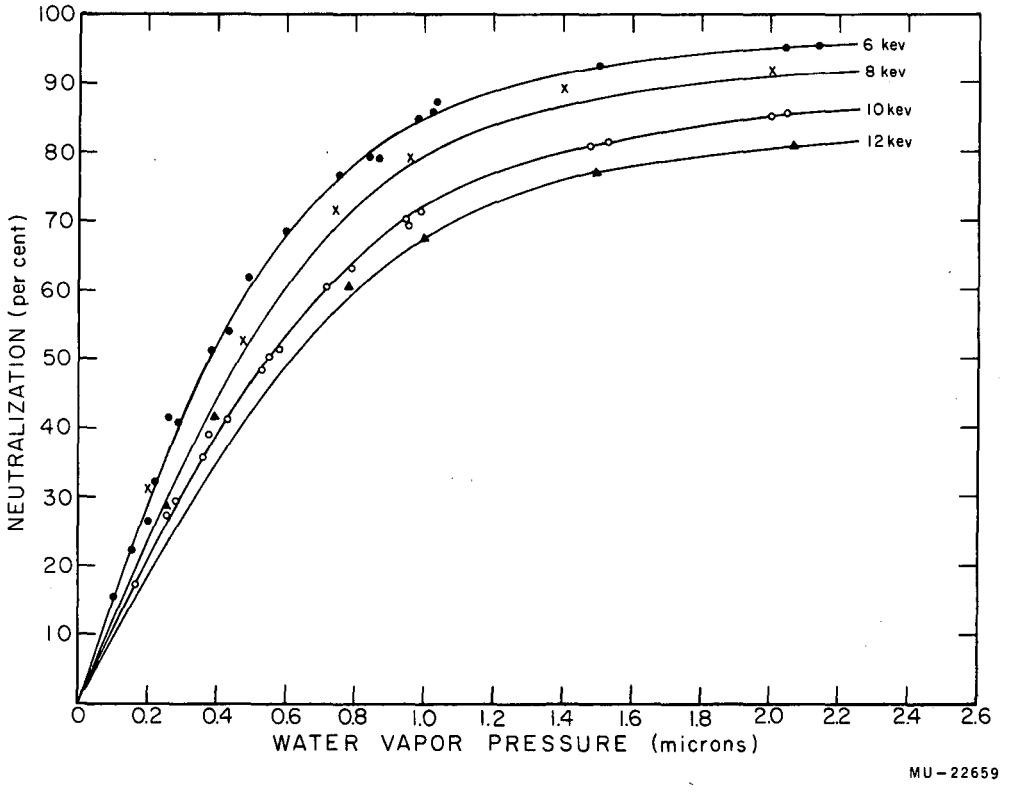

Fig. 8. Beam neutralization vs water vapor pressure.

9. BEAM NEUTRALIZATION

Charles C. Damm and Archer H. Futch

Hydrogen Neutralizer

The vacuum conditions in a system containing a hydrogen neutralizer must be determined experimentally. To test these conditions the hydrogen neutralizer, beam tube, and differential pumping chain including a simulated plasma chamber are being assembled. Delays have been encountered in the assembly, mainly because of faulty fabrication of the getter-pump leader boxes. Corrections have been made and reassembly is under way.

Water-Vapor Neutralizer

The maintenance of a suitably intense mass-separated beam of protons has proven to be a major problem in this experiment. Several changes in the source construction have been made, and a lens for refocusing of the beam after mass separation is now being installed.

With the beam available, data of a preliminary nature have been obtained. The neutralized beam fraction has been measured electrically by observation of the residual charged component on the direct or "in-line" target; or alternatively, by measuring the electrically deflected charged components on displaced targets. The charged components were deflected by a pair of charged plates. Both of these methods agree; but systematic drifts in the results occur, possibly due to a change in the neutralizing path length, or to a change in the vacuum-gauge calibration. Both these possibilities can be checked. Finally, the electrical beam measurements can be compared with a thermal calibration. The preliminary results, subject to some systematic corrections, are presented in Fig. 8. The path length of the beam through the water vapor is approximately 51 cm.

10. VACUUM AND SURFACE STUDIES

Angus L. Hunt, Charles C. Damm, and Earl C. Popp

An interesting result was obtained after molybdenum was deposited in a well-baked oil-free vacuum system. Also some observations were made with a mass spectrometer during the evaporation of molybdenum in an unbaked vacuum system.

Ionic and Sorption Pumping

As described in detail in the preceding report, a 70-liter vacuum chamber has been constructed using ionic and low-temperature sorption pumps.

After a bakeout at 200°C for 115 hr and cooling, the base pressure in this system was 4×10^{-9} mm Hg. Evaporation of one molybdenum filament reduced the indicated pressure to below 10^{-9} mm Hg. The expenditure of

two filaments reduced the two gauge readings to 2×10^{-10} mm Hg. The mass of molybdenum evaporated from the two filaments was 1.235 g.

The vacuum tank containing the molybdenum deposit then was isolated from the ionic pump by an all-metal valve. The pressure remained at 2×10^{-10} mm Hg, until the experiment was terminated at the end of 12 days. No pressure rise was found after the filaments of the two ionization gauges were turned off for periods as long as 15 hours, indicating that gauge pumping was not responsible for the static low pressure. No pressure bursts were observed as the filaments were turned on, indicating that the unknown residual gas components were not adsorbed on the cold gauge filaments.

The absence of a measurable pressure rise in the isolated tank can be attributed to the attainment of an unusually clean and leak-free system as well as to the gettering ability of the molybdenum deposit.

Gas Evolution During Evaporation of Molybdenum in an Unbaked System

The modified CEC mass spectrometer was attached to an 85-liter water-cooled stainless steel tank with a stainless tube 2 in. in diameter and 6 in. long. This tank, containing the filaments, was previously used for molybdenum evaporation and is pumped by a well-trapped MCF-300 oil diffusion pump. This system contains two nude ionization gauges and is completely bakable.

Because of the complexity of this experiment, the general experimental procedure should be described. Without baking the system and before any molybdenum was evaporated, mass spectra were obtained after the system had been pumped to 5×10^{-8} mm Hg. A molybdenum filament was outgassed at increasing power levels and the mass spectrum at each level recorded. To prevent a reduction in pressure and the resulting loss in sensitivity of the mass spectrometer during the initial evaporation of molybdenum, mass numbers 12 through 18 were scanned with the filament on. Then the filament was allowed to cool before power was restored and mass numbers 18 through 44 were scanned. The pressure was then reduced by 1-minute evaporations until the pressure would remain at 5×10^{-9} mm Hg during the evaporation. A low-pressure spectrum was obtained and a portion of it identified with the background gas in the mass-spectrometer tube. The system pressure was allowed to rise to 2×10^{-8} mm Hg over a 5-day period. Another mass spectrum was obtained as further molybdenum evaporation reduced the pressure to below 10^{-9} mm Hg. Fortunately, a mass spectrum was obtained as the molybdenum filament fused out. A new filament was degassed while the chamber walls were still active, causing a partial saturation of the previously deposited molybdenum. A correlation was obtained between the peak heights of the major degassed component and the total pressure in the system.

Before any molybdenum evaporation, at a pressure of 5×10^{-8} mm Hg, the peak heights were consistent with the presence of H_2, O_2, H_2, H_2O, A, CH_4 and CO.

Application of 50 amperes to the molybdenum filament produced an immediate increase in all peak heights and the appearance of additional mass units, indicating CO_2 and perhaps ethane in the system. The dominant component was water vapor.

Increasing the current in the filament to 75 amp gave a positive indication of ethane. The major ethane spectrum vanished as the outgassing continued.

As the current in the filament was increased to 100 amp--a power input of 400 watts--the ethane spectrum returned. After cooling and at 9×10^{-8} mm Hg, only the 15, 16, 17, 18, 28, and 44 peaks were detectable.

At a power input of 500 watts, evidence for CO or N_2, CO_2, CH_4, C_2H_6, A and H_2O appeared again. The system was pumped overnight by the diffusion pump and then showed only a trace of CO, H_2, CO_2 and a background of water vapor at a total pressure of 2×10^{-8} mm Hg. A 500-watt power input now produced no traces of ethane at a pressure of 8×10^{-7} mm Hg. On cooling and at a pressure of 4×10^{-8}, methane, water vapor, and CO_2 were detected. A check in the low-mass range showed no H_2 with the tank cold, but a large H_2 peak when 500 watts was applied to the molybdenum filament. The H_2 persisted for some minutes after the filament power was disconnected, indicating that little molybdenum had been evaporated.

As the filament power was increased to 750 watts and the molybdenum attained the temperature at which evaporation was rapid, a sweep was started at mass 12, when the pressure was 8.5×10^{-7} mm Hg; mass units 12, 13, 14, 15, 16, 17, and 18 were detected. Power was cut off after mass 18 and the sweep continued to mass 44 as the pressure dropped to 1.8×10^{-7}. No peaks were observed at mass numbers higher than 18.

In the next mass spectrum the power was increased to 750 watts as the sweep passed mass 18 and the pressures decreased from 1.2×10^{-7} to 4×10^{-8} as the sweep progressed to mass 44. Again no mass peaks were found at mass numbers larger than 18. When the filaments cooled only methane and water vapor were detectable at a pressure of 8×10^{-8} mm Hg.

The 750 watts was now applied coincident with a sweep through mass units 12 to 44. The pressure remained at about 4×10^{-8}, with only methane and water vapor detectable. By setting the mass spectrometer on the 16 and 18 peaks as 750 watts was applied to the molybdenum filament, only the 16 peaks were found to increase with the molybdenum filament temperature. This led to the hypothesis that at least part of the water vapor detected was due to background contamination in the mass spectrometer.

As the pressure decreased on subsequent molybdenum vaporizations to 6×10^{-9} mm Hg, only water vapor could be detected. The magnitude of the water vapor background could not be changed by intermittent operation of the ionization gauges. Heating the mass-spectrometer tube increased the 17 and 18 peak heights at the proper peak-height ratio for water vapor.

After a pressure rise to 1×10^{-8} mm Hg, due to saturation of the molybdenum deposit over a period of several days, 700 watts applied to the filament again produced an indication of some ethane by the appearance of small peaks at the 13.5 and 14 mass numbers during the initial part of the sweep when the total pressure was high. The total pressure dropped rapidly to 5×10^{-9}, so that the higher ethane mass units could not be observed. During the molybdenum evaporation at pressures of 5×10^{-9} no hydrogen could be detected even though the methane peaks were easily detectable. This observation was important in that it shows that the hydrogen produced with the methane was gettered so rapidly that it was not observable with the mass spectrometer, whereas methane was poorly gettered.

Degassing the ionization gauges--that is, heating the molybdenum grids--also produced methane approximately in the ratio of the indicated pressure increase. After molybdenum deposit was saturated, degassing the gauges produced detectable amounts of hydrogen.

After 5 days on the diffusion pumps with the molybdenum deposit saturated so that the total pressure rose to 2×10^{-8} mm Hg, methane and ethane were again produced in large quantities when the power was applied to the molybdenum filament. The methane peak heights followed the total pressure in the system as it cooled, after power removal, to a pressure of about 2×10^{-9} mm Hg. When the tank was completely cold at an indicated pressure of about 8×10^{-10} no methane could be detected.

Immediately before the filament fused out, methane was detectable at a pressure of 1.7×10^{-9}, but immediately after loss of the filament the methane peak disappeared at 8×10^{-10} mm Hg.

A new filament was connected immediately after evaporation of the first one, while the walls were active and the pressure in the system as indicated by the gauges was less than 10^{-9} mm Hg.

Application of the 750 watts produced ethane, methane, carbon dioxide, carbon monoxide, and a pressure rise to 8×10^{-8} mm Hg. The pressure dropped to 3×10^{-9} on cooling, and only methane could be detected. Successive applications of 630 watts, 500 watts, and 400 watts showed only the methane peak remaining, and decreasing with the power applied to total pressures as low as 2×10^{-9}.

After the experiment with the first filament, the data were consistent with the hypothesis that the trap on the diffusion pump was inadequate and that hydrocarbons collected on the walls and were cracked by the evaporated molybdenum or the hot molybdenum filament to produce ethane, methane, and hydrogen. The experience with the second filament showed that perhaps the wall contamination was not as important as the contamination on the filament or filament supports. The data from both filaments showed that methane was a major contaminating component in this unbaked system and that it was not rapidly adsorbed by the molybdenum deposit.

11. P-4 (STEADY-STATE PLASMA) SYSTEM

William L. Barr, Andrew L. Gardner, Laurence S. Hall, and Norman L. Oleson*

Circuitry

Modifications have been made to permit operation with either the cathode or the anode of the discharge chamber grounded. Operation with the anode grounded establishes a floating potential near ground for a probe in the outskirts of the plasma. This feature simplifies some of the probe measurements.

Rotating-Probe Measurements

Measurements have been made with the rotating probe assembly about half way along the system (at Port 4). These are still of a preliminary nature--the use of a more suitable ceramic insulator is planned for the probe construction and an improved measuring technique is being tested. However, these tests have shown that:

(a) The electron distribution is essentially Maxwellian all the way to the axis of the plasma column.

(b) The electron temperature on the axis is nearly 20 volts.

(c) The ion density measured by the probe is in good agreement with the electron-density measurement by microwave methods.

Figure 9 shows the approximate radial variation of electron temperature.

Probe measurements of the radial ion density are given in Fig. 10 (assuming only He^+ ions are present).

Microwave Measurement

Spherical lenses of lucite were used at the vertical arms of 4-in. glass pipe at Port 4 to focus a 4.65-mm microwave beam through the same plasma explored by the rotating probe. A phase shift of 175 deg was observed. Figure 10 shows a stepped contour, which approximates the ion distribution obtained by the probe measurements and which exactly yields the observed microwave phase shift. The remarkably close agreement with the probe measurements may be fortuitous. Such a comparison needs to be repeated when the probe technique has been further improved.

---

*U. S. Naval Postgraduate School, Monterey, California.

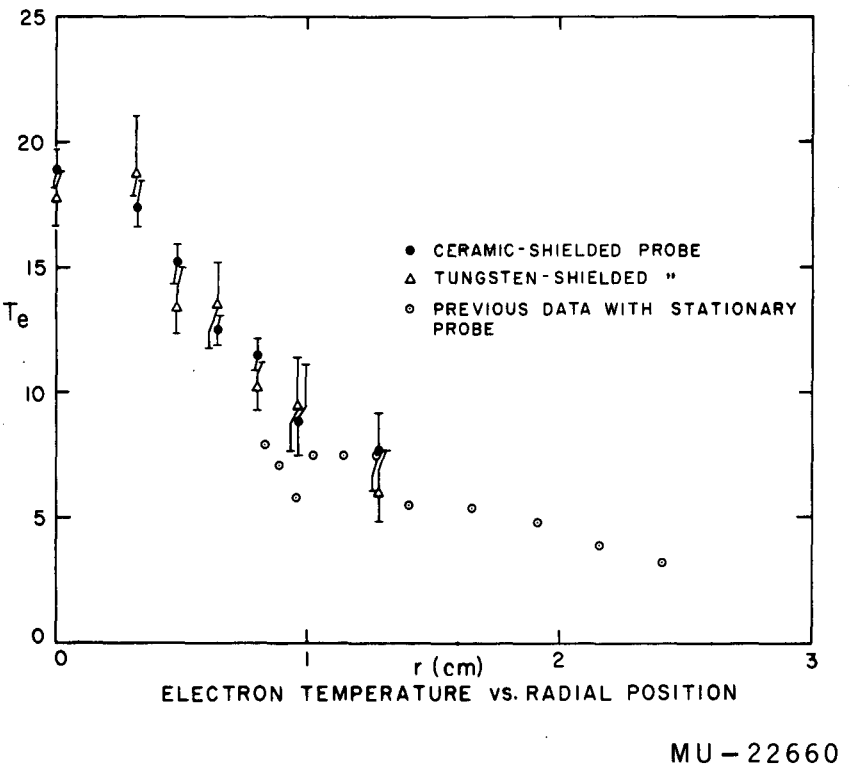

Fig. 9. Electron temperature vs radial position.

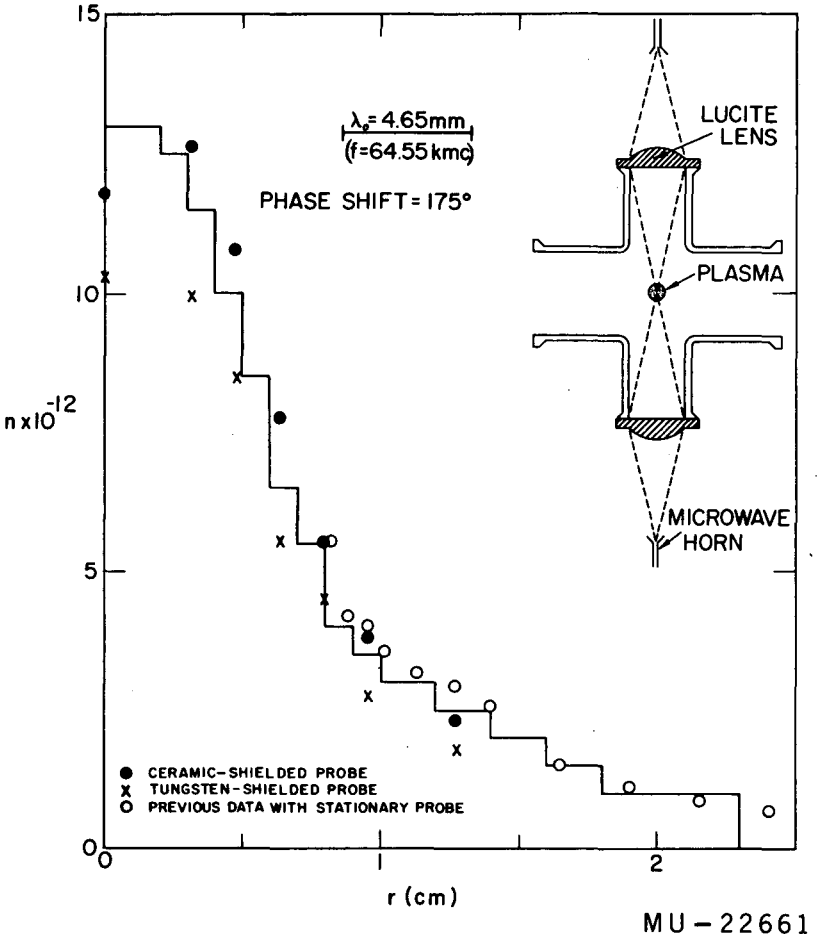

Fig. 10. Plasma density vs radius. Plotted points: ion density (probe data assuming only single ionization). Solid line: an empirical contour of electron density which yields the observed total microwave phase shift.

Optical Measurements

A study of the variation of the temperature of the He^+ ions along the axis of the P-4 system revealed an almost linear increase of temperature with distance from the PIG source. The lowest temperature observed was 1.1 ev, at the position of the window in the (PIG) discharge chamber. The highest was about 10 ev, at a point nearly midway between the two end (double) mirrors, where the field is again about 1 kG. The results are as follows.

Distance (feet)	Ion temperature (ev)	Comments
0	-	first cathode
1.5	1.1	
2.	-	second cathode
3.	2.7	1100 gauss, port No. 1
4.5	4.3	1100 gauss, port No. 2
6.	5.2	1100 gauss, port No. 3
7.5	6.7	1100 gauss, port No. 4
9.	7.6	1100 gauss, port No. 5
11.5	9.1	600 gauss, port No. 6
13	-	6000 gauss, mirror
15.3	10.1	approx 1000 gauss, port No. 7
16.8	-	6000 gauss, mirror

The study was made possible by reducing the bulkiness of the pressure-scanned interferometer used to measure temperature by Doppler broadening. Compactness of the optical system was gained by replacing the monochromator by a combination of optical filters to isolate the HeII spectral line at 4686A.

A further modification of the pressure-scanned interferometer has been tested and appears to be very promising. This modification will permit continuous monitoring of the ion temperature by displaying a rather crude profile of the ion spectrum line on an oscilloscope. Briefly, the technique is as follows. The Fabry-Perot interferometer is adjusted slightly wedge-shaped so that the interference pattern shifts by a little more than one-half fringe in going from one side to the other. A narrow collimated beam of light is then displaced (but not deviated in direction) by passing through a rotating 4-in. cube of lucite. This beam of light then passes through the combination of filters and through the interferometer. A lens focuses the fringe system on a diaphragm which intercepts all except the center spot. The light that passes through this diaphragm is detected by a photomultiplier tube, and the resulting signal is displayed on an oscilloscope. Thus, as the lucite cube rotates, the beam sweeps across the interferometer and scans a little more than half of a free spectral range. By adjusting the gas pressure in the interferometer, one can shift the range of scan to include a maximum and a minimum of intensity. The ratio of these two extremes is a measure of the line width, and, hence, of the ion temperature, if the width is due to Doppler broadening. By using two beams of light in order to observe the maximum and minimum simultaneously, one could observe the variation of the line width with time over very short intervals.

Ion Heating

The possibility of further elevating the ion temperature, in steady-state fashion, by a type of magnetic pumping is being given some consideration. If an order of magnitude could be gained by such a preheater the plasma would be interesting as the starting medium for a final high compression.

II. ASTRON PROGRAM

1. INTRODUCTION

Nicholas C. Christofilos

In the Astron program most of the effort of the group is devoted to building the Astron facility, which is expected to be ready at the end of 1961. This facility is divided into two component groups:

(a) Electron accelerator, 5 Mev, 200 amp, pulse length 0.3 μsec, 60 pps.

(b) Astron injection system and E-layer tank where the 5-Mev electrons will be injected and trapped to form the E layer.

Both component groups are proceeding in parallel. Most of the effort, however, is required in designing and testing the components of the electron accelerator. The electron gun that will accelerate the electrons up to 700 kev is now being assembled. However, tests will not start before February 1961 because the structural steel frame that will support the electron gun is expected to be in operation by June 1961. Thereafter each of the eight units of the accelerator will be installed, tested, and debugged. It is expected that by December 1961 the accelerator will be in operation at the full energy of 5 Mev. Therefore, according to this schedule, experiments pertinent to the Astron concept cannot be done before the end of 1961. For the interim some theoretical work is contemplated to clarify as much as possible the behavior of the E layer. The theoretical work Dr. Lewi Tonks was preparing in the self-consistent equilibrium solution on an infinite E layer is now completed. A report on the results of the computations will be issued soon and will be discussed in the next quarterly report.

A mathematical formulation to derive a self-consistent solution of the E layer of finite length has been prepared by Dr. Leslie Peck.[1] Dr. John Killeen is preparing the coding on the LARC. More detailed discussion on this work is in the Theoretical Section V. The formulation of this problem was very difficult. It was made possible by assuming monoenergetic electrons and very fast injection, namely to build up the layer in a few microseconds. However, the monoenergetic electrons will be all reflected at the same point, thus creating a singularity and possible blow-up of the layer. Therefore this formulation is considered as a first step which must be modified later in a more realistic way and which will be more consistent with the actual method of establishing the E layer, namely, to take into consideration the actual energy spread caused by scattering.

The stability of the E layer is an extremely difficult problem. An exact solution is rather impossible. However, attempts are made from time to time to solve this problem by assuming simplified models. The most recent work on the stability of the E layer is by V. Kelvin Neil (Section V). He assumes an infinitely thin layer. He finds that the condition for stability is

$$a^2 > 2 \pi r_e (n R/\gamma) [1 - (R/b)^2], \qquad (1)$$

[1] Consultant to Lawrence Radiation Laboratory, from Boston, Massachusetts.

where a is the half width of the velocity distribution of the electron (axial velocity spread), r_e the classical electron radius, R the radii of the E layer, b the radius of the E-layer tank, and n the electron density per unit area. For field reversal we have the conditions

$$2 \pi r_e n R/\gamma = 1 \quad . \tag{2}$$

Therefore

$$a^2 > [1 - (R/b)^2] \quad . \tag{3}$$

The ratio (R/b) in the Astron model is 0.7, whence

$$a^2 > 0.5. \tag{4}$$

This condition means that an axial velocity spread ± 0.7 c is required for stability. However, because of the drastic approximations made in these calculations whereby the layer is assumed infinitely thin, any favorable or unfavorable results are not too pertinent. The usefulness of these calculations is rather to serve as a first step to better approximations. The best answer, though, in the stability problem, rigorous without any doubts, will be the experimental evidence expected to be provided by the Astron facility.

Some results on the engineering aspects are described by W. A. S. Lamb in the accelerating column and by the Electrical Engineering group in their section of this report, on tests on thyratron tubes, the modulators, etc.

Because of the general interest in the stability of electron beams interacting with ionized gas, some thought is given to using the 5-Mev electron beam in a series of controlled experiments in which the interaction of a circular high-current (200 amp) relativistic electron beam will be studied. This matter will be discussed in more detail in the next quarterly report.

2. ASTRON ACCELERATOR COMPONENTS

W. A. S. Lamb

Two test assemblies of the 14-in. -diameter metal ceramic seals for the electron-gun accelerating column were received from the supplier. These test assemblies included the welding eyelet which joins the column at the center and mounts the unit in the gun assembly. These test assemblies were welded, demonstrating the successful design of the welding eyelet (Fig. 11).

Several 10-in. cathode assemblies were operated with appropriate gradient at 500 amp emission at a temperature of 830 °C. We now have a standard 10-in. cathode which will be used in the accelerator, as shown in Fig. 12.

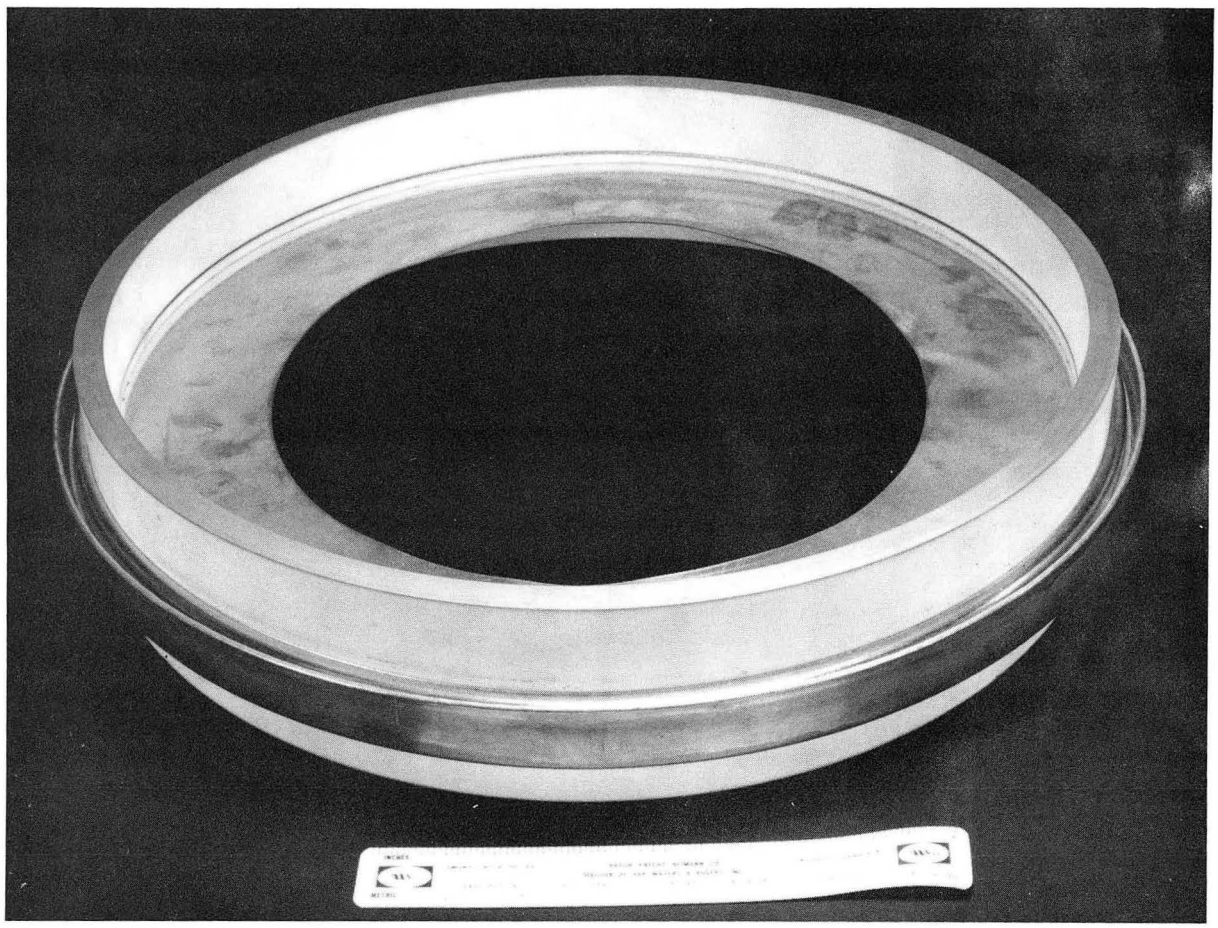

ZN-2706

Fig. 11. Fourteen-inch metal ceramic seal; welding eyelet test assembly.

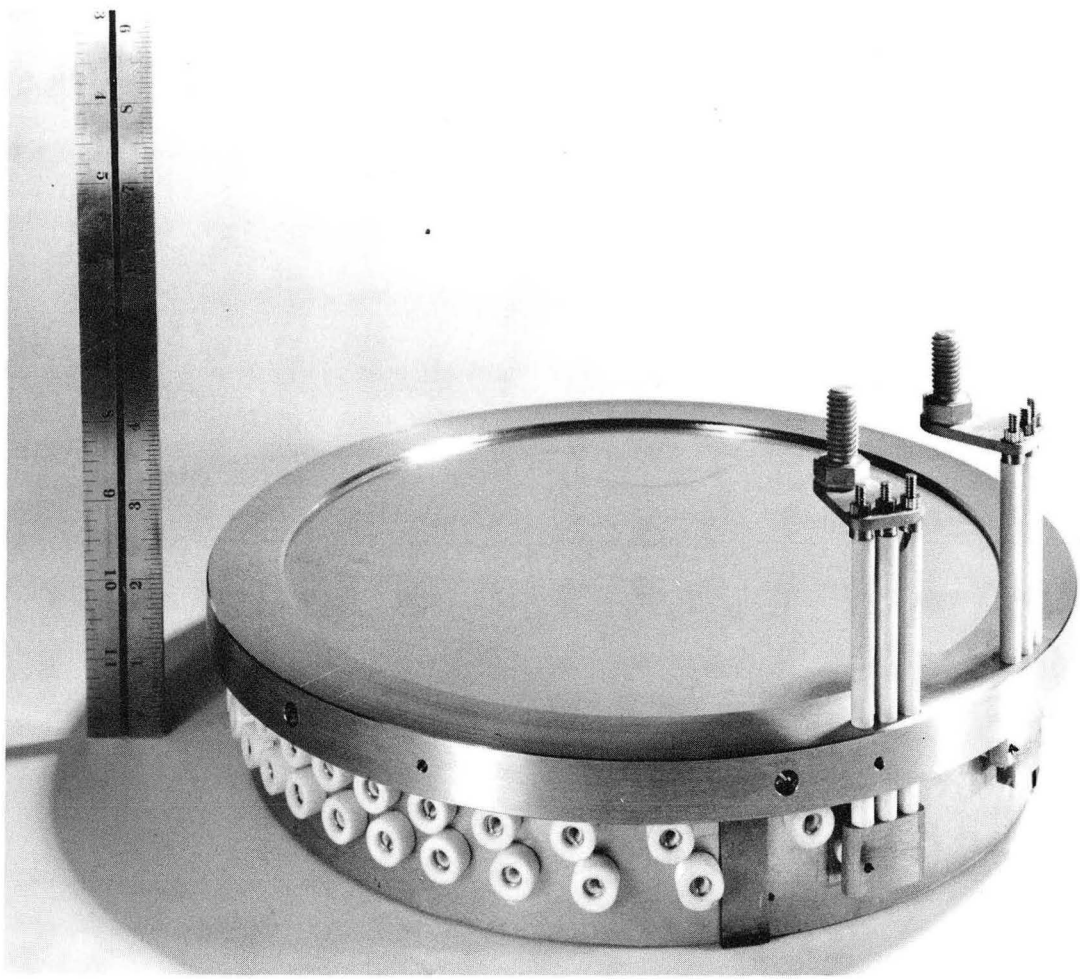

ZN-2707

Fig. 12. Ten-inch cathode heater assembly.

III. LIVERMORE PINCH PROGRAM

Dale H. Birdsall, Stirling A. Colgate, Harold P. Furth,
Fred O. Halliday, Charles W. Hartman, and Ross L. Spoerlein

1. SUMMARY

The 12-inch levitron vacuum system has been improved and is now meeting the experimental requirements. The diagnostic equipment for the levitron is also nearing completion.

The electron-beam pinch is being used to study hydromagnetic turbulence. Good consistency of results with magnetic probe data is found. Kerr-cell photographs being made of the discharge show cathode arc spots in deuterium but none in argon. No dependence of turbulence on arc-spot formation is found.

Recent measurements on the conical pinch show the efficiency of mass expulsion to be about 10%. Theoretical and experimental studies of cooperative phenomena in interpenetrating plasma streams are being made.

A 10-cm-diameter liquid sodium cusp experiment exhibits complete stability at high frequencies, but some instability when the rf skin depth is appreciable. The practical aspects of metal forming by strong transient magnetic fields are being pursued.

The "resistive" instability in sheet pinches (formation of streamers) has been shown to exist also in the E layer. Stability conditions have been calculated. A theory of aerodynamic skin friction has been developed.

2. ELECTRON-BEAM PINCH

In pinch research, the conventional test of the presence of instabilities is the shot-to-shot irreproducibility of magnetic probe traces. We have now checked this criterion with the electron-beam apparatus, and find the results largely consistent.

The "stabilized pinch" of Fig. 13 was used for this purpose. From the field distribution and the attached B_θ-probe signals taken at four different radii, one can see that the irreproducibility phenomenon starts earliest and is most pronounced at $r \approx 3$ cm, which is the region of maximum current density. The times of instability onset are seen to be roughly $r=0$ cm, $t=7.3$ μsec, $r = 1.5$ cm, $t = 4.5$ μsec; $r = 3$, $t = 3.8$; $r = 4.5$, $t = 4.8$. The electron beam is introduced either on center or at a radius $r_0 = 2.7$ cm at the cathode end, which corresponds to a B_z flux surface including 10^5 gauss cm^2. The radius at which the beam actually passes down most of the tube length in each of the three field distributions of Fig. 13 is indicated by a circle.

Figure 14 shows some typical electron-beam traces for 0.1-μsec beam pulses. When the beam is introduced on center, it is only slightly deflected during the first 6 μsec or so of the pinch. The minor departures from perfect centering seem to correspond to the small reproducible

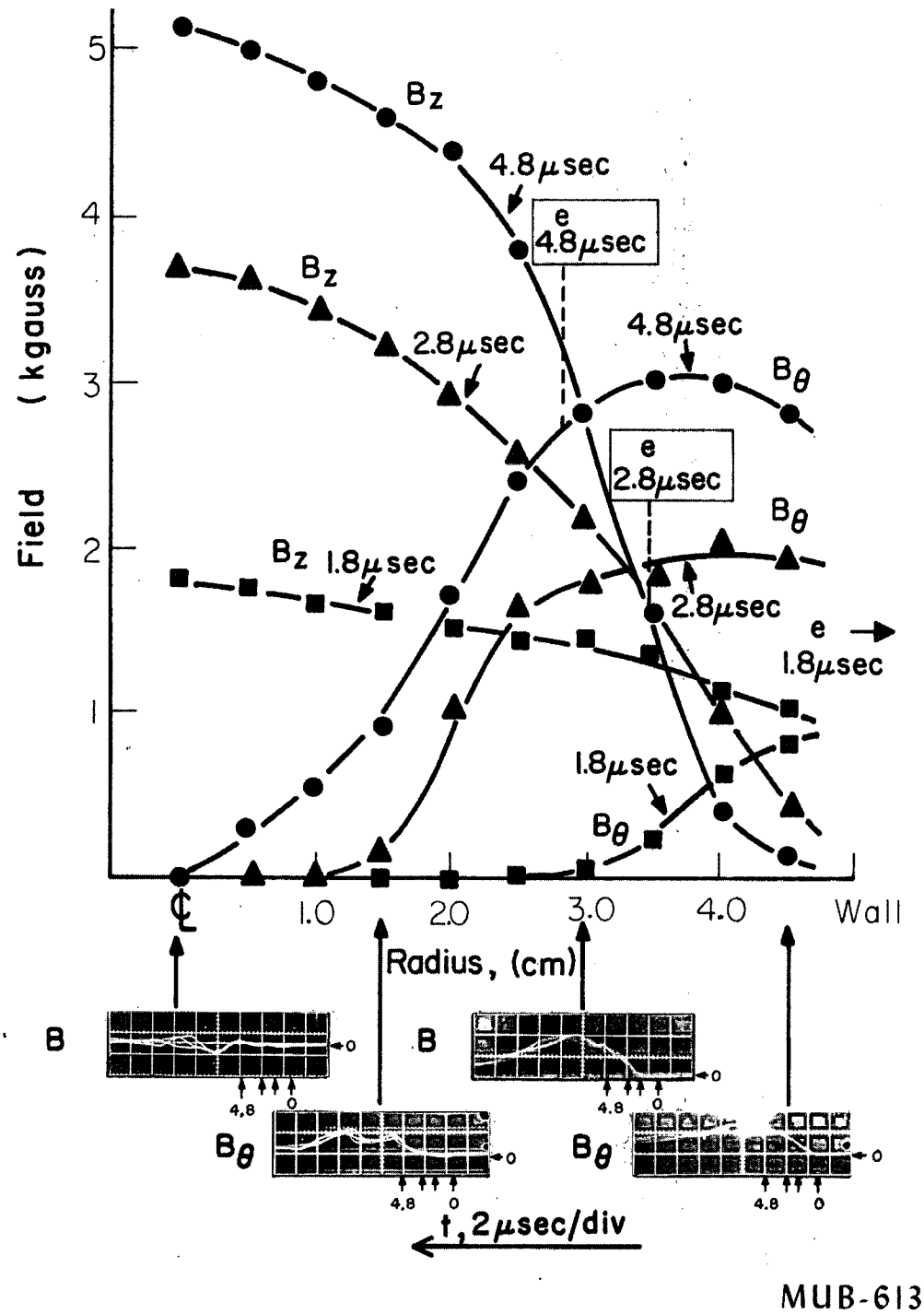

Fig. 13. Magnetic field configurations in electron-beam pinch at times 1.8, 2.8, and 4.8 μsec after pinch initiation. Radii at which the beam travels when injected at r_0 = 2.7 cm at electrode are shown by circles. Four typical B_θ probe traces are given.

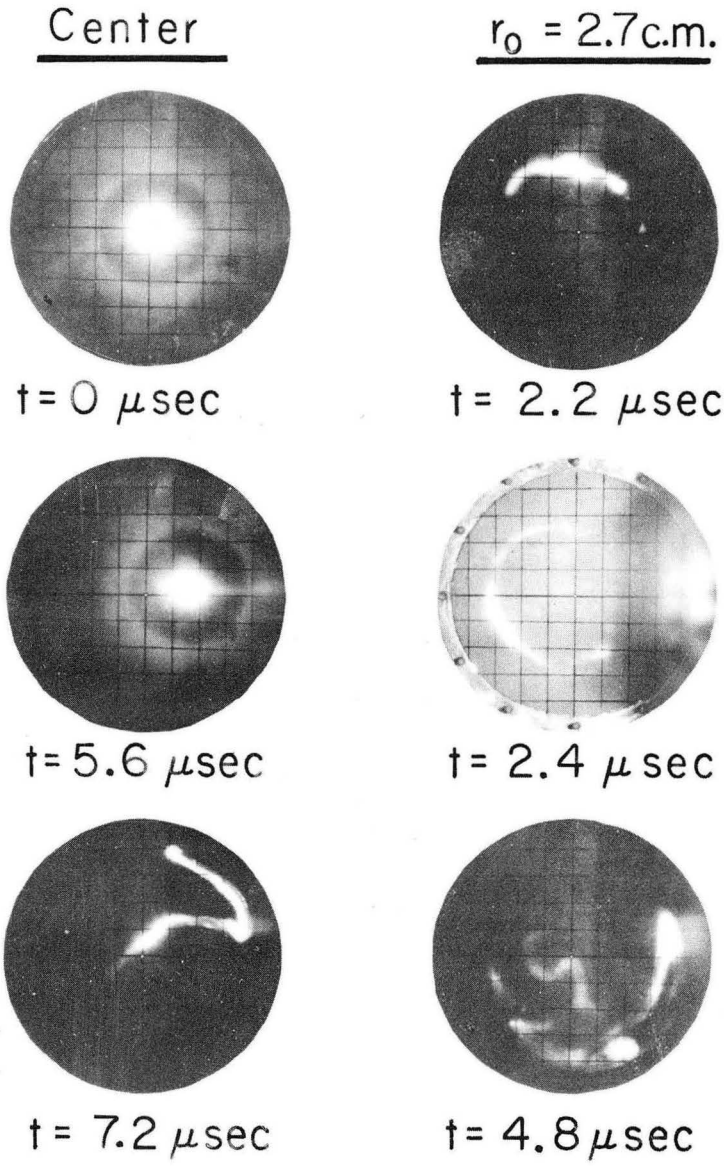

Fig. 14. Electron-beam traces with beam injected on center or at r_0 = 2.7 cm in configuration of Fig. 13.

asymmetries indicated by the B_θ probe at r = 0 (see Fig. 13). These features may be indicative of a slight "corkscrewing" of the discharge. At about 7 μsec, the beam trace becomes completely erratic (see Fig. 14), and this is just the time when the B_θ probe at r = 0 shows the onset of irreproducibility.

When the beam is introduced at r_0 = 2.7 cm, it does not appear on the phosphor until about 2.2 μsec, because prior to that the B_z-flux surface on which it moves intersects the tube wall. Unitl about 3.5 μsec, the beam traces out more or less accurate circles, but thereafter it becomes increasingly erratic (see Fig. 14). The earlier onset of B_θ-probe-signal irreproducibility in the current-carrying region is thus perfectly reflected in the earlier misbehavior of the electron beam when passing through there. The rapidity with which the beam traces out more or less regular circles prior to onset of the turbulent behavior is somewhat greater than what one would expect from the interdiffusion of B_θ and B_z fields, as measured with magnetic probes. This phenomenon may also reflect the presence of some reproducible gross "corkscrewing," even at early times in the pinch cycle.

This experiment serves, incidentally, to demonstrate in the most direct way that in a turbulent pinch the localization of particles on concentric flux surfaces breaks down. If the beam trace can wander erratically over the whole pinch cross section, then energetic particles are obviously not confined in the pinch. This confirms our previous argument based on the magnetic-probe results.

A problem that has proved to be of primary importance in beam probing is the distribution of current density at the cathode. As has been noted in earlier reports, various modifications of the cathode have changed drastically the characteristics of the beam injected on axis, the best centering of the beam being obtained with 12 symmetrical spark triggers. The screen anode enables one to photograph the cathode during the pinch cycle, and this technique has been used to explore cathode current distribution.

Figure 15 shows Kerr-cell photographs (exposure time = 0.1 μsec) of the cathode for various gases at 2, 5 and 7 μsec. Pinch radius is 5 cm, initial B_z = 1500 gauss (no program field), and current reaches a peak value of 125 ka at 6 μsec. The photographs shown were thus taken at I = 60, 110, and 110 ka respectively. The ring of triggers is clearly seen in the He 5-μsec photo. The main discharge light appears in the foreground. The trigger assembly and pinch light are also seen reflected in the tube wall.

Comparison of the three gases indicates a predominance of arc spots with D_2, some arc spots with He late in the cycle, and almost no arc spots with A. The surprising lack of arc spots with high-Z gases (air has no arc spots either) suggests a new discharge regime has been encountered, somewhat analogous to a high-pressure thermionic cathode discharge. It appears possible that suppression of arc spots can be attributed to intense photoemission supplying the necessary current at a much lower cathode-potential drop than that required to maintain an arc.

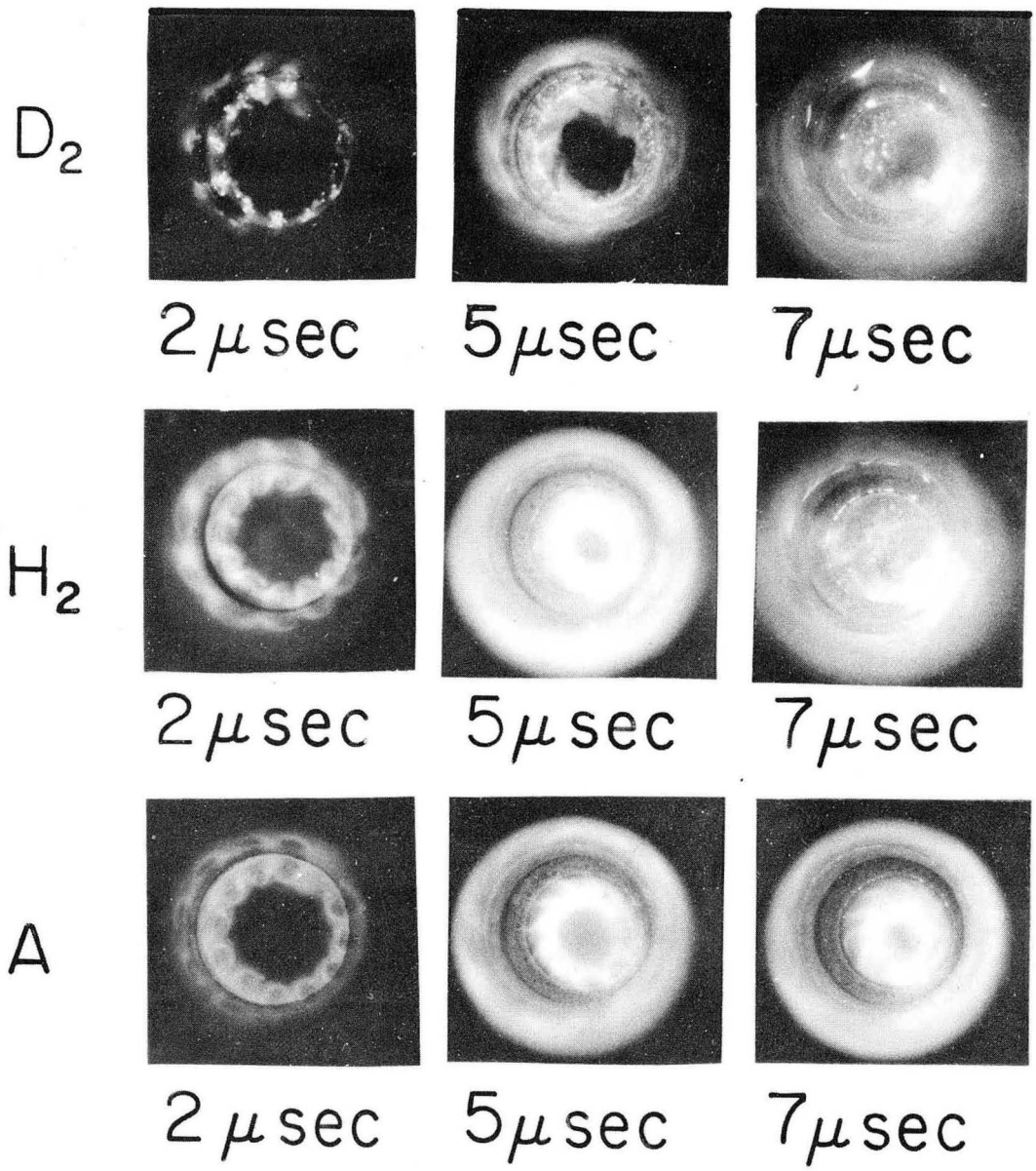

Fig. 15. Kerr-cell pictures of cathode of electron-beam pinch showing arc-spot behavior in three different gases.

The possibility of motion of the arc spots (in D_2) as current is redistributed at the cathode has been examined. It is observed that the spots generally do not move, but rather that changes in the current distribution are accompanied by formation of fresh spots.

The general filamentary character of the pinch, induced by the method of triggering, is observed most clearly in the argon photos. Some indication of this azimuthal periodicity has been observed with the electron beam.

A study was made of the possibility that arc spots induce the observed fluctuation of the electron-beam trace, either directly, by means of local magnetic field perturbations at the cathode, or indirectly, by inducing the turbulence of the discharge. To test the former possibility, a very short discharge tube was used. In that case, very little erratic behavior of the beam was found, even though the arc-spot phenomenon was the same as always. To test whether arc spots might be a causative agent for turbulence, alternative pinches were made in D_2 and He. In both cases there was comparable turbulence, wheras in He the arc spots were much less pronounced. It is tentatively concluded that arc spots are not responsible for the occurence of erratic behavior of the electron-beam probe.

3. CONICAL PINCH PLASMA ACCELERATOR

Lack of reproducibility in accelerator characteristics has been reduced from some 100% scatter to several tens of percent. Improved reproducibility is accomplished primarily by the installation in the cathode (exit electrode) of twelve symmetrically positioned spark triggers. In addition it is observed that, with multiple triggers, operation was unimpaired or slightly improved by removal of the preionization cycle.

Measurements of transient pressure build-up within the discharge chamber indicate that the empirically determined "best operation" parameters lead to firing the pinch when large pressure gradients exist in the discharge region and when the instantaneous pressure is roughly 10% of maximum. The efficiency of mass expulsion (10%) is considerably higher than previously estimated. A pinch chamber of new design will be used to investigate these properties more extensively. At present the most reliable operation is obtained at 10 to 20 μ D_2 pressure, resulting in accelerated plasma with 2 kv translational energy and 10^{14} to 10^{15} cm^{-3} density.

4. COLLISIONLESS PLASMA SHOCK

Theoretical

A machine program has been written to compute shock formation in a one-dimensional plasma. Only electrostatic forces are considered, and the plasma is idealized to a number of infinite sheets, similar to the model used by Dawson, [1] but with discrete ions as well as electrons.

[1] John M. Dawson, in Proceedings of Second Annual Meeting, Division of Plasma Physics, American Physical Society, Gatlinburg, Tenn. November 1960, p. 21.

At present the program is being checked, with 100 ion and electron sheets colliding with a like number. Careful consideration is being given to energy and momentum conservation, the effects of model discreteness, and sheet cross-over error.

Experimental

An experimental study of collisionless plasma shock formation, with no initial transverse magnetic field, has been initiated. Accelerated plasma produced with the conical pinch is allowed to collide with a stationary plasma in an axial collimating magnetic field.

Perturbation theory shows that the collective effects of the two-stream instability should pass into a nonlinear region after interpenetration of several ion plasma wave lengths ($\lambda = 2\pi v_0/\omega_{pi}$). For a typical plasma density of 5×10^{14} D^+/cm^3 and relative velocity of 5×19^7 cm/sec, traversal of the plasma through about 500 wave lengths is obtainable (50 cm axial drift). Therefore one might hope to investigate, in the nonlinear limit, the dynamic friction due to two-stream interaction.

Preliminary observations indicate some slowing down of the accelerated plasma in the manner expected; however, collisional processes have not yet been thoroughly evaluated.

5. LIQUID SODIUM EXPERIMENT

A larger model of the cusp geometry was made by using two coils 10 cm in diameter and with 5 to 7 cm spacing. When the sodium was confined at low frequency (1 kc) (see Fig. 16), it showed small random undulations, as well as standing flutes parallel to the magnetic field on the lower portion of cusp. The wave length of these disturbances (approx 1 cm) was sufficiently close to the magnetic skin depth (approx 1/2 cm) to cause one to suspect a "resistive" type of instability. Consequently, the cusp experiment was repeated with an intermittent high-frequency power source (approx 500 kc, 20 kw with pulses repeated at 120 per sec). The liquid in the cusp was in this case completely quiescent, with a perfectly smooth surface (skin depth $\approx$ 0.02 cm). Since the rf pressure was composed of a series of pulses occurring at a lower frequency even than in the 1-kc case, the possibility was excluded of explaining the instability in the 1-kc case as being of the Kruskal-Schwartzschild (accelerational) type. A tentative explanation has been proposed in terms of the local entrapment of field eddies in surface prominences of the fluid, with a resultant restoring force that is slightly phase-lagged, and therefore can result in overstability.

6. 12-INCH LEVITRON

The H-bar support of the copper liner edges has proved a satisfactory mechanical support of the vacuum load of the shell. A leaktight vacuum seal has been achieved by using silicone rubber.

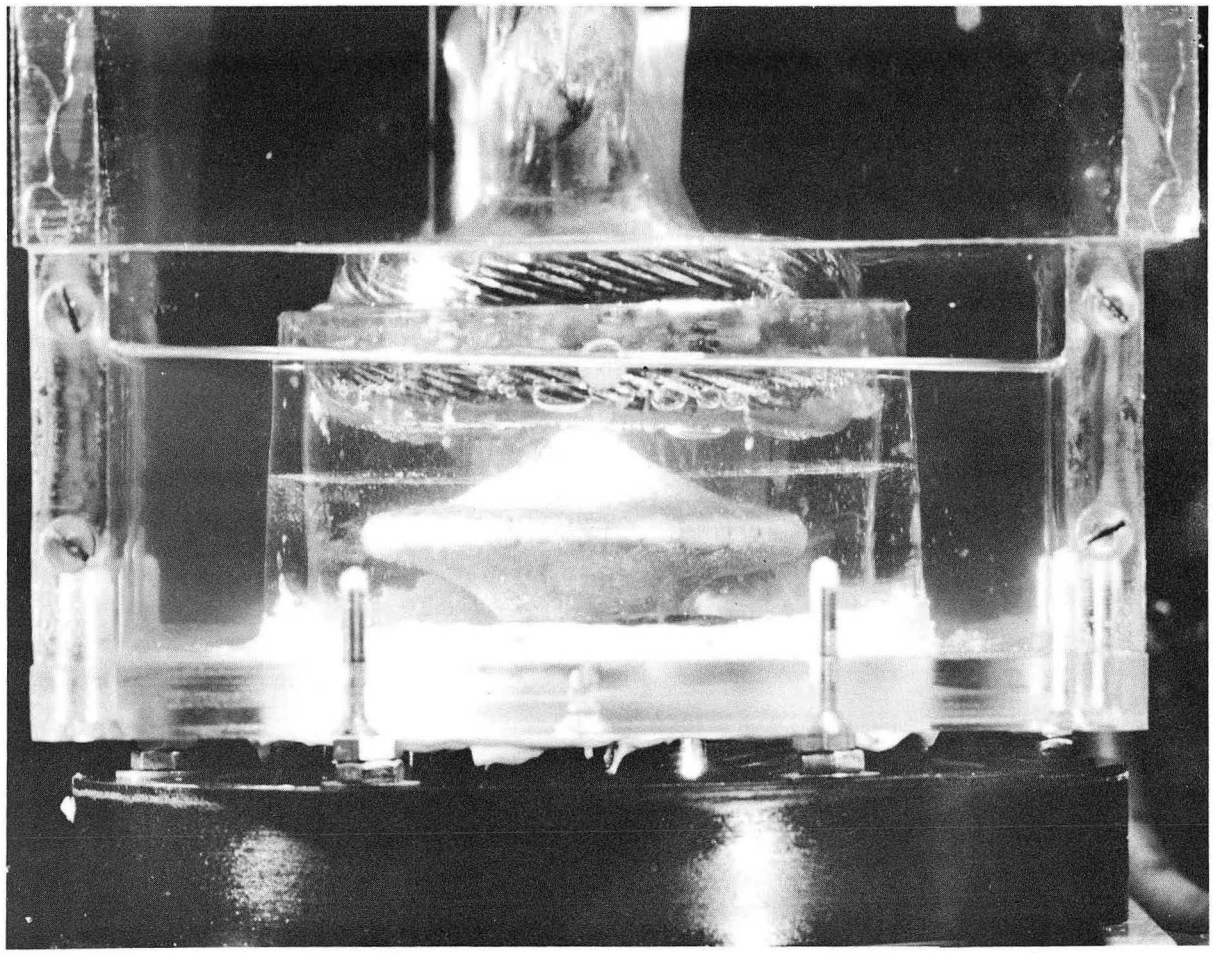

ZN-2704

Fig. 16. Liquid sodium confined in rf cusp fields.

The annular vacuum region between the inner and outer liners at first could not be held at less than about 20 microns pressure. This figure was unacceptable for obtaining a good vacuum in the inner region, because the pressure differential between the inner and outer regions was limited to a factor of 100 (because of leakage around the port seals). Outgassing of the epoxy-laminated insulating coating on the copper shell was suspected as causing the poor outer vacuum, and so the shell was heated to 350°F to bake out the plastic. As the vacuum did not improve, the levitron shell was dismantled. It was found that the epoxy laminate had delaminated from the copper and that, in addition, the epoxy had not "wetted" the glass cloth, so that a vast interconnected leak existed between the woven fibers. The laminated plastic was then completely stripped from the copper shells and they were recoated with an epoxy layer 0.030 in. thick (no glass cloth) and checked for voltage breakdown at 20 kv. The B_θ-field slit was similarly redone and checked for 20 kv voltage breakdown. (Maximum experimental voltages of 5 kv are expected.) The stainless steel liner was sealed (hard soldering) so as to become a "good" subsidiary vacuum vessel, supporting a 10^5 vacuum differential between the outer and inner volumes. (This arrangement would permit satisfactory "clean" pinch operation for an outer vacuum as poor as 1 mm.) The levitron shells with liner and core inside were reassembled and vacuum-sealed. The preliminary vacuum of 5 microns appears initially most encouraging, and the measured leak rate between the inner and outer volumes will permit a differential pressure ratio of 3×10^5.

Unfortunately, at the time of this writing a leak into the inner volume surrounding the core has been measured at 10^{-4} atmospheric cc/sec. Following the initial welding of the two core halves, the core had been pressurized with helium to 100 lb, then bagged and helium-leak checked, and finally sealed off with 1 atm of helium entrapped. If the leak rate does not increase, a satisfactory vacuum for pinch experiments (10^{-6} mm partial pressure) can be obtained; otherwise the core will be drilled and tapped in place, and fitted with a removable plug, so that the inside of the core can be evacuated when desired. This provision will insure that the outgassing of the core will not impose a lower limit on the attainable vacuum.

The following diagnostic equipment is completed:

1. Fast-read-out mass spectrometer.
2. Electron guns for aperture check.
3. High-current filaments (100-amp emission) for injection of electron ionizing current.
4. Filaments for molybdenum or titanium vacuum evaporation.
5. Removable finger trap.
6. Pulsed gas-input system.
7. Levitator position indicator.

The following equipment is partially completed:

1. High-voltage electron-gun injection (100 to 150 kev).
2. Plasma injector through diverter ports.
3. Scintillation counters for x-ray monitoring -- either of injected electron beam for aperture tests or for low-voltage (1-kev) plasma x rays; including combination of NaI and plastic phosphor with a thin Be window.

4. Threefold photomultiplier spectroscopic readout for monitoring the time history of individual lines as close as 1 A or as far as 2000 A apart, with 1/2-A resolution.

5. Core-position indicator.

6. Photomultiplier spectroscopic readout for whole or partial spectrum, 2000 to 6000 A maximum range, and with interferometer, 0.01 to 1 A minimum range; with 1% resolution over the scope sweep, repeated by a rotary mirror every 10 μsec.

The main condenser banks, lead connections, variable inductors, levitator and filament time sequences, rf-heating generator, and the cores for inductive isolation of signal and power leads are almost entirely completed, and await installation of the levitron for operation.

7. HIGH-FIELD RESEARCH

The basic ideas of the hydromagnetic analogue experiments in metal and of the high-field experimentation can be combined to advantage for the highly practical purpose of magnetic forming of metal. The forming of metal tubes against shaped insulating mandrils was first tried on a small scale in 1957. The technique has now been considerably refined. Some sample tubular forgings (1.5-in. aluminum alloy tubes pressed at 200 kilogauss for about 200 μsec) are shown in Fig. 17. A "magnetic hammer" has been used successfully to make flat stampings, such as ash trays, coin replicas, etc. The art of magnetic metal forming promises to furnish one of the most immediately useful applications of hydromagnetics.

A special 200-kilogauss magnet is being built for 1×1×4-in. emulsion stacks with a cross-field passage for a 3/4 in. beam. The purpose is to design a reliable and efficient beam-analyzing magnet to be usable (scaled up somewhat) in conjunction with the new 25-Bev accelerators, if desired.

An invited paper on the uses of high-field magnets in high-energy physics was written by Harold Furth for the 1960 International Conference on Instrumentation for High-Energy Physics, Berkeley, September 12-14, 1960, Paper I. 1.

8. THE UNIPOLAR GENERATOR

The unipolar generator has been pulsed in an open circuit, by discharging a 0.2-farad 400-v capacitor bank into the exciting-field winding (rise time, 50 msec). The voltage rise on the output showed a characteristic rise time of 0.15 sec but saturated at 2/3 of full voltage, owing to the finite volt-seconds from the capacitor. A series of such pulses changed the breakaway torque of the Unipolar operated as a motor, and in addition lowered the motoring torque. An internal short in the machine was developing, which turns out to have been the result of faulty insulation during manufacture. Repairs are under way. The preliminary pulse behavior indicated an entirely satisfactory rise time, so that a highly useful pulsed power source is still expected.

ZN-2703

Fig. 17. Magnetic forgings using 1.5-in. -diameter aluminum alloy tubes and 500- μsec half-cycle pulses at 200 kG.

9. THEORY

Calculations are being made on a "resistive" hydromagnetic instability which can result in the shredding of a sheet pinch into streamers directed along current flow lines. Details of the mathematical analysis, carried out in collaboration with John Killeen, are given elsewhere in this report (Section V, part 4).

The same type of instability might be expected to arise in a relativistic sheet pinch. A semi-intuitive analysis[2] based on examination of particle trajectories in a thin sheet yields the stability condition

$$a^2 \gamma k/2\pi r_e n_a > 1, \tag{1}$$

where a particle stream of velocity $\approx c$, with a small angular beam spread a, $f \propto \exp(-v^2/2 c^2 a^2)$, and density per unit area n_a is assumed. The instability wave number is given by k, and r_e is the classical electron radius. When two such streams are crossing at an angle $\theta \approx \pi/2$, the condition is modified to

$$\frac{a^2 \gamma k}{\pi r_e n_a} \left(1 + \frac{a^2}{\sin^2 \theta}\right) > 1, \tag{2}$$

where n_a is now the total density per unit area.

The intuitive analysis was checked by a somewhat more rigorous treatment using the Boltzmann equation, and the earlier results were confirmed. The treatment was then extended to allow for finite thickness of the layer and three-dimensional motion. The equilibrium volume-density distribution derived for a sheet E layer by Nicholas C. Christofilos was used:

$$n_v = h n_a/2(\cosh hz)^2 . \tag{3}$$

The stability criterion of Eq. (2), revised for the three-dimensional effects, can be expressed conveniently as

$$\frac{k}{2h} \left(1 + \frac{k}{h}\right) \left(1 + \frac{a^2}{\sin^2 \theta}\right) (1 + \cos\theta) > 1. \tag{4}$$

Thus the stability condition is violated for all wave lengths somewhat greater than the thickness of the E layer. For $k \ll h$, Eq. (4) reduces to

$$\frac{k}{2h} \left(1 + \frac{a^2}{\sin^2 \theta}\right) (1 + \cos\theta) > 1, \tag{5}$$

which is identical with Eq. (2), if one uses the relation between n_a and h specified by the equilibrium solution, allowing for the pressure of crossed beams.

---

[2] Harold P. Furth, On the Stability of Relativistic Sheet Pinches, UCID-4204, Oct. 1960.

When two infinitely conductive stabilizing walls are used at a distance $z = \pm d$ from the center of the E layer, one can show that the most unstable wave lengths still correspond to $k \to 0$. The stability condition in this limit involves knowledge of the zeros of fractional-order Legendre polynomials. This information was available in part from the work of David J. BenDaniel, and was supplemented with values kindly calculated by John Killeen. If, for instance, we have $a^2/\sin^2\theta \approx 0.1$ (which would correspond to standard Astron parameters) the stability condition is $d\,h < 1.3$. This value can only be considered approximate, however. For $d\,h < 1.3$, the equilibrium solution without walls (Eq. (3)) is obviously not very exact. (Note also that this entire calculation is good only for $a^2/\sin^2\theta \ll 1$.) The thin-E-layer treatment with stabilizing walls yields for Eq. (2),

$$\frac{k}{2h} \coth (dk) \left(1 + \frac{a^2}{\sin^2\theta}\right) (1 + \cos\theta) > 1. \tag{6}$$

This stability condition requires somewhat smaller values of d for stability than come out of the thick-E-layer analysis.

The preceding results have greatly benefited in credibility from the elegant and rigorous analysis of the thin-E-layer problem by V. Kelvin Neil (Section V, Part 6). Neil confirms Eq. (1), and in addition obtains instability growth rates. His solution for the thin E layer in cylindrical geometry allows us to relate the quantity d in Eq. (6) to an equivalent E layer with radius R and stabilizing-shell radius b:

$$d = R[1 - (R/b)^2]. \tag{7}$$

For $b^2 = 2R^2$, this gives, for instance, $d = R/2$. Applying this value somewhat crudely to the plane thick-E-layer calculation, one obtains $h R < 2.6$. Equation (7) applies only to the special case in which the beam is purely rotational. The more realistic case of a helical beam is still to be calculated. A feature of interest here is that "streamers" that are uniform along the beam direction (the case being considered) can exist only when $1/k$ is less than the pitch of the helical beam. For $\theta = 90$ deg, we have thus $k > 1/R$. This limit provides a slight stabilizing factor. On the other hand, the configuration with a helix of finite pitch is less advantageous from the point of view of magnetic restoring forces than is the purely rotational configuration, particularly in the case $b/R \to \infty$.

Our tentative conclusions in regard to the "streamer" instability in Astron are therefore: (a) the instability mode exists, just as it does in ordinary resistive sheet pinches; and (b) stabilization can be effected only by bringing conductive walls very close to the E layer. Richard F. Post has pointed out to us the great resemblance between the "streamer" instability and the "mirror instability" which occurs in mirror machines with excessive anisotropy in velocity space. Thus the present calculations, which were originally prompted by observations on liquid sodium pinches, furnish a fine illustration of the underlying unity of research in plasma physics.

A theory of aerodynamic skin friction has been derived,[3] in which the turbulent boundary layer is obtained on a deductive basis, starting with the concept of particle mean free paths.

It is shown the viscous damping of the minimum-size vortex determines the dimension of the laminar sublayer, which is approx $50 \lambda \frac{c}{u}$, where λ = collision mean free path, c = local sound speed, u = surface velocity of laminar sublayer. The concept of maximum momentum transport leads to the requirement of persistence of the maximum-angular-momentum vortex, which in turn results in the well-known logarithmic velocity profile. The combination of logarithmic velocity profile and laminar sublayer stress leads directly to turbulent boundary-layer growth, and a drag coefficient in agreement with experiment.

[3] Stirling A. Colgate, Aerodynamic Turbulent Skin Friction, UCRL-6256, Feb. 1961 (to be submitted to Physics of Fluids).

IV. BERKELEY PLASMA RESEARCH

1. SHEET PINCH STUDIES

Oscar A. Anderson

Stability theory for resistive plasmas has been recently developed by Harold P. Furth. His preliminary report showed that pinch-type devices are susceptible to neutral-point instability, in which resistive diffusion causes an initially stable field configuration to become unstable. [1] The tubular pinch (Triax) was considered especially susceptible to this resistive instability because of its large over-all dimension. A subsequent note suggested that the resistive instability and the rip which it generates could be utilized for plasma-acceleration purposes. [2]

These possibilities have been checked in an experiment with the 8×10 Triax. In order to promote the rip instability, quartz rods running the length of the tube were installed as shown in Fig. 18a. When the discharge was fired, these rods produced, indirectly, a magnetic field perturbation similar to the type considered in the theory. (There were also perturbations in the plasma configuration and velocity; fortunately these complications should help to promote the ripping, rather than hinder it.) Streak photographs were used to study the plasma motion. Three slits, spaced at 2.5-cm intervals, were provided in the tube electrode for this purpose (see Fig. 18b). Each slit revealed the local motion in the radial direction; comparison between slits revealed any azimuthal motion. Figure 19 shows the results. The relative absence of light in the slit directly over the rods implies that a rip was generated, but the almost normal pinches displayed in the other slits shows that the rip propagation was negligible on the 5-μsec time scale of the discharge. (The middle slit shows the pinch starting to broaden after about 3 μsec, but this is probably a different effect, perhaps caused by migration of impurities from the rods. A rip would be expected to arrive much sooner.)

Experimentally, then, no violent resistive instability occurs in the dynamic tubular pinch, even when deliberately induced. Of course, the short time scale of the discharge may be an important factor in explaining this. However, an investigation[3] of the original theory has shown that its conclusions, [1] although valid when the plasma is thick compared with a perturbation wave length, should be modified when the plasma is thin. In the Triax the plasma width (about 0.5 cm) becomes more significant than its circumference (80 cm). The severity of the rip effect should be less than the original estimates would indicate, since they were based only on the 80-cm dimension.

---

[1] Harold P. Furth, Resistive Relaxation of Perturbed Current Layers, UCRL-6071-T, July 1960.

[2] Harold P. Furth, An Instability-Type Plasma Accelerator, UCRL-6118-T, Aug. 1960.

[3] Oscar A. Anderson, Relaxation of Perturbed Current in Thin Conducting Sheet, Engineering Note 4519-41 CV-1, Dec. 29, 1960.

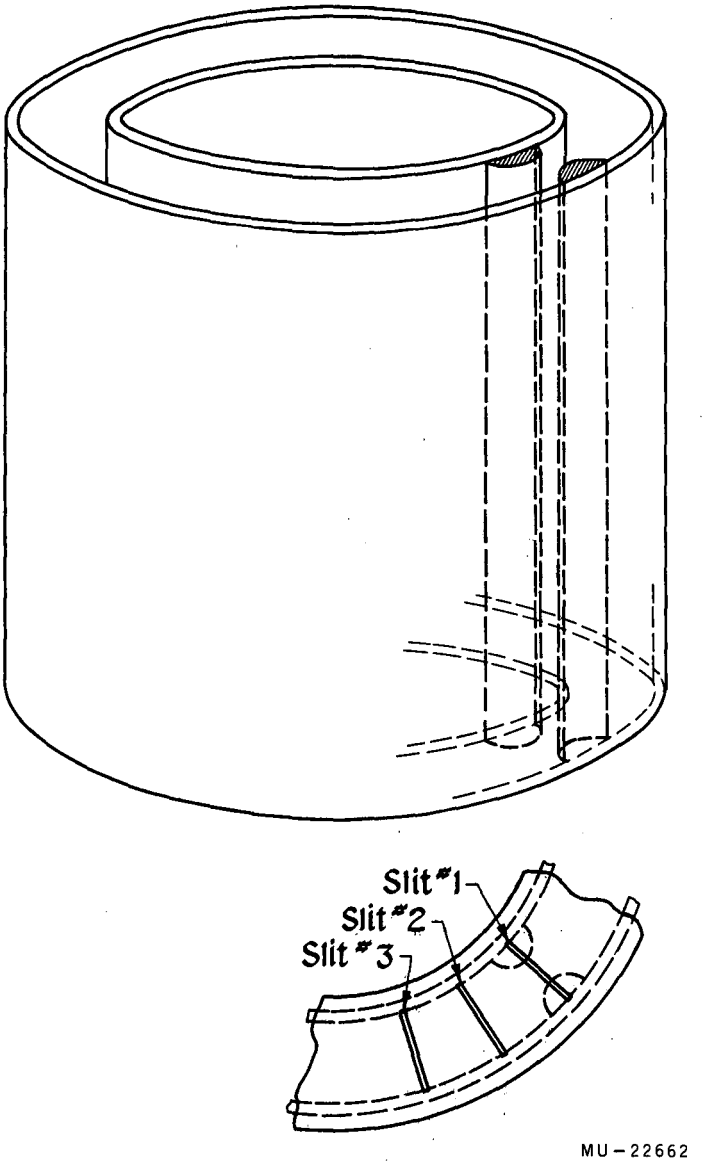

Fig. 18. (a) Rip-instability experiment. Quartz rods which produce perturbations are shown placed in 8×10 Triax. (Only the insulators are shown.)
(b) Slits for observing plasma motion in rip-instability experiment.

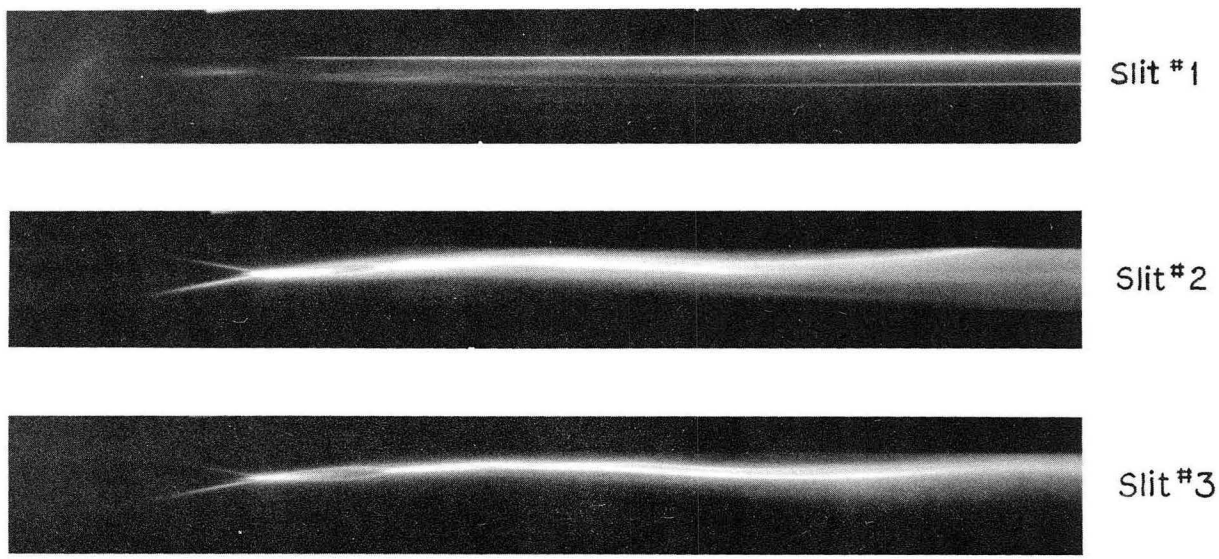

Fig. 19. Streak photographs obtained with slits shown in Fig. 18(b). Tube was operated on 200-μf condenser bank at 15 kv, with 830 μ of D_2. Half-cycle time, 5 μsec; duration of streak, 5 μsec.

So far, only the resistive diffusion part of the problem has actually been calculated, so questions about stability have been answered somewhat vaguely. A machine calculation which will give details such as instability growth rates, taking plasma thickness into account, was begun several months ago by Harold P. Furth and John Killeen. Its progress is described in Section V, Paper 4, in this report. When these theoretical results are available, further experiments may be planned.

Operation of the 6×10 Triax on the 200-μf bank has just begun. This work will be described, along with some 8×10 Triax results, in the next quarterly report.

2. HOMOPOLAR PROGRAM

Klaus Halbach, G. Donald Paxson, and Didier Veron*

During the quarter just ended, Homopolar IV went into full operation for the first time, although only during a short period, because of a break of the puff valve after a total of 490 shots and, subsequently, a leak in the vacuum system. During normal operation the voltage across the machine broke down within 0.1 μsec from 50 kv (1.5 μf with 5 ohms in series) to 25 kv about 50 μsec after the puff valve opened to fill the center region of the machine with 10 micron liters of deuterium. The back voltage of 25 kv was held by the machine for approximately 3 μsec, thereafter decaying with a time constant of 5 μsec. This back voltage together with an applied magnetic field of 20 kG indicates a rotational velocity of 3×10^5 m/sec, about ten times the Alfvén ceiling encountered in the previous homopolar machines. The velocity of 3×10^5 m/sec needs, of course, a more solid diagnostic backing (Doppler-shift measurements) in order that one can quote this number seriously.

That the machine can hold the back voltage for only 2 μsec, a time much too short for the gas to reach the insulators, suggests that something unforeseen and unwanted causes this breakdown. In order to be able to check whether or not this is an insulator breakdown, we have incorporated a probe well in one insulator, and we hope to get some useful data soon.

During operation another additional device proved to be necessary to insure reliable operation of the Homopolar IV; after many discharges the machine failed to break down properly after the release of gas by the puff valve, probably because of a clean-up process at the walls. This could be remedied by putting a spark-plug-like firing device at the outer liner in the center region of the machine.

Although the physical results we obtained so far are meager, we learned many things that will help in the design of Homopolar V. This machine, which we expect to be ready for testing by the end of January, will have the following improved or additional features:

---

*Visitor from Commissariat a l'Energie Atomique, Fontenay-aux-Roses, France.

(a) Bakability. Being able to outgas the machine at 200° C will allow us to obtain a much lower gas pressure. This in turn may enable us to leave the main bank on the machine continuously.

(b) Improved puff valve. This valve will have about the same performance characteristics as the present one, but we hope to reduce the valve failures to a minimum.

(c) Current buttons for the measurement of the current distribution both axially and azimuthally.

(d) Optical window in the center region. This will allow us to make the urgently needed Doppler-shift measurements.

(e) Provisions to operate a PIG discharge in the puff valve region. This replacement of the presently used spark plug initiator should work much more satisfactorily, from both the physical and the technical points of view.

Still another machine is being seriously considered as a promising future project in case the results obtained with Homopolar IV and V are encouraging. The basic design of this machine is represented in Fig. 20. During the first phase of operation each half of this machine operates like the present puffatron: gas is released simultaneously from the two puff valves at the ends of the two center rods. Application of two capacitor banks (charged oppositely with respect to the liner) in the presence of a longitudinal mirror field then produces two counterrotating plasma bodies with high rotational velocities. In the second phase, these two plasma bodies are brought to the center region of the machine, where they have no contact with any walls. It is hoped that after the two counterrotating plasma bodies make contact with each other, a large fraction of their rotational energy will be converted into thermal energy, thus producing a high-temperature plasma.

3. HYDROMAGNETIC WAVE AND CYCLOTRON HEATING

Hot House I

William S. Cooper, III, Alan W. DeSilva, and John M. Wilcox

During this quarter we have observed, in the hydromagnetic waveguide, reflections of Alfvén waves from high- and low-impedance boundaries and from a plasma–neutral gas interface. The variation of the wave magnetic field with radius has also been measured under various conditions, and comparisons have been made with theory.[4,5]

[4] W. A. Newcomb, in Magnetohydrodynamics (Stanford University Press, Stanford, California, 1957) p. 109).

[5] Alan W. DeSilva, William S. Cooper III, and John M. Wilcox, Alfvén Wave Reflections and Propagation Modes, UCRL-9496, Feb. 1961.

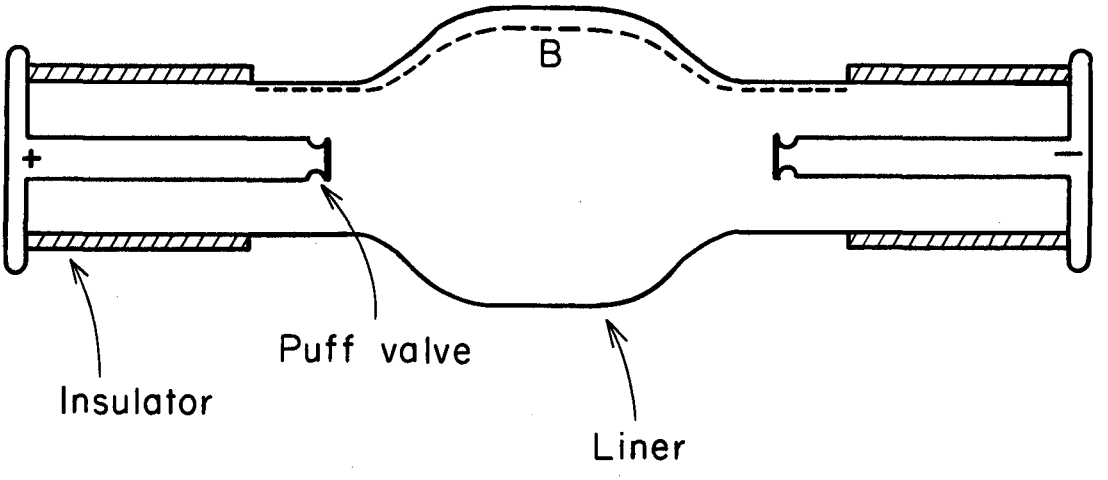

MU-22697

Fig. 20. Double-ended Puffatron.

The experimental geometry is shown in Fig. 21. The preparation of the plasma with which we work was described in an earlier quarterly report (UCRL-9243, June 1960). The plasma ion density measurements were reported in UCRL-9393 (Sept. 1960). At the time our wave measurements are made, the ion density is $> 5\times10^{15}$ cm^{-3}, corresponding to > 80% ionization of the neutral hydrogen gas initially within the tube. Plasma temperature is estimated from observed Alfvén wave damping to be about 1 ev.

Reflections of Alfvén waves have been observed from an insulating end plate, from a conducting end plate, and from a plasma–neutral gas interface. The phase relationship between incident and reflected wave fields at the boundary surface can be predicted easily from an examination of the theory.[5] For an insulating boundary the axial current density j_z associated with the wave at the boundary is zero. Theory then shows that the azimuthal magnetic field b_θ should reflect out of phase and the radial electric field E_r should reflect in phase. A conducting boundary, characterized by $E_r = 0$ at the boundary, leads to the opposite conditions: b_θ reflects in phase and E_r reflects out of phase.

Figure 22 shows $V = \int E_r\, dr$ (top trace) and b_θ (bottom trace) for the case in which a wave is reflected from a pyrex end plate at the far end of the tube. The voltage V is measured between the molybdenum electrode and the copper tube at the driving end of the tube (left side of Fig. 21) and the wave magnetic field is measured with a magnetic probe 13 cm from the driving end (not shown in Fig. 21). Thus we first see the signal from the initial wave, and then, after a time delay corresponding to two transits of the tube with a velocity equal to the Alfvén velocity, we see the signal from the reflected wave. The voltage, E_r reflects in phase and the magnetic field b_θ out of phase, as expected.

We next inserted a copper end plate in order to demonstrate reflections from a conducting boundary. The results shown in Fig. 23 were obtained; i.e., the phase relations are appropriate to a reflection from an insulating boundary. At this point we must consider the procedure for plasma preparation. After the tube is filled with plasma the ionizing current is turned off. With no external current flowing the plasma might form an insulating layer at the wall surfaces giving rise to the observed reflection. If the large ionizing current were to continue to flow this insulating layer might be removed, so that the plasma would be in electrical contact with the copper plate. We therefore reflected a wave from the copper end plate while the ionizing current was flowing and obtained the results shown in Fig. 24. The electric field E_r now changes phase on reflection and the magnetic field b_θ does not, as predicted for a conducting boundary.

We have also observed reflection of Alfvén waves from a plasma–neutral gas interface. If the ionizing current is turned off (crowbarred) when the ionizing shock wave is part way down the tube we have a tube partly filled with a highly ionized plasma and partly filled with neutral gas (or at least with gas with a very low degree of ionization). Under such conditions the wave reflections shown in Fig. 25 were obtained, which have the expected phase relations for a nonconducting boundary. The ionizing current was stopped when the ionizing shock had just reached a radial current probe

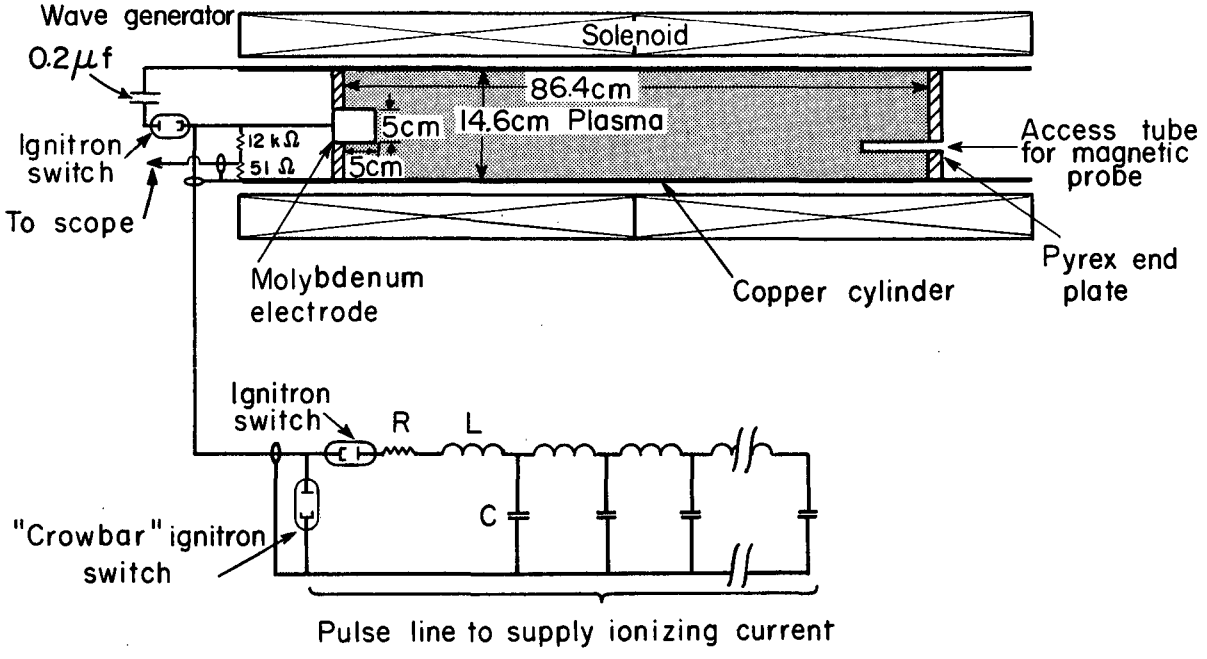

Fig. 21. Experimental geometry.

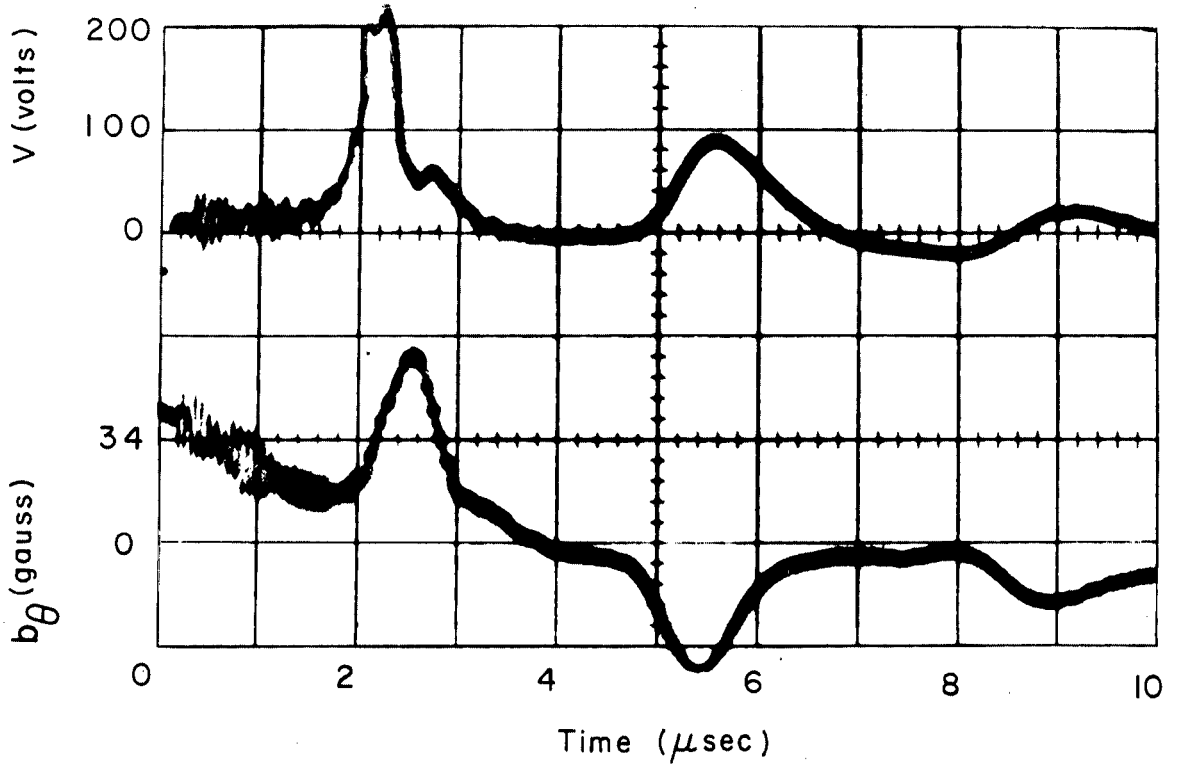

ZN-2622

Fig. 22. Oscillogram showing reflection from a pyrex end plate. Upper trace is voltage measured between the copper cylinder and the coaxial electrode at the driving end. Lower trace is azimuthal magnetic field measured with a probe located 13 cm from the driving end (not shown in Fig. 21). The first pulse is the induced wave, and the first reflection occurs about 3.5 μsec later on the voltage trace, corresponding to two transits through the tube at the Alfvén speed. The voltage reflects in phase, the magnetic field out of phase, in accord with theory for a high-impedance boundary.

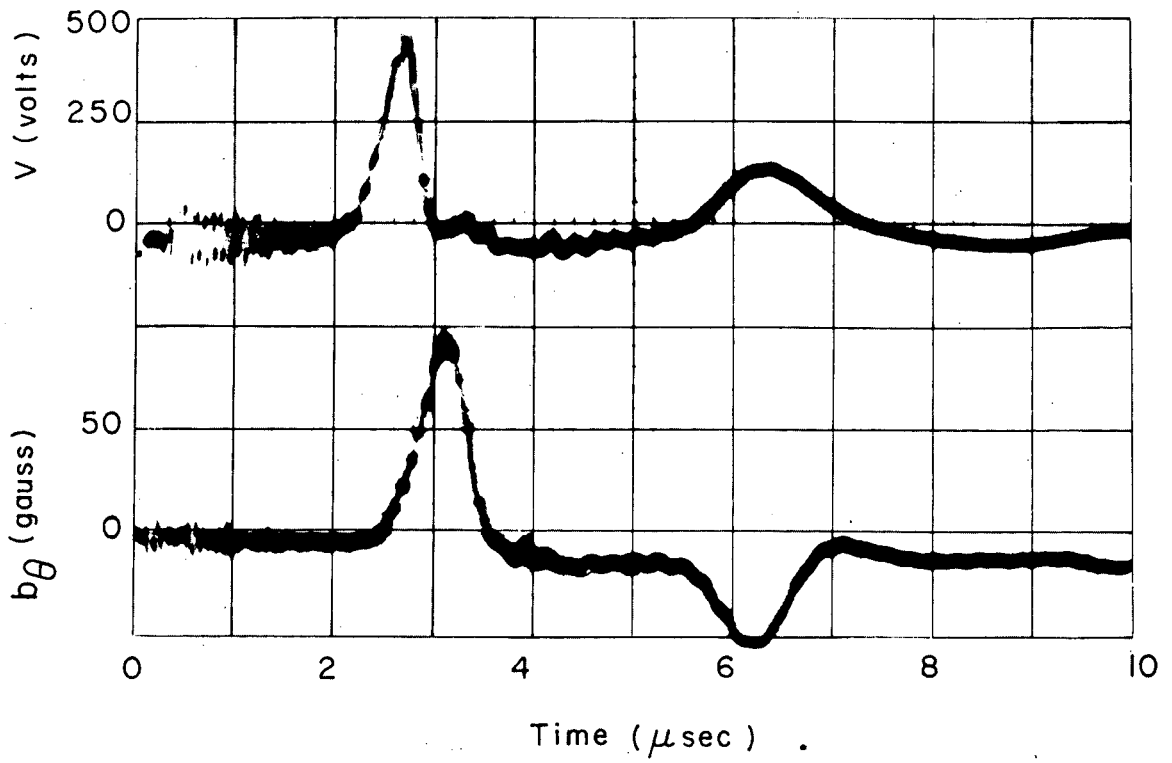

ZN-2623

Fig. 23. Oscillograms showing reflection from a copper end plate 30 μsec after ionizing current has been crowbarred. The description of the traces is the same as in Fig. 22. The phases of the reflected fields are the same as for the high-impedance boundary, showing that the copper plate is effectively isolated from the plasma.

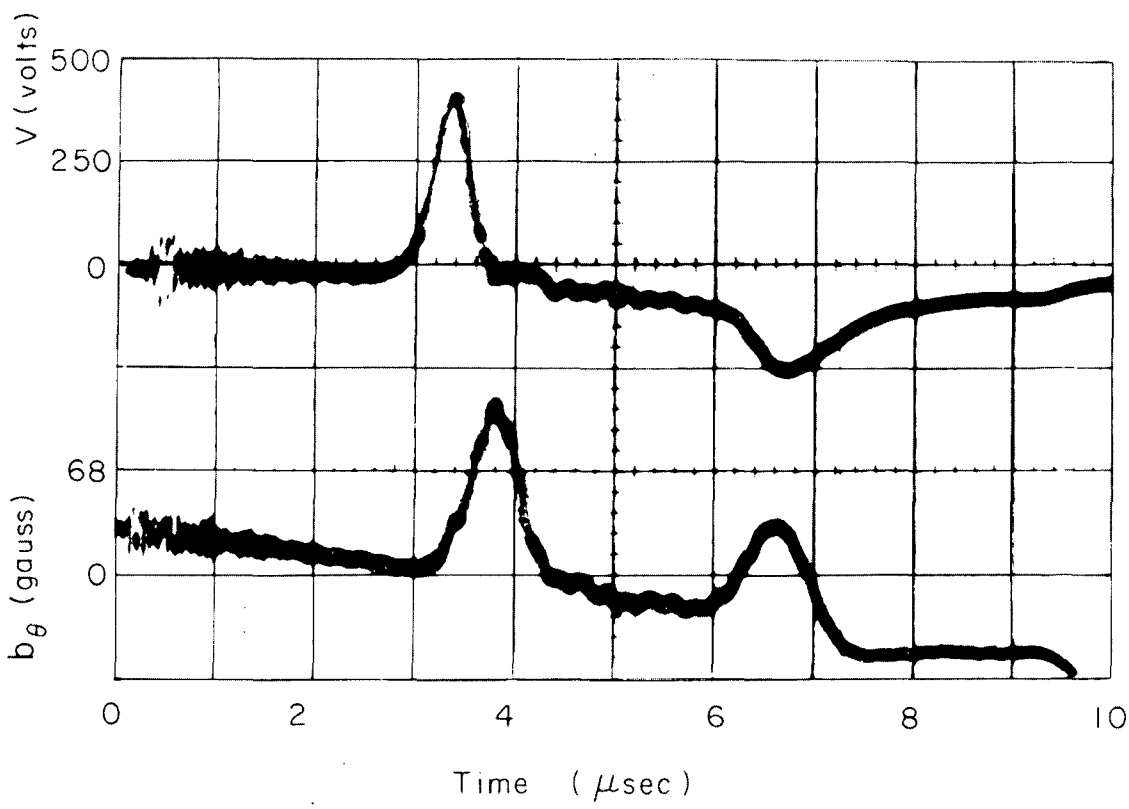

ZN-2620

Fig. 24. Oscillogram showing reflection from a copper end plate with ionizing current still running to the plate. The description of the traces is the same as in Fig. 22. The electric field has reflected out of phase and the magnetic field in phase, in agreement with theory for a low-impedance (conducting) boundary.

located 58 cm from the driving end of the tube. We wait 10 μsec for the ionizing current flow to cease and then induce the Alfvén wave. During this waiting time the interface probably continues to move on down the tube, with reduced velocity because of the plasma pressure. Using the Alfvén velocity measured under similar conditions when the tube was full of plasma, and the wave transit time measured from Fig. 25, one calculates that the reflection occurs from an interface located 68 cm from the driving end of the tube, in reasonable agreement with the estimate given above. Also, a magnetic probe located near the receiving end of the tube (in the neutral gas) detected no wave signal. Thus reflection of Alfvén waves from a plasma–neutral gas boundary seems to be established.

Radial Distributions of Wave Magnetic Field

The radial distribution of the azimuthal magnetic field b_θ associated with the wave has been measured with magnetic probes. Six probes were used, disposed near the receiving-end insulator at various radii. A typical probe location is shown at the right of Fig. 21. The result of this measurement is displayed in Fig. 26. The upper solid curve is for a wave that was induced 20 μsec after the ionizing current was crowbarred. (The lower solid curve is discussed later.) The lowest principal mode has considerably less attenuation than the higher--order modes. Therefore, after the wave has propagated a considerable distance one would expect to find the lowest mode predominant. A numerical calculation of the attenuation indicates that under our conditions a wave that has made one transit of the tube would have about 4% of the second mode remaining and less of higher modes (assuming a driving current proportional to $1/r$). The dashed curve in Fig. 26 shows a first-order Bessel function which represents the radial distribution of the wave magnetic field b_θ in the lowest principal mode.[5] Thus the observed distribution is predominantly the lowest mode.

As was discussed in an earlier quarterly report, that b_θ is zero at the tube wall implies that j_r, the radial current density, is also zero at the wall. The measurements in Fig. 26 were repeated with reversed polarity of wave-driving current, with essentially the same results. The boundary condition therefore does not seem to be associated with the well-known anode sheath which is sometimes observed in discharges where current flow to a boundary is perpendicular to a magnetic field.

The lower solid curve in Fig. 26 is the distribution of b_θ measured for a wave that was induced 90 μsec after the ionizing current was crowbarred. (For the observations discussed above the waves were induced 20 μsec after crowbar.) In this case the peak of the distribution is shifted toward the axis of the tube. This observation would be consistent with the assumption that the decaying plasma has a radial temperature gradient, with the warmest plasma (which would produce less wave attenuation) near the center of the tube.

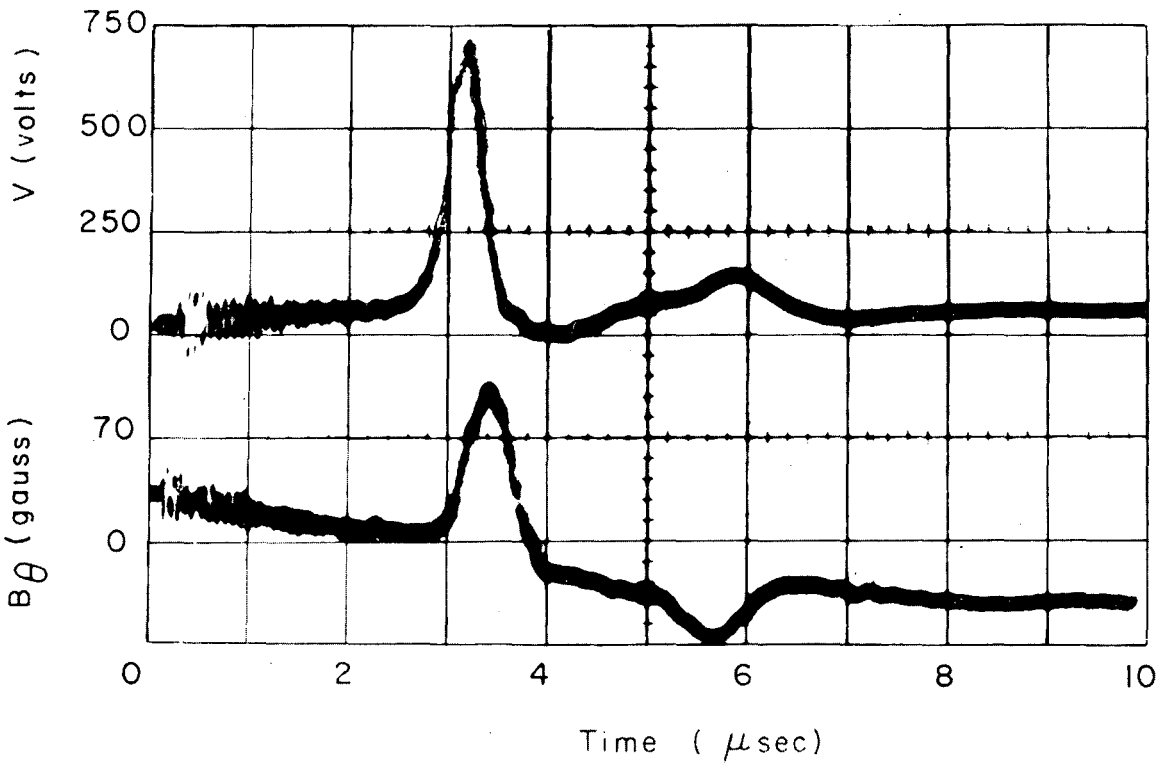

ZN-2621

Fig. 25. Oscillogram showing reflection from an interface between plasma and neutral gas. The description of the traces is the same as in Fig. 22. The phases of the reflected wave fields indicate a high-impedance boundary. The decrease in amplitude of the reflected wave cannot be explained by attenuation in the plasma, and indicates a lossy reflection.

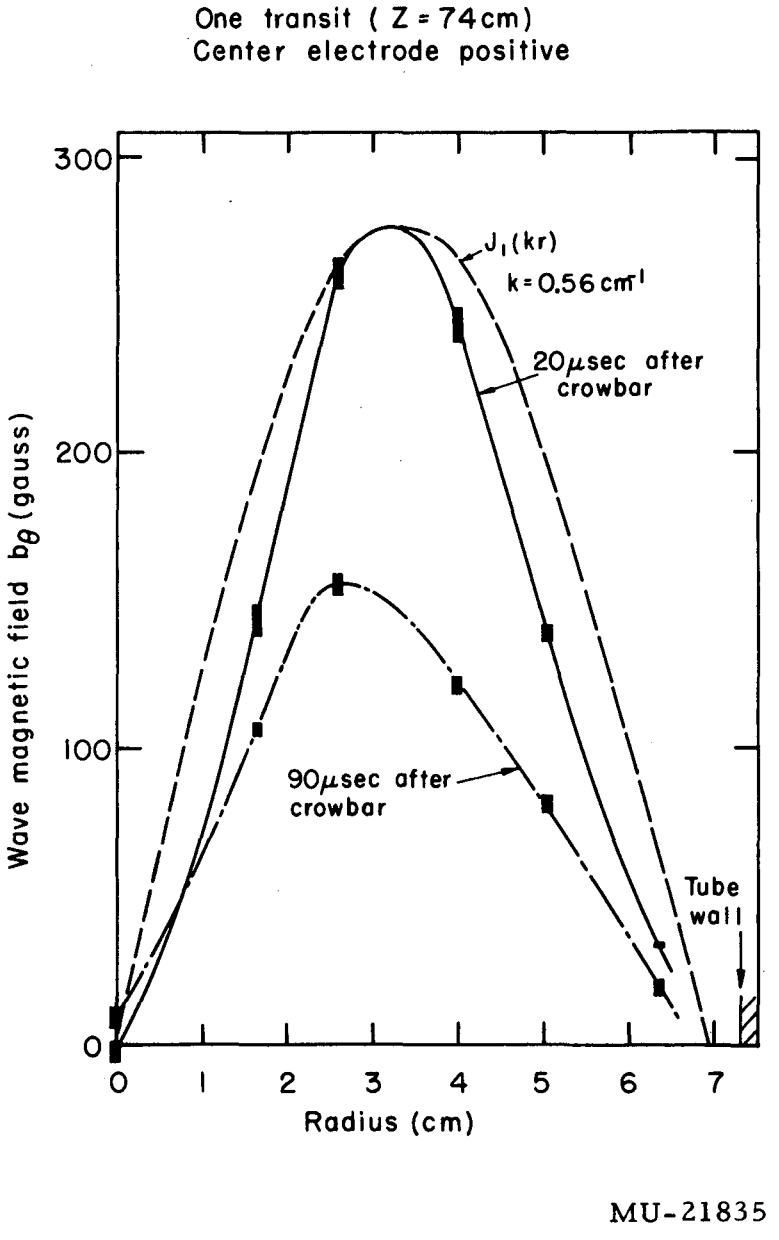

Fig. 26. The radial distribution of the wave magnetic field b_θ measured near the receiving end of the tube after the wave has made one transit. The upper dashed curve is proportional to the theoretical distribution for the lowest mode, $J_1(k_{c1}r)$. The upper solid curve is the measured distribution for a wave which was induced 20 μsec after crowbar. The lower dashed curve is the measured distribution for a wave induced 90 μsec after crowbar.

4. ION CYCLOTRON RESONANCE

Peter R. Forman, James C. Glass, Gordon W. Hamilton, and John M. Wilcox

The Berkeley ion cyclotron resonance experiment was designed to examine the possibilities of ion cyclotron heating by resonant absorption of an Alfvén wave launched at a magnetic field above ion cyclotron resonance. We have decided to operate the experiment on a pulsed basis, although in principle continuous operation should be possible. Pulsing is required by the necessity for plasma preparation by an auxiliary ionizing condenser. On a pulsed basis one can have larger magnetic fields, which greatly improve the hydromagnetic aspects of the experiment, and also larger oscillator power, so that the power input per μsec is increased. A new 5-Mw-line power installation together with some new dry rectifiers has made it possible to double the magnetic field in the region where the hydromagnetic wave is induced. Automatic timing and switching circuits have been designed and constructed to control the magnet pulsing.

The oscillators, which had been designed for continuous operation with a plate voltage of 15 kv, have been redesigned for pulsed operation with 30 kv on the plate. The grid drive loop has been reduced in order to avoid overdriving the grid. Additional rf measuring circuits have been installed. A 3-msec pulse line has been installed to supply power for the oscillators.

5. PLASMA PHYSICS AND MICROWAVE DIAGNOSTICS

I. Experiment

Donald B. Hopkins, George A. Paulikas,* Robert V. Pyle, Henry F. Rugge, and J. Warren Stearns

A. "Enhanced Diffusion" Experiment

The study of the instability at the positive column in a longitudinal magnetic field[6] is essentially complete.

Calculations of the onset and parameters of the instability from the theory of Kadomtsev and Nedospasov[7] have been made and are in reasonable agreement with our experimental results. In Fig. 27 we present experimental measurements of the wave length of the instability in helium, as well as the theoretically calculated curve. Similar agreement with theory is found for other gases and tube radii; this is somewhat surprising, as the

*National Science Foundation Fellowship.

[6]T. K. Allen, G. A. Paulikas, and R. V. Pyle, Instability of the Positive Column in a Magnetic Field, Phys. Rev. Letters 5, 409 (1960).

[7]B. B. Kadomtsev and Nedospasov, J. Nuclear Energy, Part C, 1, 230 (1960).

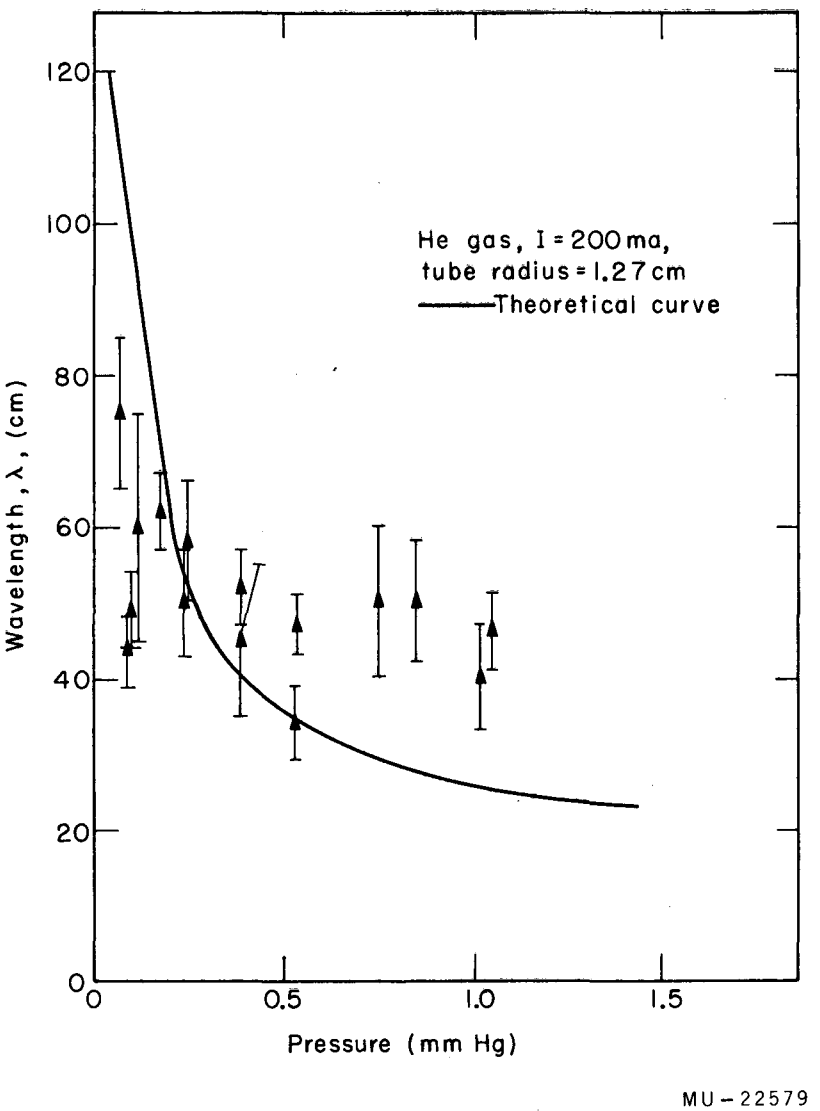

Fig. 27. Wave length of instability vs pressure; helium gas, I = 200 ma, radius of tube = 1.27 cm. Solid line is theoretical curve.

calculated values are derived from a linear theory, whereas experimental measurements were made on the fully developed instability.

A small experiment is in progress to improve techniques of measuring the radial potential distribution in the positive column. In principle, accurate profiles at the radial field can yield information regarding the presence or absence of enhanced interaction in the discharge,[8] possibly preceding the macroscopic instability of the column.

B. Thermally Ionized Cesium Plasma

Radial and longitudinal density measurements ($n = 10^{11}$ to $10^{12}/cm^3$) are continuing, using Langmuir probes with ion collection. The plasma is produced by directing a beam of neutral Cs at a W plate which is indirectly heated to about 2100°C. A similar plate serves as a stopper at the other end of the column, the radial containment being provided by an axial magnetic field.

Several operating conditions have been observed, none of which is understood as yet. Under some conditions, oscillations at approximately 40 kc, 600 kc, 5 Mc, 20 Mc, and(or) 50 Mc have been observed. Some measurements have indicated an apparent maximum in the density (at the discharge axis) in a region part way between the heated electrodes. Preliminary attempts have been made to propagate electrostatic space-charge waves along this column.

C. Microwaves

In addition to transmission diagnostic support, apparatus has been developed for launching and detecting electrostatic slow waves, propagated on a rod of thermally ionized Cs plasma. The initial attempts are at frequencies less than 1 kMc.

II. Theory

G. Ecker*

A. Theory of Probes in a Dense Plasma

As was shown in an earlier report,[9] measurement of the radial potential distribution of the positive column would enable us to detect the presence of micro-instabilities in the plasma column in a magnetic field. There are few ways to determine this distribution function with some accuracy. Probe technique is one of them.

---

[8] G. Ecker, Enhanced Interaction in the Positive Column, UCRL-9144, March 1960.

---

* Consultant to Lawrence Radiation Laboratory at the Institute of Theoretical Physics, University of Bonn.

[9] I. B. Bernstein, E. A. Frieman, M. D. Kruskal, and R. M. Kulsrud: Proc. Roy. Soc. (London) A 244, 17 (1958).

However, under the conditions of interest--that is, in collision-dominated plasma with a strong magnetic field--the application of the ordinary Langmuir theory is not possible. Langmuir's theory is implicitly based on the assumption that the mean free path is large compared with the size of the probe. But in the strong magnetic field the effective mean free path of the electrons is so greatly reduced that it is impossible to choose a probe small enough to satisfy this basic requirement.

Therefore we had to develop a probe theory which accounted for the disturbance of the plasma due to particle loss at the probe surface. To calculate this disturbance we apply a perturbation theory described in the preceding quarterly report (UCRL-9393). In the first approximation we subdivide our system into "regions of influence," each of them represented by an independent solution related to a part of the total system. The decisive question where to join these regions is answered by a criterion derived from the usual condition to choose the approximation adapted to the problem.

During the period of this report we extended this investigation of the probes in two respects.

First, we wanted to see whether higher-order contributions are negligible. Unfortunately it turned out that the calculations of these terms are very elaborate, so that we had to find a more appropriate procedure to check on the higher-order terms. These new calculations give us a means to judge in each case the limitations of our procedure.

Secondly, we have to take into account that, with the changing magnetic field, the theory of the space-charge region immediately in front of the probe is affected. The extension of this region varies with the probe dimensions and with magnetic field values. Langmuir's assumption of free fall of the ions and a Boltzmann distribution for the electrons is not generally correct any more. Because the magnetic field affects the electron diffusion and mobility much more than the ion diffusion and mobility, conditions for the electrons and ions may be completely reversed in a strong magnetic field. Also for large extensions of the space-charge region and strong fields (Larmor radius of the electrons is small), the motion of the electrons must be described by the concept of mobility and not by the concept of free fall. Let us call the magnetic field where the electron diffusion equals the ion diffusion B_s. Then we have formulated the law for the potential distribution in the space-charge region for the following cases: $B \ll B_s$; $B = B_s$; $B \gg B_s$. In general the results cannot be solved analytically. We are in the process of evaluating the formulas with the help of an analog computer.

It should be noted that knowledge of the potential drop across the space-charge region is not required for the applications described in Ref. 8, where we use only relative radial distributions. However, it is important for the interpretation of absolute values.

We are further planning to extend calculations beyond the range of the floating probe to the calculation of the complete probe characteristic.

B. Stability of the Positive Column

The gross instability of a collision-dominated positive column has been treated by Kadomtsev and Nedospasov.[7] An analysis of their calculations shows that their paper is based on a number of assumptions. As far as the calculation of the enhanced diffusion process is concerned, we would definitely feel that the small-signal theory can yield only very unreliable results. As to the calculation of the critical field B_c itself, the most serious assumption is the requirement of quasi neutrality, $n_+ = n_-$, which is applied even to the first-order terms. Also the arbitrary choice of a radial distribution for the first-order density perturbation and the solution of the averaged equations instead of the correct equations restricts the results somewhat. Without the assumption of quasi neutrality, calculations become more complicated, but one can show that the uncertainty introduced by using $n_+ = n_-$ is not more severe than that caused by the averaging process. This is true at least for the calculation of B_c. For the derivation of the enhanced diffusion rate the deviations from $n_+ = n_-$ cannot be neglected.

The work of Kadomtsev and Nedospasov is limited to the investigation of the instability of a collision-dominated plasma column with respect to certain prescribed disturbance. It is interesting to see whether it is possible to find a more general criterion for the instability of such a plasma in the form of magnetohydrodynamics. Here too, one has and one can investigate the instability of a given system on the basis of the magnetohydrodynamic equations. However, the energy principles derived by Bernstein, Frieman, Kruskal, and Kulsrud[9] give a more general and powerful means to investigate instabilities.

We are attempting to find such a more general principle for the collision-dominated plasma in the following ways: On the one hand we try, just as in the magnetohydrodynamic case, to work towards a variational principle starting from the equations of motion of collision-dominated plasma. On the other hand, we study the principles of irreversible thermodynamics in their applicability of our problem.

C. Theory of a Cs Plasma

With reference to the experimental application we investigate the following model of a Cs plasma. The whole device shows cylinder symmetry and is considered infinitely extended in the axial direction. In the center of the discharge is a core of diameter $2r_0$, which contains Cs ions and electrons of an equal temperature T_0. There is an "effective production," α, of such ions and electrons per second and per unit volume of this rod. The electrons and ions diffuse from this core outward towards the wall of the discharge, which is assumed to be a cylinder of diameter 2R. There they recombine. The neutral gas pressure in the discharge is assumed to be negligibly small.

If one assumes that electron and ion temperature (T_-, T_+) are constant throughout the discharge, then the solution of the problem is very straightforward.

However, the assumption of constant ion and electron temperature is indeed not justified, and we consequently developed a more general description taking into account the change in T_-, and T_+. This change is important because it influences the interaction term of the electrons with the ions.

Fortunately the problem is very much reduced by the assumption of quasi neutrality and by the fact that one can prove that the sum of the electron-ion temperature must be constant throughout the discharge. That is the reason why we can reduce our system of equations to only two simultaneous differential equations determining T_- and n, and with that all other quantities.

The equations do not allow an analytical solution. Moreover, we have to do with a boundary-value problem which makes machine solutions difficult. Fortunately we were able to transform the problem in such a way that the boundary-value problem is reduced to an initial-value problem. We can then start with the given initial values T_0 and n_0 and solve the two equations down to a value of the density $n = 0$ at the wall. From the transformed variables we then find the eigenvalue of the "production α" corresponding to this stationary solution. We are now preparing this problem for machine solution.

6. FURTHER ANALYSIS OF THE "SWITCH-ON" IONIZING WAVE

Wulf B. Kunkel

The nature of the ionizing process used in the "Hothouse" experiments[10] is not yet fully understood. As pointed out in the preceding quarterly report (UCRL-9393), the ionization occurs in a reasonably plane current-carrying front which propagates, like a shock wave, at uniform speed along the initial magnetic field. The current, which itself provides the driving force for the front, is transverse to the initial field and produces only a transverse magnetic field. These are the features which the phenomenon has in common with magnetohydrodynamic switch-on shock waves as defined by Friedrichs and co-workers.[11] The analogy is not complete, however, because in the case of the ionizing front under discussion here, the lack of conductivity in the region ahead of the wave uncouples the propagation speed from the particle velocity in the region behind. In fact, the shock strength or the propagation speed for a given driving current is not uniquely determined by the conservation laws alone. An additional criterion is apparently needed to specify the problem completely. In this respect the phenomenon is analogous to combustion waves in which the driving energy also is released in the propagating front itself (by exothermal reactions in the gas). In the latter case stability arguments have been used as a physical basis for the so-called Chapman-Jouguet hypothesis, which is commonly accepted as a resolution of the ambiguities and which is discussed in many textbooks. A similar treatment is suggested for this ionizing wave, but the work has not yet been completed.

---

[10] Alan W. DeSilva, William S. Cooper, III, and John M. Wilcox, Experimental Observations of Alfvén-Wave Modes and Reflections, UCRL-9258, June 1960.

[11] J. Bazer and W. B. Ericson, Hydromagnetic Shocks, Astrophys. J. 129, 758 (1959).

From the conservation laws alone in a one-dimensional treatment, and under the assumption that a steady wave propagates with equilibrium behind as well as ahead of the discontinuity, relationships between any two of the dependent variables are readily derived, of course. The algebra tends to be fairly complex. Even assuming that complete dissociation and ionization exists behind the front so that the gas composition, internal energy, and equation of state are simple, the resulting equations are always cubic in the velocities. A relatively simple quadratic form which may be useful for any further analysis has been derived by using the following new dimensionless variables:

$$Y = U^2/a_\perp^2,$$

$$X = v_\parallel U/a_\perp^2,$$

$$A = a_\parallel^2/a_\perp^2 = H_\parallel^2/H_\perp^2,$$

$$\epsilon = e/a_\perp^2 - \tau_0/(\gamma_0 - 1),$$

$$\tau_0 = p_0/\rho_0 a_\perp^2,$$

where U is the speed of the front, v is the speed of the gas, $a_\perp^2 = (\mu_0/\rho_0)H_\perp^2$, $a_\parallel^2 = (\mu_0/\rho_0)H_\parallel^2$, e is the dissociation and ionization energy per unit mass, μ_0 is the permeability of free space, and γ, p, ρ, and H have the usual meaning. The subscript 0 refers to the state ahead of the wave and the subscripts $\perp$ and $\parallel$ are meant to indicate components transverse and parallel to the initial magnetic field, respectively. In these variables the solution becomes

$$Y = \frac{(\gamma+1)X^2 - (2-\gamma - 2\gamma\tau_0)X + (\gamma-1)A}{2X + 2(\gamma-1)\epsilon + \gamma - 2 + 2\tau_0} . \qquad (1)$$

It should be kept in mind that the requirement of equilibrium on both sides of the front implies that no currents are flowing there; hence the solution is independent of the conductivity behind the wave. On the other hand, if the conductivity ahead of the wave is not negligible, a second condition results, i.e., the electric field there must vanish, which in this terminology implies we must have

$$Y = X + A. \qquad (2)$$

When Eq. (2) is substituted in (1) the usual magnetohydrodynamic switch-on shock relation is recovered for a gas in which energy is absorbed by dissociation and ionization. Without the condition (2), however, Eq. (1) does not determine the phenomenon completely. For very large X, Eq. (1) approaches the well-known strong shock relation of ordinary gas dynamics. Very much as in the analysis of combustion waves, Y(X) displays a minimum which may have a special physical significance, although the relationship to the Chapman-Jouguet point of ordinary combustion wave theory is not yet completely clear. The situation is certainly more complicated here because of the existence of three signal speeds in hydromagnetics, as compared with a single sound speed in gas dynamics. The minimum propagation speed for the front is

given by the relationship (neglecting τ_0 and taking $\gamma = 5/3$),

$$9Y^2 - (5-32\epsilon)Y - 16A + 0.25 = 0. \quad (3)$$

This equation, with the appropriate simplifying approximations, yields again the results quoted in the preceding quarterly report.

V. THEORETICAL AND BASIC EXPERIMENTAL PLASMA PHYSICS

1. THE INTERCHANGE INSTABILITY

William A. Newcomb

Rosenbluth and Longmire have investigated the stability of a mirror machine against the interchange of neighboring magnetic field lines.[1] Assuming that the plasma pressure is small compared with the magnetic pressure, and restricting their attention to the outermost field lines, they obtain the following stability condition, in which $d\ell$ is an element of arc length along a field line, $P_\perp$ and $P_\parallel$ are the components of plasma pressure perpendicular and parallel to the field, r is distance from the axis, B is the magnetic field intensity, and R is the radius of curvature of the field line, counted as positive when the line is concave outward:

$$\int \frac{d\ell\,(P_\perp + P_\parallel)}{rB^2R} > 0. \qquad (1)$$

The integral is taken along the part of the field line that passes through the plasma. If the ends of the field lines are not tied, the stability condition is that the inequality (1) should be satisfied on the field lines just within the outer edge of the plasma. It is quite difficult to find plasma distributions that satisfy this condition.

Using the TA energy principle,[2] I have found the stability condition for field lines within the body of the plasma:

$$\int \frac{d\ell}{r^2B^3}\left[\frac{1}{R^2}\,\frac{\underline{\tau}\cdot\underline{\nabla}\,(P_\perp + P_\parallel)}{\underline{\tau}\cdot\underline{\nabla}\log B} - \frac{1}{R}\,\underline{n}\cdot\underline{\nabla}\,(P_\perp + P_\parallel)\right] > 0, \qquad (2)$$

where $\underline{\tau}$ and $\underline{n}$ are, respectively, the unit vectors in the r, z plane parallel and perpendicular to the field line. The sign of $\underline{n}$ is chosen so that n_r will be positive. In deriving this condition, we have made one more assumption: The mirror regions have a much smaller volume than the weak-field region between the mirrors. If this is true, and if $P_\perp$ and $P_\parallel$ are everywhere small in comparison with the magnetic pressure $B^2/2$, then the stability condition is that the inequality (2) should be satisfied on every field line. It is easily shown that our condition reduces to that of Rosenbluth and Longmire on the outermost field lines, provided that $P_\perp + P_\parallel$ approaches zero at the outer edge with $\underline{n}\cdot\underline{\nabla}\,(P_\perp + P_\parallel)$ remaining finite.

It should be emphasized that the pure interchange instability cannot occur when the field lines are tied at the ends, in which case every displacement involves a certain amount of line-bending. This may be the explanation for the observed stability of mirror machines that violate condition (1).[3]

---

[1] M. N. Rosenbluth and C. L. Longmire, Ann. Phys. 1, 120 (1957).

[2] W. A. Newcomb, in Controlled Thermonuclear Research Quarterly Report, UCRL-9243, June 1960, p. 101.

[3] R. F. Post et al., Phys. Rev. Letters 4, 166 (1960).

2. CYCLOTRON RADIATION FROM A PLASMA

Donald P. Geesaman

Some calculations are being made of the cyclotron radiation losses from cylindrical and slab plasma geometries.[4] Trubnikov's derivation of the absorption coefficients is assumed, and in particular his constant-phase evaluation of an integral in his derivation is taken to be satisfactory. The expressions for the absorption coefficients are left in the form

$$a^{\perp} = h^{\perp} e^{-\frac{m_e c^2}{T_e}\left[1 - 2\frac{T_e \psi \omega}{m_e c^2 \omega_c} + 2\left(\frac{T_e \omega \sin\theta}{m_e c^2 \omega_c}\right)^2 \left(1 + \frac{\psi^2}{2} - \cosh\psi\right)\right]^{1/2}},$$

where $\psi(\omega,\theta)$ satisfies $\psi - \sinh\psi = \dfrac{m_e c^2 \omega_c}{T_e \omega \sin^2\theta}$, and where there is a similar expression for the other polarization.

The radiation intensity at the plasma surface is then given for one polarization by

$$I^{\perp} = \frac{\omega^2}{8\pi^3 c^2} T_e \left[\frac{1 - \exp(-a^{\perp} s)}{1 - R\exp(-as)}\right],$$

where R is the reflectivity of the surface and

$s = \dfrac{t}{\sin\theta\cos\phi}$ for a slab of thickness t, and

$s = \dfrac{2a\cos\phi}{\sin\theta}$ for a cylinder of radius a.

The sum over frequencies and surface directions is done by a machine integration. At each ω, θ of this evaluation the transcendental equation for $\psi(\omega, \theta)$ is solved.

So that an estimate of critical size can be made, it is assumed that all the thermonuclear energy that goes to heat the ions is transferred to the electrons by collisions. Results are not complete, but for a representative deuterium plasma in a slab geometry with $B = 10^4$ gauss, $n = 2.8 \times 10^{13}$ particles/cm^3, $T_e = 40$ kev and $R = 0$, a critical size of 6.5 meters is obtained. This conclusion is compatible with the earlier results of Trubnikov and Kudryatsev.

---

[4] Donald P. Geesaman, Cyclotron Radiation From a Plasma, in Controlled Thermonuclear Research Quarterly Report, UCRL-9394, Aug. 1960, p. 68.

3. THE MAGNETIC COMPRESSION OF A PARTIALLY IONIZED GAS

Donald P. Geesaman and John Killeen

The ionization and heating of a deuterium gas and the formation of a current layer have been treated in an earlier paper.[5] In that paper plasma motion is not included, i. e., the calculation is stopped at a time when the magnetic field due to the current layer is large enough to cause an implosion of the ionized sheath. In this work the hydrodynamic motion is included, and cylindrical coordinates are used. We are still treating a partially ionized gas, so that there are two equations of motion and two continuity equations. The two fluids are the ionized gas and the neutral gas. There are three temperatures (electron, ion, neutral) and thus three energy equations. The electromagnetic variables are j_θ, j_θ, B_θ, B_z, E_θ, E_z. The problem is one-dimensional, i. e., all the dependent variables are functions of r and t only. The effects of ionization, excitation, charge exchange, viscosity, and runaway electrons are included. A coupling between the plasma equations and the external circuit equations is included. A new code, PLASMA II, is planned which will solve the system of partial differential equations discussed by finite-difference methods. The purpose of the code is to study various experimental situations such as hard-core pinches, theta pinches, etc. By keeping the code flexible we can determine those processes which are important in explaining the experimental results.

4. RESISTIVE RELAXATION OF A PERTURBED SHEET PINCH

Harold P. Furth and John Killeen

In an earlier report[6] the effect of finite conductivity on the stability of a sheet pinch was investigated. In that calculation the approximation of an inert fluid was used. In the present treatment the plasma motion is included, but the density is kept constant.

The equations used are

$$\rho\left(\frac{\partial \vec{v}}{\partial t} + \vec{v}\cdot\nabla\vec{v}\right) = \vec{j}\times\vec{B} - \nabla p,$$

$$\operatorname{div}\vec{v} = 0,$$

$$\frac{\partial \vec{B}}{\partial t} = -\operatorname{curl}\vec{E},$$

$$\vec{E} = \eta\vec{j} - \vec{v}\times\vec{B},$$

$$\operatorname{curl}\vec{B} = \vec{j}, \qquad \operatorname{div}\vec{B} = 0.$$

---

[5] J. Killeen, G. Gibson, and S. A. Colgate, Boundary Layer Formation in the Pinch, Phys. Fluids 3, 387-394 (1960).

---

[6] Harold P. Furth, Resistive Relaxation of a Perturbed Current Layer, UCRL-6071-T, July 1960.

The following model is used:

$$B_x = B_0 [F(\zeta) + \frac{\partial}{\partial \zeta} \psi(\zeta, t) \cos kx],$$

$$B_y = B_0 \, k \, a \, \psi(\zeta, t) \sin kx,$$

$$B_z = 0,$$

$$p = B_0^2 \{p_0 - \frac{1}{2} [F(\zeta)]^2 + p_i(\zeta, t) \cos kx\},$$

$$v_x = u_x(\zeta, t) \sin kx,$$

$$v_y = u_y(\zeta, t) \cos kx, \quad v_z = 0,$$

where $\zeta = y/a$. In this model there is no z dependence. The resistivity η is assumed isotropic, and is a given function of ζ. In the above model the unperturbed configuration is specified by F and p_0, and the first-order perturbations are given by ψ, p_i, u_x, u_y. If we substitute the above expressions into the given equations and keep only zero- and first-order terms we obtain the two equations

$$\frac{\partial \psi}{\partial \tau} = - \beta F(\zeta) w + \eta(\zeta)/\eta_0 \left\{ \frac{\partial^2 \psi}{\partial \zeta^2} - a^2 \psi \right\},$$

$$\frac{1}{a^2 \beta} \frac{\partial}{\partial \tau} \left\{ \frac{\partial^2 w}{\partial \zeta^2} - \zeta^2 w \right\} = F(\zeta) \left\{ \frac{\partial^2 \psi}{\partial \zeta^2} - a^2 \psi \right\} - \frac{d^2 F}{d\zeta^2} \psi,$$

for $\tau \geq 0$, $0 \leqslant \zeta < \infty$.

In the above equations we have

$$w = [\rho^{1/2}/B_0 \; u_y],$$

$$\tau = [\eta_0/a^2] \, t,$$

$$a = ka, \; \beta = B_0 \, a \, \eta_0^{-1} \, \rho^{-1/2}.$$

The field $F(\zeta)$ and the resistivity $\eta(\zeta)$ are given. The initial perturbations $\psi(\zeta, 0)$ and $w(\zeta, 0)$ are also specified. The boundary conditions are

$$\left. \frac{\partial \psi}{\partial \zeta} \right|_{\zeta = 0} = 0, \qquad w(0, t) = 0, \quad t > 0,$$

$$\frac{\partial \psi}{\partial \zeta} + a\psi = 0, \qquad \frac{\partial w}{\partial \zeta} + a \, w = 0,$$

as $\zeta \to \infty$, $t > 0$.

The partial differential equations for ψ and w are solved by replacing them by a pair of implicit difference equations. The solution of the difference equations is effected by an IBM 709 code called RIPPLE, which has been completed and is now being used for some test problems. The results of these calculations, together with some details of the method of solution of the difference equations, will appear in a forthcoming report.

5. A COMPUTATION FOR STUDYING THE FORMATION OF THE ASTRON E LAYER

John Killeen

Dr. Leslie Peck has prepared a mathematical formulation of the self-consistent formation and build-up of the Astron E layer.[7] Cylindrical symmetry is assumed and the field can be specified by one component of the vector potential. The equation to be solved for $A_\theta(r, z, t)$ is

$$\frac{1}{c^2}\frac{\partial^2 A_\theta}{\partial z^2} - \frac{\partial^2 A_\theta}{\partial z^2} - \frac{\partial}{\partial r}\left[\frac{1}{r}\frac{\partial}{\partial r}(r A_\theta)\right] = j_\theta,$$

where $j_\theta(r, z, t)$ is the current density given by

$$j_\theta = e p_\theta \iint \gamma^{-1} \rho(r, z, p_r, p_z, t)\, dp_z\, dp_r,$$

$$\gamma = (1 + p_z^2 + p_r^2 + p_\theta^2)^{1/2}.$$

The function ρ is the electron distribution in phase space, which satisfies the Boltzmann equation (neglecting scattering),

$$\frac{\gamma}{c}\frac{\partial \rho}{\partial t} + p_z\frac{\partial \rho}{\partial z} + p_r\frac{\partial \rho}{\partial r} + q p_\theta \frac{\partial A_\theta}{\partial z}\frac{\partial \rho}{\partial p_z} + \frac{p_\theta}{r}\left(p_\theta + q\frac{\partial (r A_\theta)}{\partial r}\right)\frac{\partial \rho}{\partial p_r} = 0.$$

It is proposed that the above set of equations be solved by finite-difference methods making use of the new fast computer LARC.

The relevant difference equations are now being studied in preparation for the organization of the LARC code.

---

[7] Leslie G. Peck, A Computation for Studying Build-Up of the E Layer in the Astron, private communication, Aug. 1960.

6. STABILITY OF INFINITELY THIN ELECTRON LAYERS

V. Kelvin Neil

A particular instability of an infinitely thin layer of electrons has been investigated theoretically. A plane sheet, infinite in extent, and neutralized by positive ions, was considered as an initial model. All electrons travel with a relativistic velocity $\bar{v}$. A small disturbance with time and space dependence exp i $(\omega t - \bar{k} \cdot \bar{r})$, with $\bar{k} \cdot \bar{v} = 0$, is taken as a perturbation to the equilibrium distribution. Displacement currents are neglected throughout the treatment. This problem has been treated previously by Harold P. Furth. The linearized hydromagnetic equation and Maxwell's equations are solved self-consistently to yield a dispersion relation for the allowed values of the frequency ω. It is found that a pair of pure imaginary values of ω are always allowed. If the electron energy is greater than 5 Mev and the ions are protons, these imaginary values of ω are given approximately by

$$\omega^2 = - 2 \pi e^2 n k \beta / (\gamma m M)^{1/2},$$

where n is the number density of electrons per unit area, γm is the relativistic electron mass, M is the ion mass, and β is the electron velocity divided by the velocity of light. For heavy ions and an electron energy less than 2 Mev, the growth rate may be found from

$$\omega^2 = - 2 \pi e^2 n k (\gamma^2 - 1)/M.$$

When the electrons are assumed to be monoenergetic, but to have a small angular spread in velocities, the hydromagnetic equations are replaced by the linearized relativistic Vlasov equation. If the half width of the angular spread is designated by a, the condition for stability is found to be

$$a^2 > 2 \pi r_0 n / \gamma k,$$

where r_0 is the classical radius of the electron. This is a condition previously derived by Harold P. Furth. It at first appears that, for any a, instability prevails for sufficiently long wave lengths (small k). However, the validity of the treatment is limited to values of a such that $a^2 \ll 1$, and the above criterion is not applicable when this limitation is violated.

The same type of perturbation has been applied to an infinitely thin cylinder of radius R inside a perfectly conducting cylinder of radius b. The system is infinite in the axial direction, and radial motion of the particles is not considered. The electrons move in the azimuthal direction, and the disturbance moves in the axial direction. In the absence of any axial velocity the instability is found to be present as in the plane sheet. For wave lengths much less than the circumference of the electron cylinder, the growth rate is only slightly less than those found for the plane sheet. For wave lengths much longer than $2 \pi R$ and $2 \pi b$, the growth rate is significantly reduced. For $k R \lesssim 0.2$, and for $b/R = 1.4$ (typical of the Astron device), the growth rate is given approximately by

$$\omega^2 = - 4 \pi e^2 n k^2 R/M.$$

Consideration of an axial velocity spread in this model indicates that the condition for stability is

$$a^2 > 2 \pi r_0 n R [1 - (R/b)^2]/\gamma.$$

By applying this criterion to Astron, for 5-Mev electrons and a surface current of 400 amp/cm, it is found that $a > 0.45$ radian is required for stability. This implies a total angular spread of 50 deg, which is very large. Here again, however, the condition $a^2 << 1$ is a basic assumption in the calculation, and therefore the accuracy of this result is questionable.

7. PLASMA POTENTIAL IN A MAGNETIC MIRROR SYSTEM

David J. BenDaniel

Kaufman has shown that the mirror ratio of a magnetic mirror system is diminished from its theoretical value by the presence of a plasma potential.[8] This potential arises from the more rapid initial loss of electrons. The potential then develops to bring the electron and ion loss rates into balance. He calculates that the effective mirror ratio R_e is given by

$$R_e = (B_c/B_0)/[1 + (T_e/T_i)\gamma],$$

where B_c/B_0 is the theoretical mirror ratio, T_e/T_i is the ratio of the electron temperature to the ion temperature, γ is the absolute magnitude of the potential between the center of the mirror system and the outside, in units of electron temperature.

The value of γ calculated by Kaufman neglects the spatial properties of the magnetic mirror system. Post points out that the plasma potential is considerably modified by the magnetic mirror geometry.[9]

In a separate report,[10] a new estimate of the effective mirror ratio is made which takes the spatial properties of the system into account and more realisticly estimates the electron and ion loss rates.

Figure 28 gives the value of γ calculated in this report as a function of the theoretical mirror ratio and the temperature ratio. Figure 29 gives the effective mirror ratio R_e as a function of the theoretical mirror ratio and the temperature ratio.

In this report, the plasma potential is shown to be set up throughout the body of the mirror system and to affect the motion and loss rate of the ions considerably.

---

[8] A. N. Kaufman, Ambipolar Effects in Mirror Losses, TID-7520 (Pt. 2) Sept. 1956, p. 387.

[9] R. F. Post, Some Aspects of the Economics of Fusion Reactors, UCRL-6077, Dec. 1960.

[10] David J. BenDaniel, Plasma Potential in a Magnetic Mirror System, UCRL-6235, Feb. 1961.

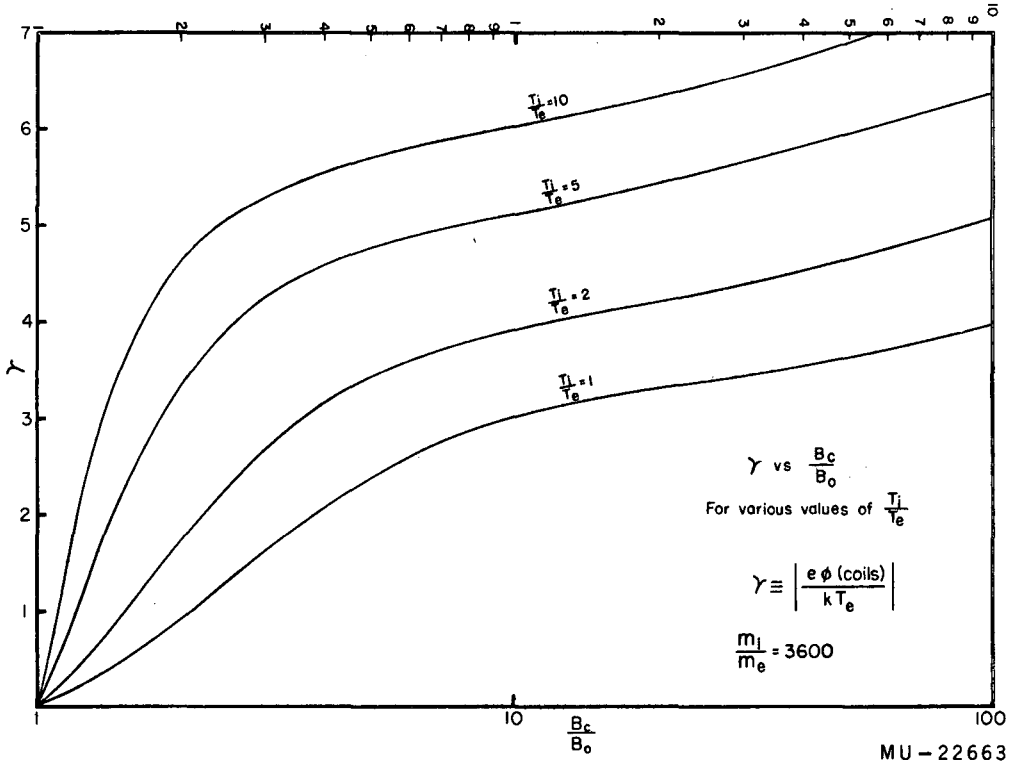

Fig. 28. Plasma potential (in units of electron temperature) as a function of theoretical mirror ratio.

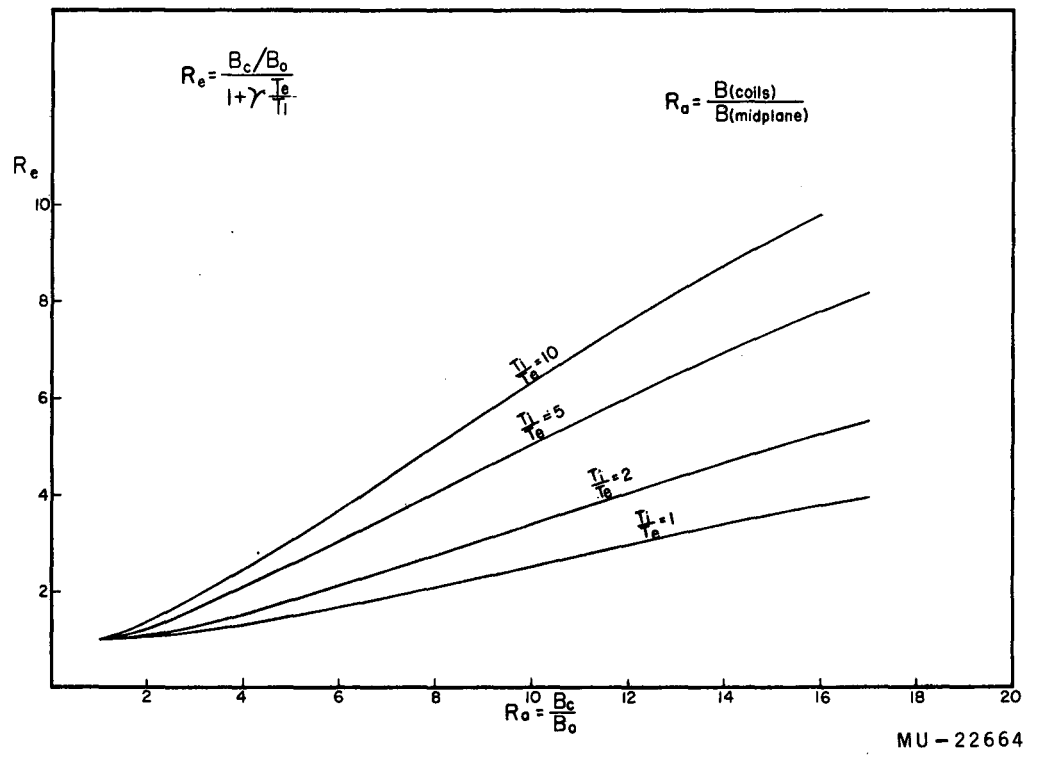

Fig. 29. Effective mirror ratio as a function of theoretical mirror ratio.

8. SECONDARY PROCESSES IN A HYDROGEN GAS NEUTRALIZER

Daniel Z. Freedman, John R. Hiskes, and C. H. Woods

Various atomic and molecular reactions which would be expected to occur in a hydrogen gas beam neutralizer are studied. A set of simultaneous differential equations has been solved giving the density of cold ions and atoms along the beam trajectory. The variable components generated in the H_2 gas by the high-energy beam considered here are H, H^+, H_2^+, H_3^+, and e^-. It has been shown previously[11] that unless charge neutralization can be maintained in the neutralizer a large angular distribution of the high-energy beam will occur; consequently, we assume charge neutrality will be maintained, and take the e^- density equal to the ionic density. We consider fifty reactions occurring between the two fast components, H and H^+, the H_2 gas, and the five cold components H, H^+, H_2^+, H_3^+, and e^-. The H_2 gas density is held fixed at 5×10^{13} molecules, corresponding to a base pressure of approximately 10^{-3} mm of Hg. The end effects--that is, the spatial dependences in the problem--are ignored. The cross sections involving H and H^+ are taken for 10 kev and the cross sections involving the cold components are those at approximately 1 v energy. We make three assumptions regarding the effects of recombination at the walls: In the first case we assume a loss rate of 10^5/sec for each of the cold components, which is intended to simulate the recombination of these components at the wall for form H_2 gas in a time comparable to the wall distance divided by the mean velocity. For the second case we assume a loss rate of 10^5/sec for the cold charged components but no loss rate for the H component. The third corresponds to no loss rate to the walls for any component.

These equations have been solved for three initial values for the H^+ current--1 ma/cm^2, 10 ma/cm^2, and 100 ma/cm^2--and over a time scale ranging from 10^{-8} sec to 10 sec. In Fig. 30 are shown the results for the initial condition of 10 ma/cm^2 and for the first and second assumptions regarding the wall recombination. In Fig. 31 are shown the results for 10 ma/cm^2 initial current and for no wall recombination. The data for 1 ma/cm^2 and 100 ma/cm^2 indicate that the asymptotic densities are approximately linear functions of the incident H^+ current.

For the reactions considered here we have used the experimental cross-section data whenever available, but have had to rely on theoretical estimates and extrapolation for many of the processes. Consequently, the data presented here must be considered to be indicative only.

These data suggest the following general conclusions: Referring to the curves shown in Fig. 30, we note that the asymptotic density of cold ions is roughly an order of magnitude larger than the density of the fast ions and neutrals. For the second assumption, in which it is assumed no recombination of H occurs at the walls, the asymptotic density of H is approximately 40% of the H_2 density. If this were to occur in the beam neutralizer it would have the favorable result of increasing the ratio of fast neutrals to fast ions by several percent.

[11] C. H. Woods, Space Charge Effects in a Beam Neutralizer, UCRL-5902-T, March 1960.

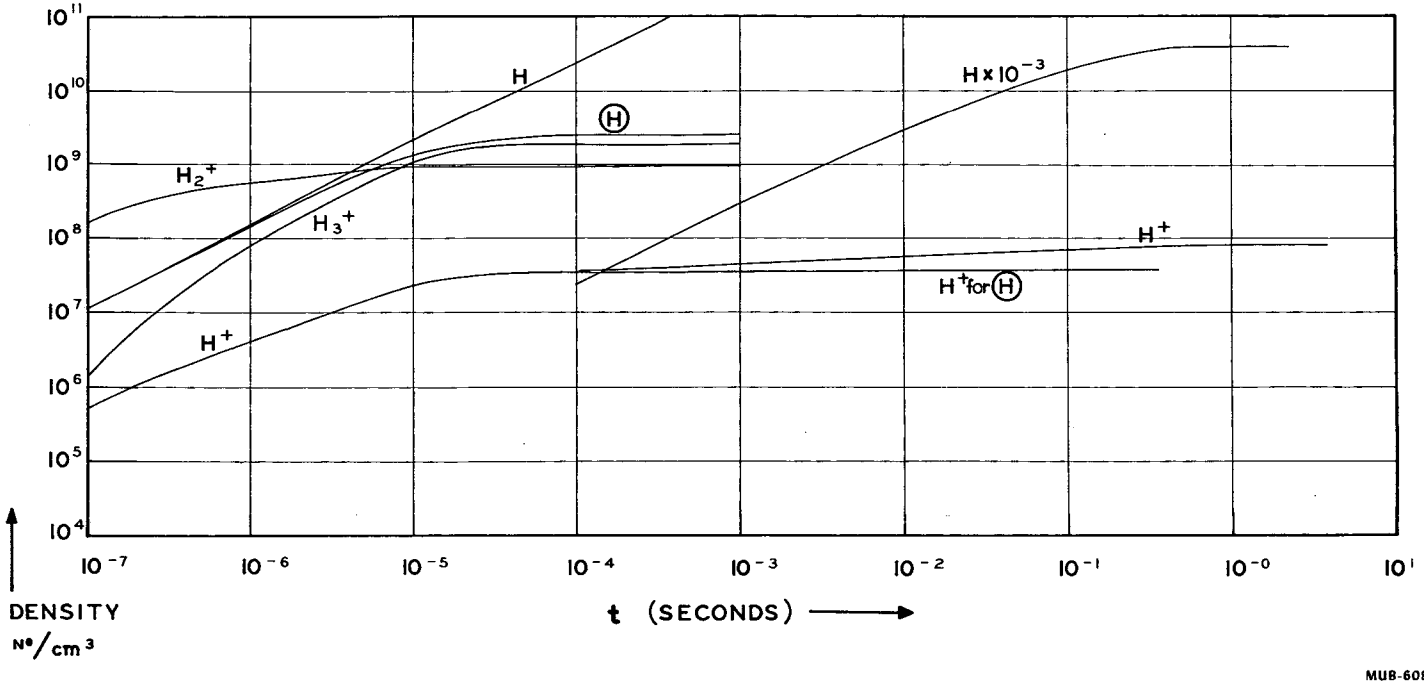

Fig. 30. Cold ion density plotted as a function of time for the first two assumptions regarding recombination at the walls. Incident ion current = 10 ma/cm^2 → 4.2×10^8/cm^3; 10-kev protons. Ion loss rate to walls = 10^5/sec; H loss rate to walls = 0.0; Ⓗ :H loss rate to walls = 10^5/sec.

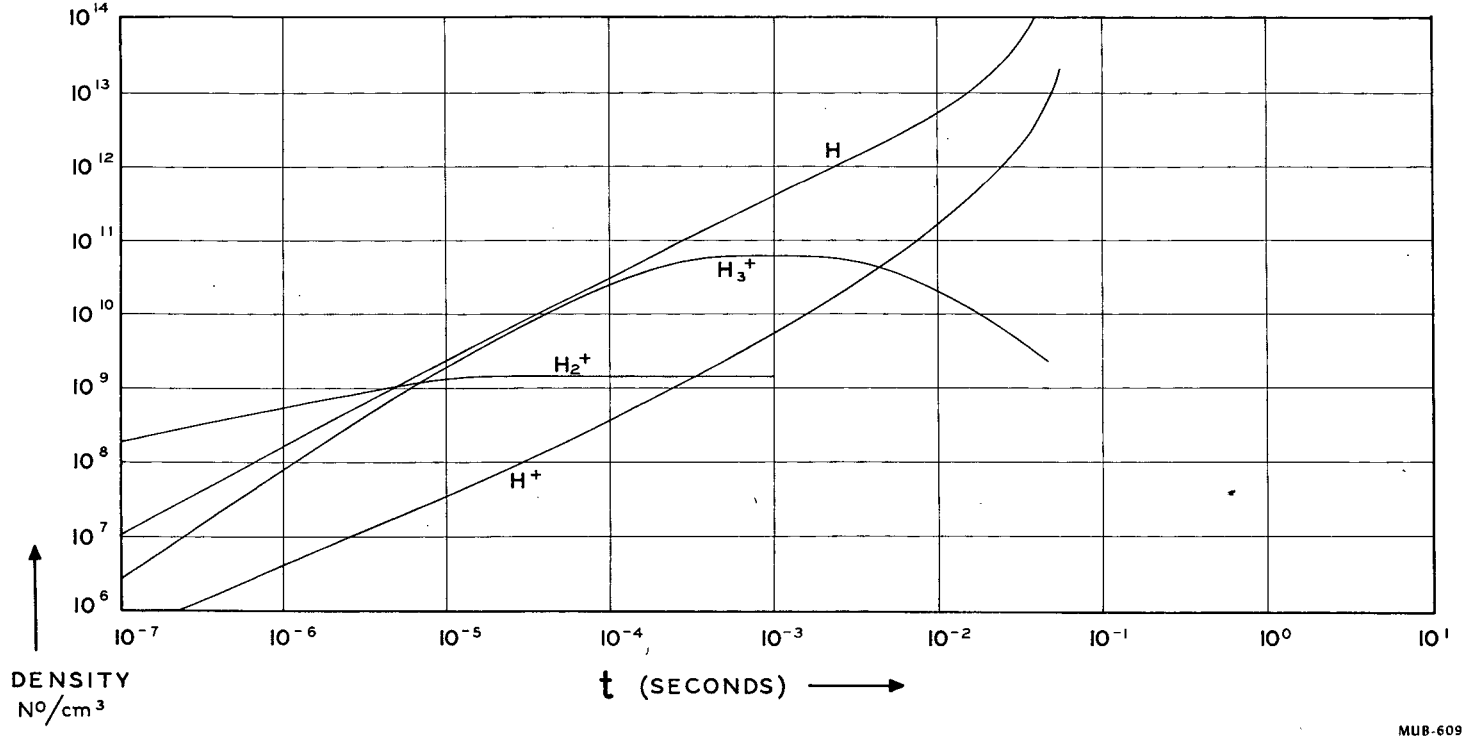

Fig. 31. Cold ion density plotted as a function of time for the case of no recombination at the walls. Incident beam current = 10 ma/cm^2 → 4.2×10^8/cm^3; 10-kev protons. Ion loss rate to walls = 0.0.

The data of Fig. 31, for which no recombination occurs at the walls, indicate that the cold ion density will be of the same order of magnitude as the H_2 density in a time of roughly 0.1 sec. When the cold ion density approaches the H_2 density we would expect that the normal operation of neutralizer would be altered. The time for the cold ion density to reach a particular value is inversely proportional to the incident H^+ current.

9. VIBRATIONAL STATES OF THE HD^+ AND HT^+ IONS

John R. Hiskes

It has been shown that the HD^+ and HT^+ ions are more susceptible to electric dissociation than is H_2^+.[12] As a first step toward determining the threshold fields necessary for dissociating the successive vibrational levels of these ions we report here the results of calculations giving the vibrational levels for the unperturbed HD^+ and HT^+ ions. These calculations have been done for the J = 0 rotational state, neglecting the dynamic corrections to the potential. For the HD^+ ion we find twenty-two bound states, and for the HT^+ ion twenty-three bound states. The eigenvalues, expressed in Rydberg units, are listed in Table I.[13] These calculations are discussed in greater detail in a separate report.[13] Calculations are in progress to determine the vibrational levels of the remaining hydrogenic isotopic molecular ions, D_2^+, DT^+, and T_2^+.

---

[12] John R. Hiskes, Dissociation of Molecular Ions by Electric Fields, UCRL-9182, May 1960.

[13] S. Cohen, J. R. Hiskes, and R. J. Riddell, Jr., Vibrational States of the HD^+ and HT^+ Ions, UCRL-9414, Sept. 1960.

Table I. Vibrational eigenvalues for the HD^+ and HT^+ ions

V	HD^+	HT^+
0	-1.1958037	-1.1963171
1	-1.1783752	-1.1798348
2	-1.1618234	-1.1641346
3	-1.1461231	-1.1491957
4	-1.1312519	-1.1349986
5	-1.1171900	-1.1215261
6	-1.1039202	-1.1087623
7	-1.0914283	-1.0966944
8	-1.0797030	-1.0853109
9	-1.0687371	-1.0746040
10	-1.0585270	-1.0645688
11	-1.0490734	-1.0552037
12	-1.0403816	-1.0465109
13	-1.0324619	-1.0384967
14	-1.0253301	-1.0311711
15	-1.0190081	-1.0245493
16	-1.0135246	-1.0186506
17	-1.0089152	-1.0135004
18	-1.0052240	-1.0091300
19	-1.0025007	-1.0055752
20	-1.0007944	-1.0028782
21	-1.0000948	-1.0010814
22		-1.0001982

Dissociation limit = $W_0(\infty)$ = -1.0000000

10. PENETRATION OF CHARGED PARTICLES THROUGH THE PICKET FENCE

N. W. Hetherington and C. H. Woods

Further calculations of trajectories of charged particles colliding with the picket-fence field[14] have made it possible to plot a curve showing the effective slot width versus the angle of deviation from normal incidence for the approaching particle. This curve, given in Fig. 32, holds for particles having no initial component of velocity along the conductors, and having the ratio of gyro radius (between the conductors) to conductor spacing equal to 0.1. If the angle of deviation is greater than 30 deg, the particle is always reflected.

In the case of the moving picket fence (established by alternating the conductor currents in appropriate phase relation) we have found that the particle is always reflected if the fence moves at least twice as fast as the particle.

11. ATOMIC AND MOLECULAR BEAM RESEARCH

Forrest Baker, Gilbert O. Brink, and Edmund S. Chambers

The electron gun that was mentioned in the preceding quarterly report has been improved and modified so that it will operate down to thermal energies. No attempt has yet been made to measure its energy spread. The current and focusing abilities of the gun appear to be adequate for its intended use.

A potassium beam has been produced and crossed with the electron beam from the above gun. Potassium ions have been detected but as yet no quantitative measurements have been made. The detection system of the machine is being tested in order to optimize its performance.

The design of the machine for the K^{42} experiment is essentially complete. The main machine structure, including the vacuum system, is finished with the exception of the installation of some of the electronic components for the high-vacuum system. Leak hunting and sealing is in progress. An electron gun is being built and will be tested as soon as completed. All the electronic units for the gun either have now arrived or are being fabricated.

A 20-channel pulse-height analyzer is being installed. The main units and cabling are completed but a vent system is still needed. The lead pig for the photomultiplier tube assembly has arrived and has been setup near the analyzer.

In collaboration with Mr. Al Taylor and the Hazards Control Group, the following has been accomplished: The 2-inch lead-shielded glove box

[14] N. W. Hetherington and C. H. Woods, in Controlled Thermonuclear Research Quarterly Report, UCRL-9393, Sept. 1960, p. 69.

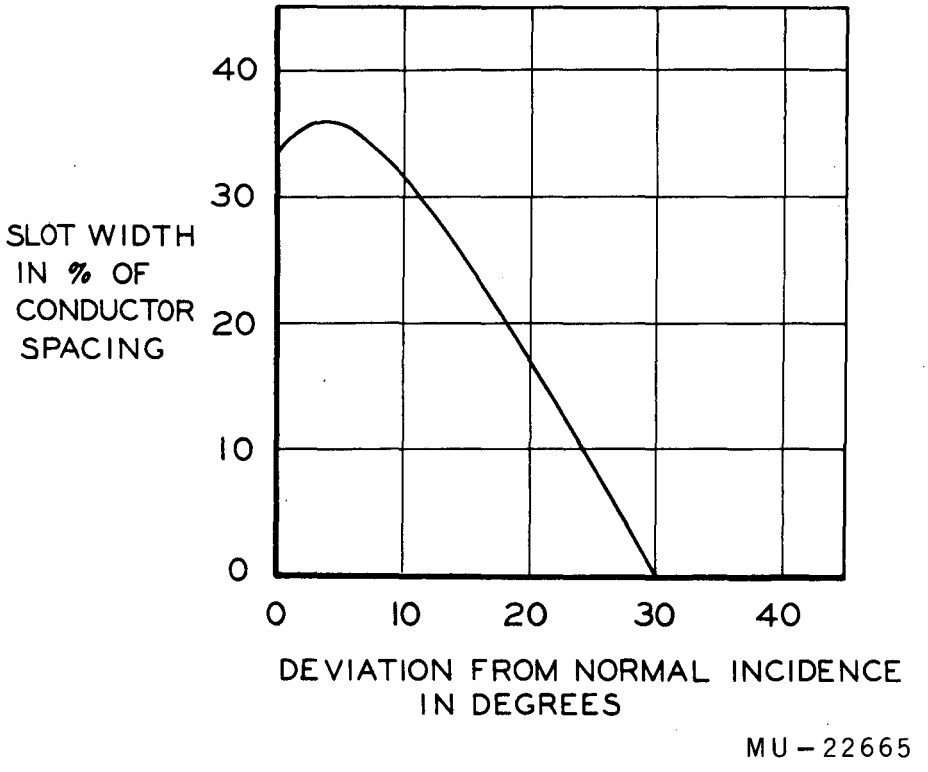

Fig. 32. Slot width in the picket fence.

(cave) is due to arrive from Allied Engineering Associates this week. In association with this, the northeast alcove is being modified for the cave installation. The utilities are being brought to the alcove and the necessary ducting, blower system, personnel barrier, and radioactivity shielding designs are completed and will soon be installed. A chemical fume hood is on order and should arrive very soon.

Preliminary designs of the 2-inch lead shielding for the machine are being roughed out. Actual construction will not begin, however, until the machine itself is more fully developed.

The reactor people have been extremely cooperative in developing tentative arrangements for the neutron bombardment of our samples. There is every expectation that this facet of the experiment will go very smoothly.

All those phases of the experiment which may be of potential danger are being worked out in close cooperation with the Hazards Control Group.

60-kev Hydrogen Ion Source

The new low-energy dispersion rf ion source, in which ions are extracted directly from an aperture at the surface of the plasma, has produced a beam of 0.5 ma. Although this current will probably be adequate when properly focused, modifications of the extraction geometry are being tried in order to increase it.

The vacuum system for the energy selector is now being assembled on the framework of the Varian V2200A magnet.

We propose to determine the charge-transfer cross section in proton-hydrogen atom collisions. This should extend the work of Fite et al.,[15] from 40 kev to 60 kev. We plan on detecting the hot neutrals formed during transfer as well as the slow protons.

We also propose to study the dissociation of atomic or molecular ions by electric fields. This will be based on the theoretical study by Hiskes.[12]

---

[15] Wade L. Fite, R. F. Stebbins, David G. Hummer, and R. T. Brackmann, Phys. Rev. 119, 663 (1960).

12. CONTAINMENT OF POSITRONS IN MIRROR AND CUSP GEOMETRIES

Gordon Gibson,* Willard C. Jordan,† and Eugene J. Lauer

Introduction

In the preceding quarterly report a summary and analysis was given of the observed containment times of positrons which escape on the axis of a mirror machine.[16] It was stated that data had also been obtained for particles escaping in orbits that could not encircle the axis. These data are now presented along with some results obtained with the coils tilted with respect to each other. The field coils used were the smaller set (76 cm mean diameter) mentioned in the preceding report. The separation was again 81 cm center to center, which results in a mirror ratio of about 1.8. The central field was 1300 gauss, and neon was used as the scattering gas.

In addition, some preliminary data were obtained with the current reversed in one coil (cusp geometry) of the larger set of coils (152 cm mean diameter).

Symmetric Mirror Field

Table II lists the containment times observed with the counter at two different off-axis positions, 11.4 cm in one case and 15 cm on the opposite side in the other case. The values listed for the time constants are averages of several runs and are reproducible within about ±10% except for the negative and large positive bias points, for which counting rates are low. A comparison with the results reported previously[16] shows that the containment times off axis are about the same as observed on axis. Furthermore, the fractional part of the counting rate due to trapped particles (zero-time intercept) is comparable to the on-axis case.

In order to establish that wall effects were not influencing the above results, probes were inserted in the mid-plane along a radius opposite to the counter position. No effects on the data were observed when the tip of the probe was more than 20 cm from the axis. Since the intersections of the precessional surfaces with the mid-plane are circles centered on axis, this means that the trajectories of the detected particles did not traverse radial distances greater than 20 cm from the axis. The minimum radius of the vacuum tank wall is 25.4 cm.

---

*Westinghouse Electric Corporation.

†Bendix Corporation.

[16]Gordon Gibson, Willard C. Jordan, and Eugene J. Lauer, in Controlled Thermonuclear Research Quarterly Report, UCRL-9393, Sept. 1960, p. 73.

Table II. Containment times for the symmetric machine

Distance of counter from axis (cm)	Energy of positrons detected (Mev)	Bias (%)	Scattering gas pressure (10^{-6} mm Hg)	τ (sec)
		4	0.5	6.5
		4	1.0	3.4
		4	2.0	1.75
15.2	0.5 ± 0.15			
		-1	1.0	4.3
		19	1.0	3.6
		39	1.0	3.2
		59	1.0	3.1
		79	1.0	3.0
		19	0.5	4.6
		19	1.0	2.95
		19	2.0	1.4
11.4	1.0 ± 0.23			
		-1	1.0	2.5
		1.5	1.0	2.85
		39	1.0	3.0
		59	1.0	2.8
		79	1.0	2.8
		99	1.0	2.25

Asymmetric Mirror Field

The measurements of containment times in an asymmetric field were made with an angle θ = 360 deg/128 = 2.81 deg between the planes of the coils (76 cm mean diameter). (Each coil was rotated by $\theta/2$ without displacement from the symmetric position.) The counter was located 3.8 cm off the vacuum tank axis in the direction of minimum coil separation, where a maximum trapped fraction was observed. The coil current was that which would result in a 1300-gauss field on axis at the mid-plane if coils were parallel. The energy of the particles was 0.5 ± 0.15 Mev and the neon pressure was 1.0×10^{-6} mm Hg. The data obtained to date for these conditions are summarized in Table III, and yield containment times that are about 30% shorter than in the symmetric case.

Table III. Containment time as a function of bias for tilted coils

Bias (%)	-1	9	19	39	59	79
τ(sec)	2.0	2.6	2.55	2.5	2.3	1.6

As above, probes were inserted to test for wall effects. In this case the time constants were not appreciably affected when the tip of the probe was 15 cm or more from the axis.

In addition to the containment-time measurements, an attempt was made to locate the drift surfaces in the asymmetric case by observing the effect of probes on the steady-state counting rates observed at various counter positions. Four probes located in the plane that bisects the angle θ were used. One of the probes was moved along a radius from the axis of the vacuum tank toward the point of minimum separation of the two coils. A second was moved along a radius in the opposite direction toward the point of maximum separation. The other two were at right angles to these.

As a probe is moved in along a radius the steady-state counting rate undergoes a transition from an unperturbed value to a lower value as the tip of the probe prevents trapped particles from reaching the counter. When the tip of the probe is not in this transition region the counting rate is, in general, independent of position. (An exception occurs when the tip of the probe and the scintillator are near the same field line so that particles may scatter directly into the scintillator.) A "cutoff" point, r_c, may be arbitrarily defined as the radius at which the counting rate is at the mean value between those obtained with the probe tip on the vacuum-can axis and with it all the way out.

Data were recorded for θ = 0 deg, 360 deg/512, 360 deg/256, 360 deg/128, and 360 deg/64 with the coil spacing, center to center, constant at 81 cm. The counter position was varied along a line parallel to the motion of the first two probes.

In the symmetric case ($\theta = 0$) the value of r_c for each of the probes is related to the position of the counter, as one would expect. For example, if the counter position is changed from 7.5 cm to 15 cm the value of r_c for each probe also increases about 7.5 cm (from about 11 to 18.5 cm). However, for θ = 360 deg/256 and larger, r_c is almost independent of the position of the counter. (θ = 360 deg/512 is an intermediate case.) For example, at θ = 360 deg/128 a change in counter position as large as 19 cm results in a change of r_c of only about 3 cm.

A plausible interpretation of these data is that scattering results in a radial "drift surface diffusion"[17] which occurs at a rate that is rapid compared with the rate at which particles enter the loss cone. If this is correct, location of the precessional surfaces will have to be done with probes whose position can be changed quickly without introducing gas into the high vacuum. Equipment to do this is being assembled.

The radial "drift surface diffusion" is apparently important only in a central region, the extent being determined by the angle θ. This behavior is also predictable from the calculations, since the curves of longitudinal invarient vs position for different magnetic moments become more similar with increasing distance from the central region. As has been stated above,

[17] Gordon Gibson, Willard C. Jordan, and Eugene J. Lauer, Phys. Rev. Letters, 4, 217 (1960).

long time containment is observed for θ = 360 deg/128. Therefore, particles cannot diffuse rapidly as far as the walls of the vacuum tank in this particular case.

Cusp Geometry

Some preliminary measurements of containment times in a cusp geometry have been made, using the same techniques as for the Mirror Machine. The magnetic field resulted from passing equal but oppositely directed currents through two coaxial coils of 76 cm mean radius whose center-to-center distance along the axis was 76 cm. Figure 33 illustrates the geometry and gives some estimates of field strengths obtained by an approximation which treats the coils as single-turn loops having radii equal to the mean radius of the coils. When the counter is at its maximum position off axis (15.2 cm), field lines similar to A and B intersect the scintillator. That is, along a line of force, the field increases in moving away from the scintillator ($z \approx -0.38$), reaches a maximum ($z \approx -0.15$), then decreases until it reaches a minimum and once again increases. Hence, one should observe long containment times just as in a mirror machine. Furthermore, the field at the "mirror" which is near the counter is weaker than the field along the line of force as it passes through the vacuum can near the midplane. Therefore the trapped particles should tend to escape out of the end of the device, if they are lost because of multiple scattering. The field behavior along a line of force closer to the axis is similar; however, the field intensity at its minimum is quite weak and the adiabatic approximation is not valid. Therefore no predictions can be made concerning the containment times from these arguments when the counter is very near the axis. Data were recorded with the counter at three positions--on axis, and 10.1 cm and 15.2 cm off axis.

When the counter was on axis and also 10.1 cm off axis, no long containment time was observed. That is, if a fraction of the particles was initially trapped, their "mean containment time" was less than 1/2 sec, which is the "pumpout" time. At 15.2 cm off axis a containment time of 2.7 sec was observed. In each case the counter was set to detect particles in the energy interval 0.50 ± 0.15 Mev. The base pressure during these runs was quite high, ≈ 2 or 3×10^{-7} mm Hg of unknown gases; as a result, mean containment times associated with various amounts of a known scattering gas could not be determined, nor could the dependence of the containment time on pressure. Also the ratio of the field strengths at the scintillator and at the near mirror was close to unity, so that the pitch angle of the trapped particles as they hit the counter was quite large (approx 70 deg), and some collimation and attenuation may have resulted. Future runs in the cusp geometry are planned.

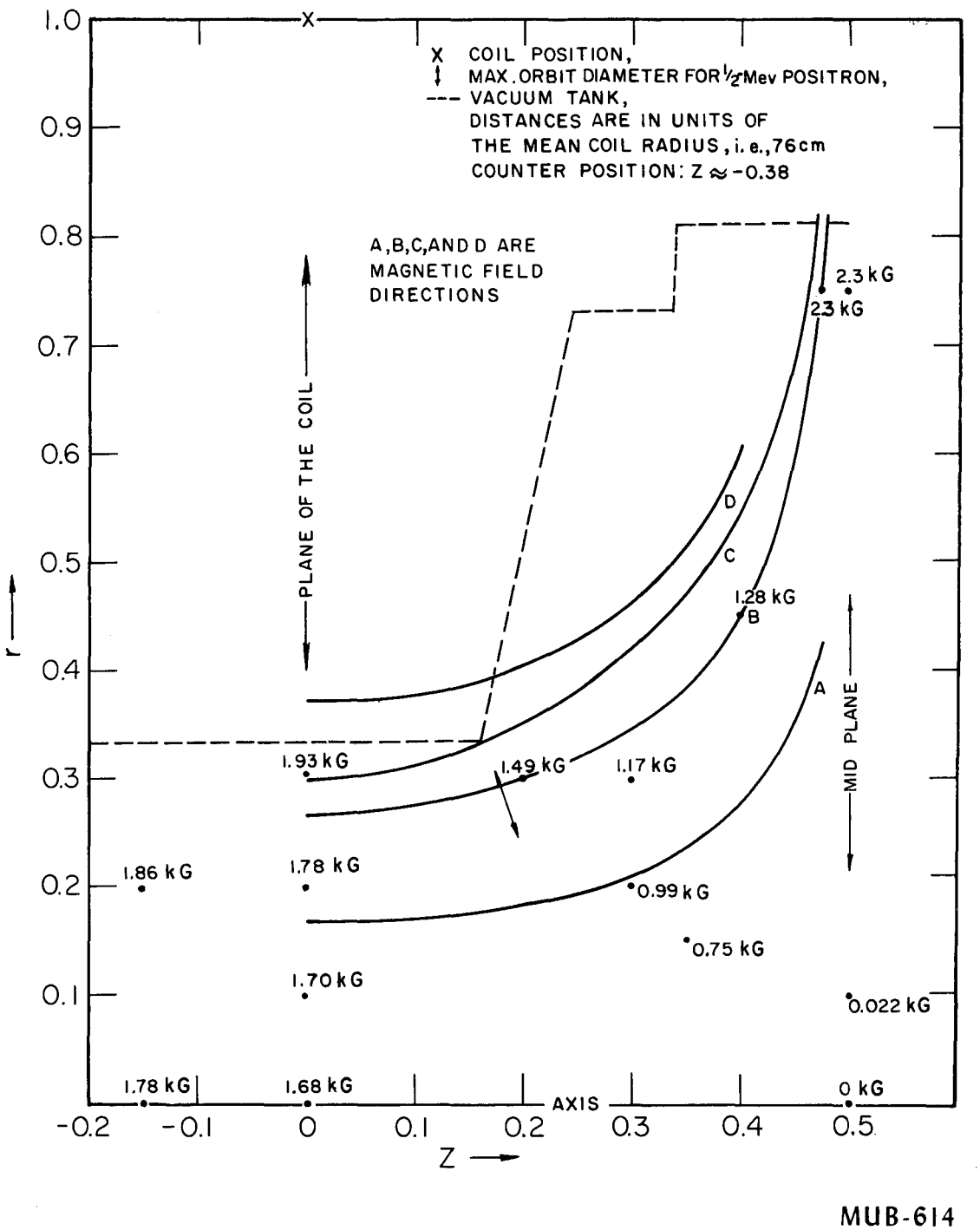

MUB-614

Fig. 33. Cusp geometry.

VI. ENGINEERING AND TECHNOLOGICAL DEVELOPMENT

1. ULTRAHIGH-VACUUM DEVELOPMENT

Norman Milleron and Leonard L. Levenson

Introduction

Pursuing our goal of optimizing diffusion pump systems, we worked on

- a new heater for oil,
- pumping-speed measurements,
- a contamination analyzer,
- conductance measurements,
- large bakable valve design,
- properties of trap materials.

A New Heater for Oil

This new heater provides (a) superheated oil vapor; (b) no eruptive boiling; (c) 5-sec starting and stopping; (d) a directed vapor stream; (e) maximum heating efficiency of the oil vapor; (f) a nearly independent supply of vapor to each D. P. jet. The construction of the heater is simple.

Nichrome strip, 0.001 in. thick and 1 in. wide, is wound with about three turns of glass string per inch of length. The strip is then rolled into a spiral, the glass string spacing the turns about 1/20 in. apart and electricically insulating each. Up to 13 amp of electric current may then be run through the spiral when the spiral is half immersed in oil. Oil runs up the small flues of the spiral and is superheated. A moving picture of the action of this heater was made.

Pumping-Speed Measurements

With three separate heaters of the above type, 5000 watts was put into convoil 20 oil in a 10-in. pump.[1] The base pressure was 5×10^{-7} torr, and the forepressure tolerance was 0.8 torr for air. The speed ratio was 2.3/1 for H_e and N_2 when a modified stack to the top jet was used. The absolute speed will be measured with the dp/dt method[1] in the future.

Contamination Analyzer

Construction is continuing on this device.[1]

---

[1] Norman Milleron and Leonard L. Levenson, Discussion of Optimization of Large Oil-Pumped Ultrahigh-Vacuum Systems, UCRL-5597-T, Sept. 1960.

Conductance Measurements

The data reported[2] on measurements of molecular flow conductance were expanded.

Large Bakable Valve Design

A bakable valve model with a 16-in. -diam orifice has been constructed. This valve model will be used to test a seal actuated by hydraulic pressure.[1]

Properties of Trap Materials

An experiment has been devised to examine the amount of oil vapor that can be trapped by various materials, e. g., artificial zeolite, activated alumina.[1, 3] Construction has just begun on apparatus for this experiment.

2. MECHANICAL ENGINEERING DEVELOPMENT

Thomas H. Batzer

Beat-Ray Experiment

J. Ralph Ullman

A fast-acting oscillating probe has been designed (UCRL Dwg. No. L19D4395). Two of these probes are being fabricated by Chalet Tool. They will be located on the horizontal ports of the 44-inch-diameter vacuum tank and will be placed in service in December. Each probe will be actuated by a special air cylinder, supplied by Rotex Punch Company, having a variable stroke between 5 and 18 in. Stroke time will be 100 msec or less. These probes will permit study of the orbit diameters versus other parameters for both asymmetric and symmetric mirror configurations.

Mirror modifications have been made to the Waldo coil containers to handle 18,000-lb. coil bucking forces involved in the case of the cusp geometry under study during the latter part of November. Center-line coil separation is set at 30 in., the minimum permitted by the 44-inch-diameter vacuum tank.

System operation has been routine and satisfactory with a base vacuum between 6×10^{-9} and 5×10^{-8} mm Hg. In October-November, system base pressure rose to 5×10^{-7} mm Hg. The steps taken (which we hope will correct this) were to change the oil in the 32-inch diffusion pump and replace three burned-out boiler heaters.

---

[2] Leonard L. Levenson, Norman Milleron, and Donald H. Davis, Optimization of Molecular Flow Conductance, UCRL-6014, Aug. 1960.

[3] M. A. Biondi, Nonrefrigerated Isolation Traps for Ultrahigh-Vacuum Systems, Transactions, Seventh National Vacuum Symposium, 1960.

Toy Top

John R. Benapfl

A magnetic analyzer is being designed that will be capable of measuring the maximum ion energy expected in the foreseeable future. The analyzer is of the pot type, having a circular pole face with a concentric cylinder as a flux return path. The field will be about 6000 gauss in a 1-in. gap, and the HR will be 198,000 gauss cm, which is capable of handling a D^+ ion with an energy of more than 10^6 ev.

The design deceleration voltage is 50 kv. Experiments are in progress now and so far we have held 35 kv. The problem seems to be one of field emission, and it seems likely that, with a larger radius on some corners and a decreased voltage gradient, the 50-kv figure will be attainable.

Table Top

James F. Ryan

The mechanical crowbar switch closed under load 530 times between October 20 and 26, with the saturable reactor in place to limit initial rate of current rise. On disassembly the contact cylinder showed heavy pitting. We conclude that the saturable reactor was working properly, but that errors were made in assembling the switch. The moving cylinder struck the making contact at least 0.020 in. off center and the contact pressure was too low. There was no pitting at the point of initial contact such as we found on the previous test. Redesign is needed to insure proper alignment of the parts and less dependence on the skill of the mechanic who assembles the switch.

Low-Energy Neutral-Beam Experiment

William S. Neef, Jr., William T. Crothers, and Eugene T. Bradley

The beam tube from the neutralizer to the dummy reaction chamber is nearly complete, and pumping tests on that portion of the machine will begin in December. All 6-in. elbow traps have been received; two are operating, and four are in the final stages of assembly and leak testing. Drawings for all the reaction chamber components and a new beam neutralizer are complete and have been released to fabrication.

Electrical pulse tests of coil No. 1 were accomplished to the rated current of 3000 amp. No further cracking of the epoxy resulted and no electrical problems were encountered. It was not possible to reach 78°K coil temperature. Heat losses through lines on the storage Dewar and from the ambient to the coil surface prevented us from reaching the desired value of coil resistance. Additional insulation of Dewar delivery lines has been completed. Insulation blankets around the coil improved the situation, and point to the need for thorough lagging around the mirrors of the ALICE machine. Coil section No. 2, composed of six two-pancake units, was completed and is awaiting test.

A button-type beam scanner has been developed and designed which has thirty-five 1/2× 1/2-in. targets electrically isolated and individually

cooled contained in a volume roughly 6×5×5 in. A pressure probe for the main reaction chamber is being designed. It consists simply of a few lengths of pipe with cooling tubes and a bakeout facility with two ion gauges and a place for attaching a mass spectrograph.

A stainless steel tank 37 in. in diameter and 72 in. long will be used as the beam burial chamber. It will be lined with a water-cooled copper cylinder acting as a burial wall for the gases in the chamber. Twelve centrally located titanium filaments provide the active burial materials.

An electrically and thermally insulated copper target will provide three measurement possibilities: (a) cooling-water temperature increase for a steady-state beam; (b) target temperature increase without cooling water for a pulsed beam; (c) electrical current flow caused by beam impact on target. The tank will be pumped by a 6-in. diffusion pump with a liquid nitrogen baffle and gate valve.

Astron

Charles A. Hurley, James F. Ryan, James E. Blades, and Edward G. Scarlett

A trial assembly of the core stack for the 720-kv electron gun was completed and difficulties were uncovered. The fiberglass spacer strips between cores were too narrow and not located accurately. They have been increased to 3/4 in. wide and are now located with a jig. The 1/8-in. thickness has been changed to 5/32 in. to allow more insulation around the primary straps.

The general status of mechanical work on the 720-kv electron gun and the 6-Mev accelerator is shown in Fig. 34. The general status of the mechanical work for the Astron main chamber is shown in Fig. 35.

The status of the modifications to Bldg. 157 for the installation of the Astron experiment are as follows: The restacking of the shielding blocks is on schedule and should be complete by December 15. Installation of cranes inside the shielding will begin December 1. Bids for the platform steel inside the shielding have been received, and this work should be complete by February 15, 1961, which will then allow the installation of the gun and accelerator.

Component Developments

J. Ralph Ullman

As indicated in an earlier report (UCRL-9243, p. 119 and 120), the test results on the double-pinch bakable seal demonstrate its reliability. Since that time the effort has been switched to understanding the behavior of the single-pinch bakable seal. A number of tests with an 8-in. diam single seal show conclusively that if the outer portion of the gasket is clamped or coined to exclude air from the pinch areas the seal remains tight through bakeout. In order to extend the test to larger-diameter seals, one of the ALICE pump boxes (UCRL Dwg. No. 7HL9114A), carrying five

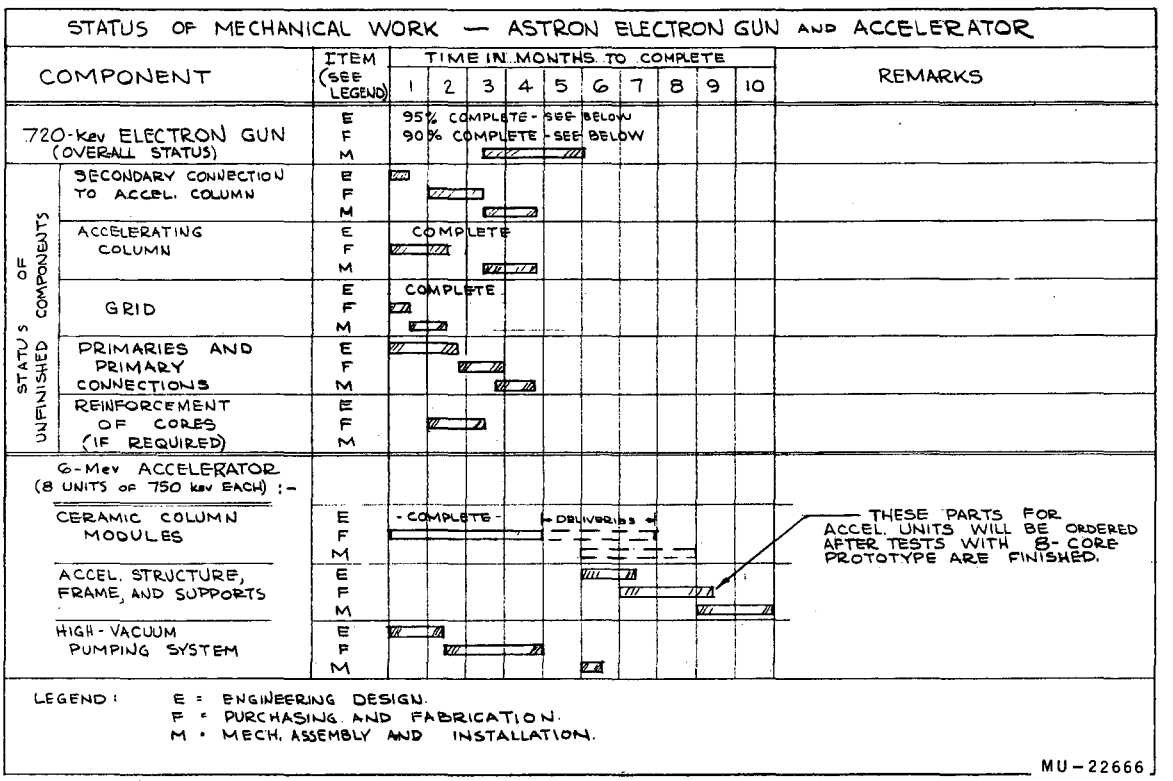

Fig. 34. Status of mechanical work--Astron electron gun and accelerator.

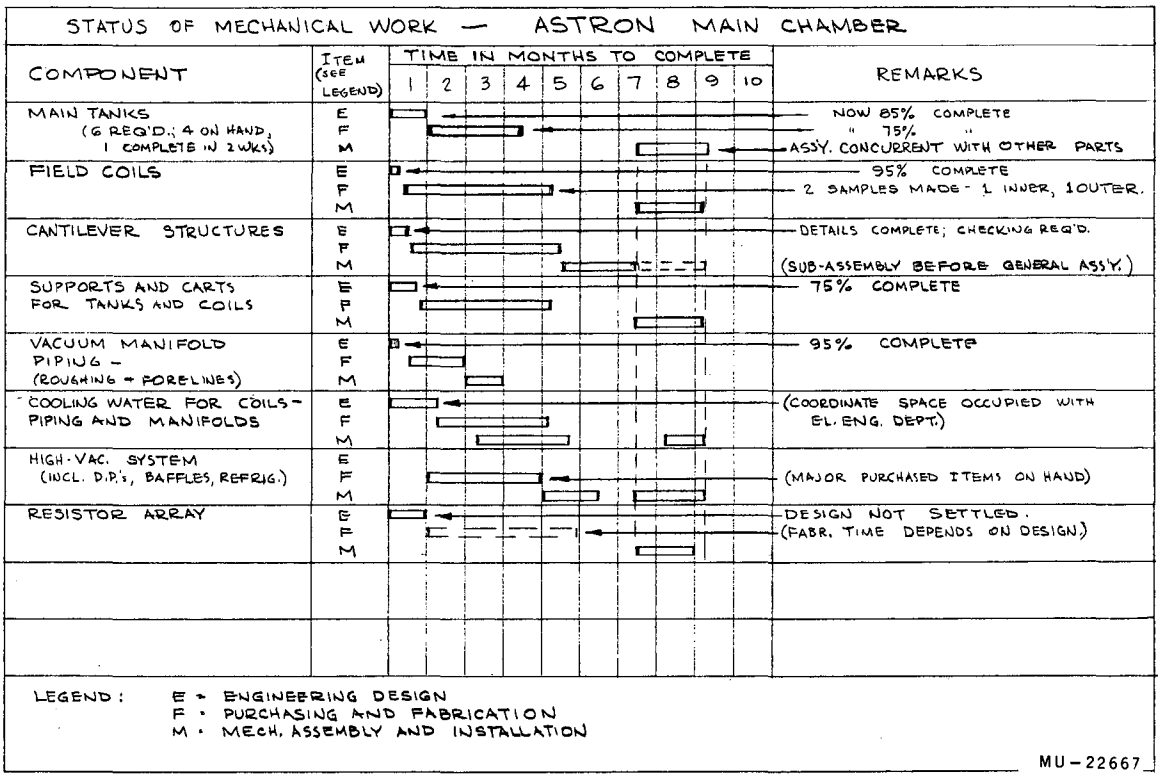

Fig. 35. Status of mechanical work--Astron main chamber.

15-in. single seals, has been set up for testing. Upon the successful conclusion of the seal development an Engineering Note will be issued showing the standard design details for both the single- and the double-pinch seals.

The 6-in. bakable gate valve (UCRL Dwg. No. L19D3865) to be used on the ALICE reaction chamber has been detailed. The valve utilizes the new stainless steel pressure diaphragm developed on the 4-in. bakable valve. The diaphragm is vacuum-welded to isolate the pressurizing fluid from the vacuum. The diaphragm drives the copper seal ring into sealing contact with the gate.

The 3-in. bakable angle valve installed on ALICE Mopu No. 2 manifold has been modified to permit actuation during bakeout. Further, the gate operator has been redesigned to eliminate torque transmission through the bellows. To date, the valve has been baked and the gate closed at 200°C.

In an effort to determine the best kind of elastomer O ring material for use in the ALICE beam tube, a test system was assembled. The system will check the base pressure for a variety of elastomer materials at given temperatures up to 300°C. The residual gas will be analyzed by a mass spectrometer.

Low-Temperature Refrigeration

Clyde E. Taylor

Two different prototype refrigeration systems are now operating continuously, cooling baffles in two 20-in. diffusion pumps. The original three-stage cascade system, which had two-stage compression in each refrigeration stage, has been modified to single-stage compressor operation. Although the two-stage compression system operated successfully, our immediate requirements can be met with the new systems, which are simpler but do not reach -285°F.

One of the two systems currently in operation is the modified system described above, which uses hermetic compressors, three refrigeration stages, suction pressures above 1 atm, and single-stage compression, and maintains a baffle temperature of -220°F. All heat exchangers and compressors are mounted in a single package. The refrigerator is connected to the baffle with a vacuum-insulated refrigerant line.

The other system uses much larger open-type two stage compressors, two refrigeration stages, and vacuum suction pressures, and maintains baffle temperatures at -230°F. The heat exhangers are mounted at the baffle and the compressors are remotely located, using noninsulated refrigerant lines. Both systems operate successfully. Similar systems will be built to meet Sherwood vacuum system requirements as the need arises.

Cryogenic Coil Project

Clyde E. Taylor, Robert L. Nelson, David C. Holten, Arturo Maimoni,* Jack W. Savage,† and R. Sewell†

Progress has been principally confined to paper studies, measurements of resistivity and magneto-resistivity in sodium and resistivity in aluminum; development of an ultrapure sodium distillation process; design and partial construction of an 8-in. i.d. test coil and a low-temperature coil test facility. Many of the pertinent data are summarized in a paper, by Clyde E. Taylor and Richard F. Post, Progress of the Cryogenic Coil Project at LRL--Preliminary Report, UCRL-6224, Nov. 1960.

All major components of the coil test facility are under construction in outside shops with the following exceptions: the coil test design is completed but not released by Purchasing; the valve box designs are completed but are being held pending tests of actuating mechanisms. Installation of major piping, wiring, switchgear, bussing, and instrumentation has not yet begun. The batteries and charging supply are installed; control switchgear has been ordered.

3. ELECTRICAL ENGINEERING DEVELOPMENT

Vernon L. Smith

Pyrotron

David R. Branum

Table Top II

During the past three months the machine has been in use in the experiments by Dr. Walton A. Perkins and Dr. Thomas Passell.

There were 9644 bank operations at an average level of ± 11 kv. The total is now 91,046 pulses on the bank since it was installed.

The mechanical-crowbar relieving switch was installed in October and operated satisfactorily until a vacuum switch in the saturable-reactor core-reset power supply failed and the bank discharged through the power supply. The switch has now been removed from the experiment.

There have been no major bank problems during the past 3 months. One charge vacuum switch failed in the bank after 73,000 operations.

A fast bank consisting of twelve 7.5-mf 20-kv "Green River" type capacitor-ignitron setups is under design for the future modification of the machine. Two Perkins-type 300-kw 2,000-amp dc supplies are to be installed in the machine area.

---

*Chemistry

†Electronics Engineering

The output bus networks of the main bank will be suspended from the ceiling away from the shield can that now supports it.

From now on the main 10^6-joule-maximum bank will be known as Bank No. 1 and the new fast bank will be known as Bank No. 2. The rise time of Bank No. 1 will be about 7 msec and that of Bank No. 2 will be between 10 and 20 μsec.

Toy Top III

The past three months have been spent in constructing the third-stage components (banks, pulse lines, etc.) during the day and running the two-stage experiment during a night shift. There were 5800 Bank 1 and 4 operations at ± 14 kv.

The new type of transmission lines for Bank 4 has proven to be very satisfactory. The lines are made of double-flex braid and are a glass-epoxy encapsulated line.

Work is continuing on Banks 2, 3A, 3B, and 3C. The transmission lines for 3A, 3B, and 3C are completed and are also of the flex-braid, glass-epoxy encapsulated construction.

In order to obtain longer L/R decay times in the third-stage coils, additional crowbar ignitrons are being added to Banks 3A, 3B, and 3C. At a later date additional crowbar ignitrons will be added to bank sections of Bank No. 4.

Banks Nos. 3A and 3B are being converted over to positive 20-kv banks, and a third kenotron hv charging supply is being connected to charge only these two banks. This will give Toy Top III three 20-kv 4-amp dc bank-charging supplies.

Two additional Perkins-type 300-kw 2000-amp dc magnet supplies are being added to the experimental area. This will give the machine seven of this type of dc supplies.

P-4

The electronics of the arc source control were modified so that the PIG arc could be run at either polarity cathode or anode ground.

Pyrotron--Miscellaneous

Hubert W. Van Ness, Alfred F. Waugh, Kristian Aaland, and Gilbert A. Reeser

ALICE

The cable trench work into the m. g. set room in Bldg. 156 has been completed. Installation of the 480-volt primary power cable and circuit breaker panel in this area is also now complete. The installation of cope tray and cables from one of the m. g. sets to the ALICE Ion Source in Bldg. 180 is in progress.

A specification sent to 18 companies requesting proposals on equipment for dissipating inductively stored energy in ALICE coils yielded only two replies. A design has been completed for the mounting and cooling of the previously purchased thyrite assemblies. The design of the required bus-bar connections to the ALICE cryogenic coils is also complete. A specification and purchase order have been written for a dc current interrupter which, together with the thyrite, should satisfy the performance requirements.

The installation of equipment required for the ALICE beam tube experiment is essentially complete. The purpose of this experiment is to determine if the required vacuum pressures and pressure differenials can be maintained along the ALICE beam tube from the ion source to and including the confinement chamber.

Fabrication has been started on a 20-kv 1-amp power supply, regulated to 0.2%. Prior to fabrication, an extensive analysis was made of the design, which basically is the same as the design of the Astron dry run $\phi\pi$ supply that was engineered early in 1958. The regulation required in this supply necessitated a closed-loop negative-feedback system with a very high gain, and the analysis of the supply was concerned primarily with the operation of this feedback system. The small signal gain, large signal gain, time response, and Nyquist plot were all investigated to assist in the engineering. An overcurrent-interrupt feature with 1-msec automatic reset has been included. The plan calls for the supply to be ready for test early in January.

Source Development

The ALICE ion source began operating October 18. The initial operation has been satisfactory and encouraging. A 250-ma 20-kv beam has been produced down a 3-foot beam tube.

The ion-source field coils have been temporarily energized by a 300-kw Perkins power supply. Field-strength measurements and corresponding coil current and voltage measurements have been made so that now the gauss/amp and power requirements are definitely known. The motor generator set has been operated into a pair of 9-in. i. d. modular magnet coils which exactly duplicate the ion-source field coil load. The excitation requirements and response characteristics of the m. g. set have thus been determined.

The combination of the J. C. Carter Model 601 rotating-coil fluxmeter unit and a power control unit No. 4504 made by Control, a Division of Magnetics, Inc., looks like a promising solution to the regulator problem.

High-Vacuum Research

Measurements have been made of pumping speeds and base pressures obtainable by using Varian Associates Vac-Ion Pump and Vac-Sorb Pumps on a completely bakable oil-free system. Preliminary data are very encouraging.

A slow-sweep bakable mass spectrometer system has been successfully operated to analyze the composition of the residual gas in ultrahigh-vacuum systems.

Constituents of the residual gas have been observed at base pressures in the region 10^{-8} mm.

P-4

A complete pulse-powering system for an electron gun was designed and built. The system is ready for testing with the gun.

The characteristics are line-synchronized pulses up to 60 pps, 0 to 20 kv amplitude, and of 2 to 20 μsec adjustable duration. Cathode bombardment power is 2 kv, 1.5 amp dc, isolated for a 20-kv pulse. A number of dc focusing voltages are also furnished. The system is shown on LE 6971-1.

Pinch and Collapse

Hubert W. Van Ness

Gamma Bank Area

The 40-kw 450-kc oscillator has been installed and made operational. It will be used for inductively heating the inconel liner in the "Levitron" experiment.

Fast-Scan Mass Spectrograph

Testing and calibration of the hyperbolic waveform scanning system is in progress. This circuit will provide scanning rates from 10^{-3} to 10^{-1} sec to cover the mass ranges 2 to 100. Use of the hyperbolic scan waveform will provide a linear oscilloscope presentation of mass numbers.

Sodium Radio-Frequency Analog Experiment

The 40-kw oscillator was connected to a coil system tuned to resonate at 300 kc. Sufficient coil current was obtained to produce the desired experimental forma in sodium.

Energy-Storage System Investigation

The unipolar generator was installed and successfully run as a motor a few times, but vibration troubles were encountered at speeds above 3000 rpm. Allis-Chalmers provided a service engineer who balanced the machine, permitting operation up to 10,000 rpm without excessive vibration. Initial field pulsing tests with a 0.2-farad capacitor bank at 400 v produced one-third open-circuit output voltage with a rise time of about 0.2 sec. Additional troubles that developed in the machine prevented further tests. Investigation disclosed internal plugging of the machine NaK passages and probable insulation damage, resulting in internal short circuits. A decision has been reached to dismantle the machine to determine the extent of the trouble, which will then be corrected by Allis-Chalmers. The machine should be dismantled around the first week of December.

300-kv Marx Capacitor Bank

An investigation of the internal characteristics of the Tobe Deutschmann capacitors is under way. These tests will be made in the 100-kc frequency range. The object will be to determine differences that may exist between capacitors, and that could account for the poor service obtained in Marx operation. Such information will aid in the future planning and design of Marx-type capacitor banks.

Switch Development

David B. Cummings

Mechanical Switching

The mechanical-crowbar relief switch with the saturable-reactor modification was tested on Table Top. This change eliminated contact burning on the leading edge. However, the difficult problem of contact alignment remains unsolved.

Ignitron Development

Tube Tests

The rest of the tube types were tested. Some production troubles on tubes prevent clear conclusions. However, it appears that (a) single-pantleg anode seals are comparable to double-pantleg seals, (b) vacuum-melted mild steel anodes are comparable to vacuum-melted molybdenum, and (c) ceramic ignitor seals still wet badly from metal anodes. Greater emphasis will be placed on having smooth anode and wall surfaces.

The ignitron development and testing program was terminated with the dismantling of the Engineers Bank on October 3, 1960. Further tests will be done on operating machines.

New Designs

A modified single glass pantleg tube with a vacuum-melted mild steel anode has been ordered for evaluation.

The long, high-current pulses used on Table Top have caused arc transfer from the cathode to the steel wall. This has wetted the ignitors, made them difficult to fire, and shortened the life of the tubes. To cure this problem a design has been ordered in which the spacings are arranged to inhibit arc transfer. This results in other advantages also, such as lower inductance and greater stability.

Cryogenics Coil Experiment

Jack W. Savage

The helium-system compressor is being installed along with the refrigeration units.

The battery and charger are in their final locations and operating switches have been ordered. The main 45,000-amp switch is being tested and adjusted and its control circuit modified to work with the balance of the experiment.

Main current control, valve control, instrumentation, and over-all system design are complete.

The microvolt bridge is now installed and working.

Present major concern is prediction of effect of 100,000-gauss main coil field on instrumentation, since it is not possible to move instruments to a definitely low-field area.

Atomic and Molecular-Beam Experiment

David R. Branum

The development of a low-energy and a high-energy gun system has been completed. A focus-detection system using an X-Y recorder is being used to determine beam position.

Microwave Diagnostic Development

Charles B. Wharton and Joseph E. Katz

Most of the effort this quarter has been in getting the group going again. So far we have no technician and the cleaning up has been slow.

We have investigated several new ideas for microwave diagnostics. The first of these is aimed at measuring the density of a compressed plasma of dimensions comparable to wave length. The usual transmission methods fail, owing to scattering around the plasma. The new method involves measurement of the frequencies of plasma resonances as a function of

propagation angle. At 0 deg (along B) the resonance is at the cyclotron frequency, independent of density. At 90 deg the resonance is at the "hybrid frequency," $\sqrt{\omega_c^2 + \omega_p^2}$. Measurement of more than two resonances as a function of angle simultaneously yields the electron density. To tilt the microwave beam at a known angle we have investigated microwave prisms. Field plots of various radiators and prisms indicate that tilts of as much as 60 deg are possible without much attenuation in the tilting system. We had planned to apply the method on both Table Top and Toy Top, but were not able to get machine time yet. The equipment is being set up on P-4, but the 1000-gauss field is so low that there is a question whether or not we can resolve the two resonances, since they will lie very close together.

The second idea involves polarization-angle measurements. We have constructed a polarization duplexer which gives > 30 db isolation between cross-polarized components. The duplexer will allow time-resolved measurement of Faraday rotation angle, or will permit simultaneous measurement of $E \perp B$ and $E \parallel B$ components in propagation across a plasma. We have used the duplexer in a radiation experiment on Toy Top III to view the two polarizations. In addition, a tilting of the beam, as mentioned above, was done with prisms, giving 90, 60 and 45 deg in respect to the field. Some data were obtained and are being analyzed, but the experiment was terminated by failure of a pulse coil in Toy Top. We hope to resume after Christmas. The only conclusions we wish to draw yet are that the electrons in the compressed (two-stage) plasma do not seem to be very hot. The electron temperature appears to be about 100 ev near peak compression, but occasional spurious, anomalously large radiation signals, corresponding to several kev, occur during warm-up of the experiment. The radiation intensities coming from the plasma source itself (without compression) correspond to 1 to 3 kev. We presume that this value represents only the high-energy tail of electrons, occurring in sufficient density ($10^{13}/cm^3$) to appear opaque to our receiver. Further investigations are definitely indicated before valid conclusions can be drawn.

Electron Beam Instabilities Experiment

The electron gun, capable of producing a 5-amp 20-kev dc beam, is in place on the end of P-4. Initially we plan to pulse the beam with 10-μsec pulses. A pulser, cathode-bombarding supply, and all the necessary electronics to operate the gun have been furnished by Kristian Aaland's group, and the system will be operative as soon as minor vacuum problems have been corrected.

To view the effect of the pulsed beam on the P-4 plasma we have set up a microwave receiver which sweeps over the spectrum near the electron gyro frequency, viz., 2 to 4 Gc. We also have receivers to sample the spectrum at 25 Gc and 35 Gc, corresponding to plasma frequencies at various locations in the plasma. A dual-frequency waveguide duplexer (J. A. 1238 issued to H. Bunn) will permit both receivers to view the same region, using only one antenna. Langmuir and rf pickup probes will also be used to detect plasma oscillations. Various optical instruments in place on P-4 may also be useful.

Astron Electron Beam Experiment

We have begun thinking of methods of measuring the electron density, temperature, and collision rates. The densities will be quite high, so we have obtained a few pieces of 2-mm-wave-length plumbing, to get the feel of using 140-Gc equipment for diagnostics. The first measurements will be done at 70 Gc and 90 Gc, and at 140 Gc by harmonic generation from 70. So far only dry-lab setups have been made. The major problem we must face is the excessive losses in waveguide transmission paths. Various high-mode, low-loss transmission lines and mode transducers are being investigated.

The circular TE_{01} mode seems to be most promising. Mode transitions have been electroformed and are being evaluated.

Astron

System Engineering

Clelland D. Nail

The Electron Accelerator

The entire Astron machine is shown in simplified block layout in Fig. 36. Progress on the various portions of this system can be reported as follows.

The Core Pulsers

Pulse-forming networks (PFN) will consist of six lengths of RG-218/U coaxial cable. One carload of this cable has arrived--more is expected soon. Reels for holding and handling the PFN's have been designed and a sample built. An overhead storage rack for these reels has been drawn up. This enables access to any PFN for repairs or replacement and occupies otherwise lost space. The details of this plan are being reconsidered because of the delay and cost of the overhead structure.

The Pulser Chassis

Performance specification L 468-1 has been written covering the high-voltage connectors and thyratron housing which form the principal special parts of the pulser chassis. Delivery of three samples similar to those called for in the proposed specification have been received from Franklin Engineering Company and are undergoing test. Preliminary results indicate that only minor revisions will be necessary.

Requisition No. 1845-13 calls for bids on quantities of 3, 30, and 440 to the specification. The request has not been approved by AEC or Budget to date.

Informal conferences with prospective bidders on this hardware have resulted in proposals from six companies, at least three of which wish to

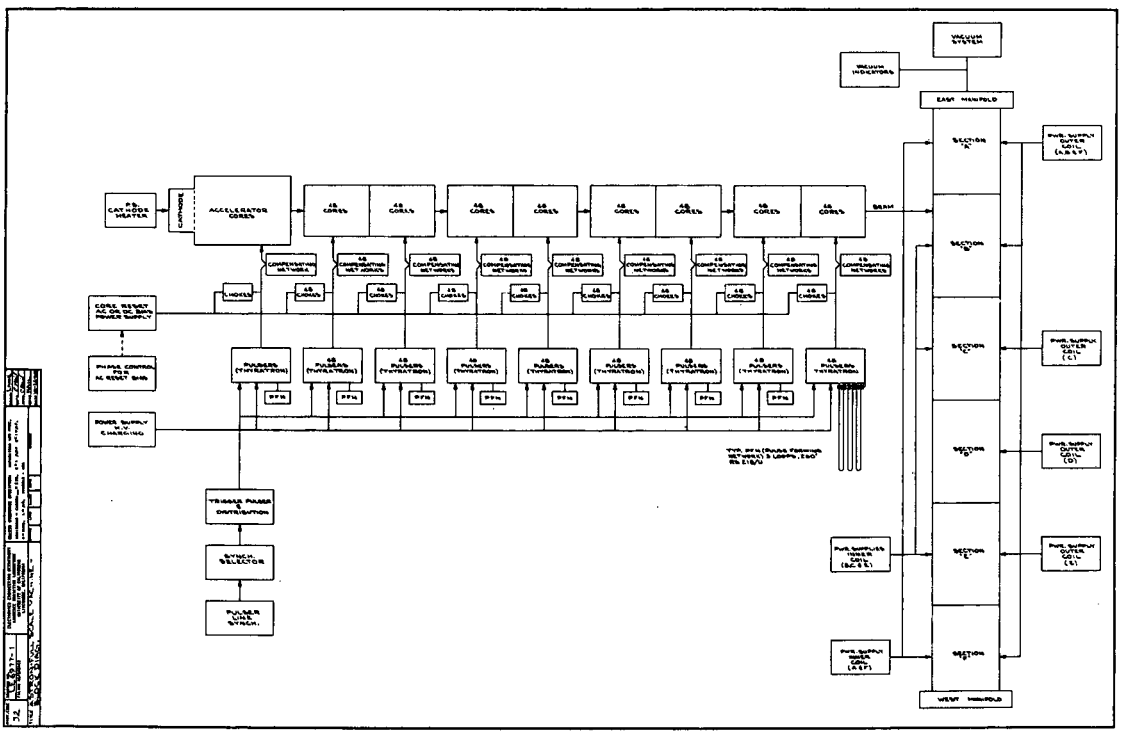

MU-22675

Fig. 36. Full-scale Astron machine.

be considered for construction of the entire chassis. One company has submitted detailed price and delivery information on the complete pulser, which has sufficient merit to justify further consideration. A performance specification is being written for the entire chassis, based on the 6587 thyratron and the input-output requirements, in order that comparative bids may be obtained.

Thyratrons

Nicholas C. Christofilos has suggested tests be conducted with the 5949/1902 hydrogen thyratron, which has a higher voltage and current rating than the present 6587. This tube is nearly twice the physical size of the 6587 and costs about two times as much ($80.).

Samples of the tube are on order, as well as filament transformers and other hardware to mount the tube.

Power Supply

The design of the hv power supply has not been completed. However, a performance specification is being prepared to permit soliciting proposals on this unit. The total output power requirement of this supply is of the order of 500 kw. For this large power demand, line charging from a single-phase power source such as was used on the Astron "Dry Run" experiment is not feasible. A design being considered is three-phase-supplied and will also delay recharging the pulse-forming lines until just before needed. This should reduce corona damage and the tendencies for the tube to "fire through."

System Trigger

A trigger generator to fire 100 chassis has been constructed by Kristian Aaland. No difficulty is seen in extending the design to a larger system of 500 outputs. A completely solid-state pulser with 500 outputs is being considered by Aaland, which will also incorporate variable delay in each output.

The Load Cables

The load cables will be RG-213/U coaxial (successor to RG-8/AU). Tests have indicated this cable is generally able to withstand the service except at points where stress concentrations occur. This indicates the need for special construction at all joints to prevent early failure. This cable has been received and is in storage.

The Core-Excitation Windings

The design of the primary core winding remains a major obstacle in the design of the accelerator. Some promising results are indicated with special wire with oil-impregnated teflon or polyethylene insulation. It seems necessary to completely exclude air as a dielectric in any part of the field, since the gradient is well above its breakdown strength. This imposes a difficult fabrication problem in bonding the large cores and secondary

surfaces with epoxys or silicone rubber to prevent air voids and attendant corona failure.

Mr. Christofilos has indicated that a single strap at one location on the core may not be satisfactory. Three are suggested, at equal spacing. Alternatively, he proposes a solid sheet conductor as a primary.

The latter will be tested in the near future, but it is believed that the large capacity of such a structure will make it impossible to excite or compensate.

Compensators

The networks necessary to compensate the core windings so as to produce a rectangular voltage pulse have been designed and built, using various commercial components. These circuits have been successful at distances up to about 15 feet from the core in achieving a flat top to about 1%. The capacitors available that have been tested so far have not been reliable in the compensator circuit. Others are in the process of evaluation and more are being ordered. All work to the present has been done with one strap per core.

Bias Methods

The core-reset bias can be either ac, dc, or pulsed dc. In each case the requirements are 30 to 50 amp of bias at the time of pulsing for each core. Because of the simplicity in circuitry and balanced primary loading, dc is favored as the method for reset. Because of the very large total current (25,000 amp) the power supplies will probably have to be located inside the shield wall as close to the machine as possible. Even so, fairly large bussing will be necessary if reasonable efficiency is realized.

Of the three methods, dc reset will create maximum core heating. If adequate cooling becomes difficult, it may be necessary to resort to pulsed dc bias. This will require development of a large switch or a large number of small switches to handle the total bias current. This is further complicated by low circuit voltage (10 to 20 v).

Main-Field Power Supplies

A precise set of specifications for the main field is being prepared. These are given low priority at present because of the need for effort elsewhere and because these items are not for immediate purchase. Fifteen companies have shown capabilities for producing our needs.

Beam Inflector

Specifications for a high-current power supply for the beam inflector is being worked on in cooperation with Mr. Ryan of the Mechanical Engineering Department.

Beam-Analyzing Magnet

A current-regulated power supply has been requisitioned (Requisition No. 1845-29) for the beam-analyzing magnet.

Research and Development

Kristian Aaland and Bernard M. Loth

Train Pulse Investigation

A transistorized computer-type unit was completed which could remove the correct number of pulses at the correct times from a 10-Mc/sec pulser (LE 6906-1 to 6906-10). This, then, was the first stage of the train pulse. Development of amplifier stages, investigation of high-power tubes, and examination of pulse transformers for 30-nsec train pulses was continuing when the decision was made to "mothball" the project for two months.

Hard Tubes

A Machlett experimental tube type DP11 was successfully operated at 150 kv plate voltage. Load was 400 ohms resistive. A 120-kv pulse was observed, yielding an output power of about 36 Mw. We have received one DP11L for faster pulses and one DP15 for a possible plate voltage of 200 kv.

65-Megawatt Pulse Amplifier

Construction was started on a 65-Mw 0.3-μsec hard tube pulser. The pulse output was calculated to be 64 kv, with a top flat to ± 1% and a peak output current of up to 1000 amp.

This unit was designed to permit testing of the Astron electron gun cores. The test method was to have been the same as used on the accelerator cores, outlined in LE 409-1.

The pulser was designed as a multistage pulse amplifier with the last two stages immersed in insulating oil. This was to provide both cooling and dielectric strength.

Work has been suspended on this unit. The design and construction are complete up to the final output stage. Because of the amount of effort and manpower this pulser has taken, a word about the problems encountered seems in order.

A study of switch tubes has been made (LE 413-1). This has indicated that a hard tube pulse of this power could be built.

In the course of construction, two main problems came up. Both are associated with the high power and high voltage of the final stages. The first is water absorption by the insulating oil. The dielectric strength of common insulating oils is reduced by as much as 50% by as little as a few parts per million of absorbed water. This alone has caused the rebuilding of the final stage in order to reduce the voltage gradient to a safe value for

contaminated oil. The second difficulty associated with high voltage has been faulty components. Several of the paralleled capacitors have failed at below their rated voltage. In each case the high energy dissipated in the fault has resulted in the damage of associated components and equipment.

The necessity of rebuilding the output stage many times has resulted in a long construction time for the unit.

Reports Written This Period

B. M. Loth, Hard Tube Switch Performance, LE 413-1 (UCID-4212).

K. Aaland, Trigger Distribution Transformer, LE 476-1.

VII. TALKS AND PUBLICATIONS

International Conference on Instrumentation for High-Energy Physics, Berkeley, California, Sept. 12-14, 1960

R. F. Post and C. E. Taylor, Cryogenic Magnet Coils for High-Energy Physics Experimentation, UCRL-6133-T Abst., Sept. 1960.

Thirteenth Annual Gaseous Electronics Conference, Monterey, California, October 12-15, 1960

George A. Paulikas, T. K. Allen, and Robert V. Pyle, Instability of a Positive Column in a Magnetic Field, UCRL-9370 Abst., Aug. 1960.

W. S. Cooper, III, A. W. DeSilva, and J. M. Wilcox, Experimental Observation of Stark Broadening of Balmer Lines, UCRL-9371 Abst., Aug. 1960.

The 7th National Vacuum Symposium, Cleveland, Ohio, October 12-14, 1960

L. L. Levenson, N. Milleron, and D. H. Davis, Optimization of Molecular Flow Conductance, UCRL-6014-T Abst., June 10, 1960.

Norman Milleron and L. L. Levenson, Discussion on Optimization of Large Oil-Pumped Ultrahigh-Vacuum Systems, UCRL-5597-T Abst., Sept. 12, 1960.

University of California, College of Engineering, Berkeley, California, Air Force Research and Development Course 801, Richmond Field Station, Richmond, California, October 20, 1960

Norman Milleron, Effects of High Vacuum on Engineering Materials (invited paper).

The Fifth Sherwood Vacuum Technology Meeting, Oak Ridge, Tennessee, October 31, 1960

L. L. Levenson, Preliminary Observations of Operating Characteristics of Nude Gauges (invited paper).

Norman Milleron, Results on Optimization of Diffusion Pump System (invited paper).

T. H. Batzer, Recent Successful Test Results with Modified High-Vacuum Copper Pinch Gaskets (invited paper).

J. R. Ullman, On the Application of the Marman Conoseal as a Seat in an Angle Bakeable Valve (invited paper).

Mechanical Engineering Seminar, College of Engineering, University of California, Berkeley, California, November 14, 1960

Norman Milleron, Knudsen Flow in the Design of Ultrahigh-Vacuum Systems (invited paper).

Department of Electrical Engineering, College of Engineering, University of California, Berkeley, California, November 15, 1960

F. H. Coensgen, Multistage Magnetic Compression Experiment and Results (invited paper).

Second Annual Meeting American Physical Society Division of Plasma Physics, Gatlinburg, Tennessee, November 2-5, 1960

A. L. Gardner and N. L. Oleson, Rotating Probe Measurements in the Interior of the P-4 Steady-State Plasma, UCRL-6158-T Abst., Sept. 22, 1960.

H. P. Furth, Sheet Pinch Instabilities Caused by Finite Conductivity, UCRL-6160-T Abst., Sept. 22, 1960.

J. F. Steinhaus and C. C. Damm, Trapping and Confinement of 20-kev Hydrogen Atoms in a Magnetic Mirror Machine, UCRL-6131-T Abst., Sept. 19, 1960.

E. S. Chambers, Ion Heating by Alternating Radial Electric Field in a Mirror Machine, UCRL-6159-T Abst., Oct. 27, 1960.

T. O. Passell, Plasma Calorimetry in the Table Top Mirror Machine, UCRL-6153-T Abst., Sept. 20, 1960.

F. H. Coensgen, W. F. Cummins, W. E. Nexsen, Jr., and A. E. Sherman, Ion Energy Distributions in Magnetically Compressed Plasma, UCRL-6151-T Abst., Sept. 23, 1960.

R. F. Post, Velocity Space Instabilities in the Mirror Machine (invited paper).

E. C. Taylor and F. A. Wolf, The Effect of Charge Separation on Large Amplitude Pulses in a Cold Plasma, UCRL-6137-T Abst., Sept. 12, 1960.

F. A. Wolf and E. C. Taylor, The Effect of Charge Separation on Large Amplitude Pulses in a Plasma with Isotropic Pressure, UCRL-6138-T Abst., Sept. 12, 1960.

G. G. Comisar, The Ion Structure of Plasma Shock Waves in a Transverse Magnetic Field, UCRL-6140-T Abst., Sept. 12, 1960.

R. F. Post, Ambipolar Potentials in a Mirror Machine, UCRL-6155-T Abst., Sept. 20, 1960.

A. H. Futch, C. C. Damm, W. Heckrotte, J. Killeen, and L. Mish, Gas Density Variation During Plasma Buildup by Neutral Atom Injection, UCRL-6150-T Abst., Sept. 19, 1960.

L. S. Hall, A. L. Gardner, R. L. Kelly, and N. L. Oleson, A Qualitative Model of P-4, a Steady-State Plasma Source, UCRL-6156-T Abst., Sept. 20, 1960.

S. A. Colgate, C. W. Hartman, and R. L. Spoerlein, Electron Beam Probing of the Pinch, UCRL-6157-T Abst., Sept. 22, 1960.

W. L. Barr, A Method for Computing the Radial Distribution of Emitters in a Cylindrical Source, UCRL-6154-T Abst., Sept. 21, 1960.

Melvin J. Bernstein, Measurement of α/p for H_2 across a Strong Magnetic Field, UCRL-9406 Abst., Sept. 1960.

Alan W. DeSilva, William S. Cooper III, and J. M. Wilcox, Experimental Observations of Hydromagnetic Wave Modes and Reflectors, UCRL-9407 Abst., Sept. 1960.

Jet Propulsion Laboratory, California Institute of Technology, Pasadena, California, September 1960

Norman Milleron, Ultrahigh-Vacuum Techniques (invited paper).

University of California Extension, Alameda Naval Air Station, Alameda, California, October 1960

Norman Milleron, Properties of Surfaces at Ultralow Pressures (invited paper).

American Nuclear Society, Burlingame, California, November 14, 1960

R. F. Post, LRL Magnetic Mirror Program (invited paper).

F. H. Coensgen, Recent Results in the Multistage Magnetic Compression Experiment (invited paper).

The Physics of Fluids

W. E. Nexsen, Jr., F. H. Coensgen, A. E. Sherman, and W. F. Cummins, Plasma Injection into a Magnetic Field of Cusped Geometry, 3, 764 (1960).

Lewi Tonks, Diffusion through a Finite Plasma in a Uniform Magnetic Field, 3, 758 (1960).

H. P. Furth, Sufficient Conditions for Hydromagnetic Stability of a Diffuse Linear Pinch, 3, 977 (1960).

S. A. Colgate and H. P. Furth, Stabilization of Pinch Discharges, 3, 982 (1960).

The Physical Review

W. F. Cummins, F. H. Coensgen, A. E. Sherman, and W. E. Nexsen, Jr., Collision of Two Plasma Streams, 119, 1457 (1960).

The Physical Review Letters

T. K. Allen, George A. Paulikas, and Robert V. Pyle, Instability of a Positive Column in a Magnetic Field, 5, 409 (1960).

F. H. Coensgen, W. F. Cummins, W. E. Nexsen, Jr., and A. E. Sherman, Evidence of Containment of a 3-kev Deuterium Plasma, 5, 459 (1960).

Information Division
sa